Musculoskeletal Ultrasound

Author(s) Beggs, Ian

Imprint Lippincott Williams & Wilkins, 2014

ISBN 9781451144987, 1451144989

Permalink https://books-scholarsportal-info.myaccess.library.utoronto.ca/en/xml/chapter?id=/ebooks/ebooks1/lww/2014-07-29/1/01762492&chapterId=B01762492-C4

Chapter 4
Elbow
Theodore T. Miller

INTRODUCTION

The elbow is commonly injured in sports and occupational activities. Elbow injuries account for approximately 20% of upper extremity sports injuries[1] and the elbow is the second most commonly dislocated joint after the shoulder.[2] The elbow is well suited to sonographic evaluation: it is small and easily manipulated by the examiner, enabling dynamic assessment; it is accessible around its entire circumference, allowing long and short axis scanning of every segment of the joint; and the structures of interest are superficial and linear and thus easily examined.

ANATOMY AND TECHNIQUE

Linear high-frequency transducers should be used since the ligaments, tendons, and nerves about the elbow are superficial and linear. Unlike the shoulder, which has a standard scanning protocol, the elbow is scanned by placing the transducer over the site of clinical concern. Nonetheless, for the purpose of the description of anatomy, the elbow can be divided into four quadrants: anterior, lateral, posterior, and medial.[3]

Anterior Quadrant

The anterior quadrant contains the biceps muscle and tendon, the radial and median nerves, and the anterior aspects of the radiocapitellar and humeroulnar joints. Scanning is performed with the elbow extended and supinated (Fig. 4.1). The transducer is placed transversely across the distal arm. The pulsating brachial artery is midline and is a major landmark. Lateral to the brachial artery is the distal biceps tendon, and medial to the brachial artery is the median nerve. The biceps aponeurosis (also called the lacertus fibrosus) is a fascial layer that extends from the flexor pronator muscle group to the biceps tendon (Figs. 4.2 and 4.3).

Tip:

You may have to rock the transducer cranially to make the tendons and nerves echogenic.

Figure 4.1. Scanning of the anterior quadrant. The transducer is placed transversely across the antecubital fossa.

As the transducer slides distally, the anterior aspects of the radiocapitellar and humeroulnar joints come into view. The curvilinear bony surfaces are covered by anechoic articular cartilage. The radial nerve is visible deep to the brachioradialis muscle at this level (Fig. 4.3). As the transducer moves distally, the deep branch of the radial nerve can be identified as it enters the supinator muscle between the superficial and deep muscle heads (Fig. 4.4). Rotating the transducer 90 degrees over either the radial or median nerves demonstrates the hypoechoic fibrillar appearance of the nerve in long axis (Fig. 4.5).

The radial nerve is the terminal branch of the posterior cord of the brachial plexus (C5-8, T1). In the arm it courses posterior to the humerus in the spiral groove, and pierces the intermuscular septum in the distal arm to lie anterior to the lateral condyle of the humerus. The radial nerve supplies the triceps, anconeus, brachioradialis, and the lateral half of the brachialis.

At the level of the elbow joint, the radial nerve divides into a superficial sensory branch, which courses in the forearm along the deep surface of the brachioradialis, and a deep motor branch, which enters the radial tunnel. The radial tunnel extends from the

level of the radiocapitellar joint to the proximal aspect of the supinator,[4] and is bounded by the joint capsule posteriorly, the
P. 50

brachialis muscle and biceps tendon medially, and the brachioradialis muscle and the extensor carpi radialis brevis and longus muscles laterally.[5]

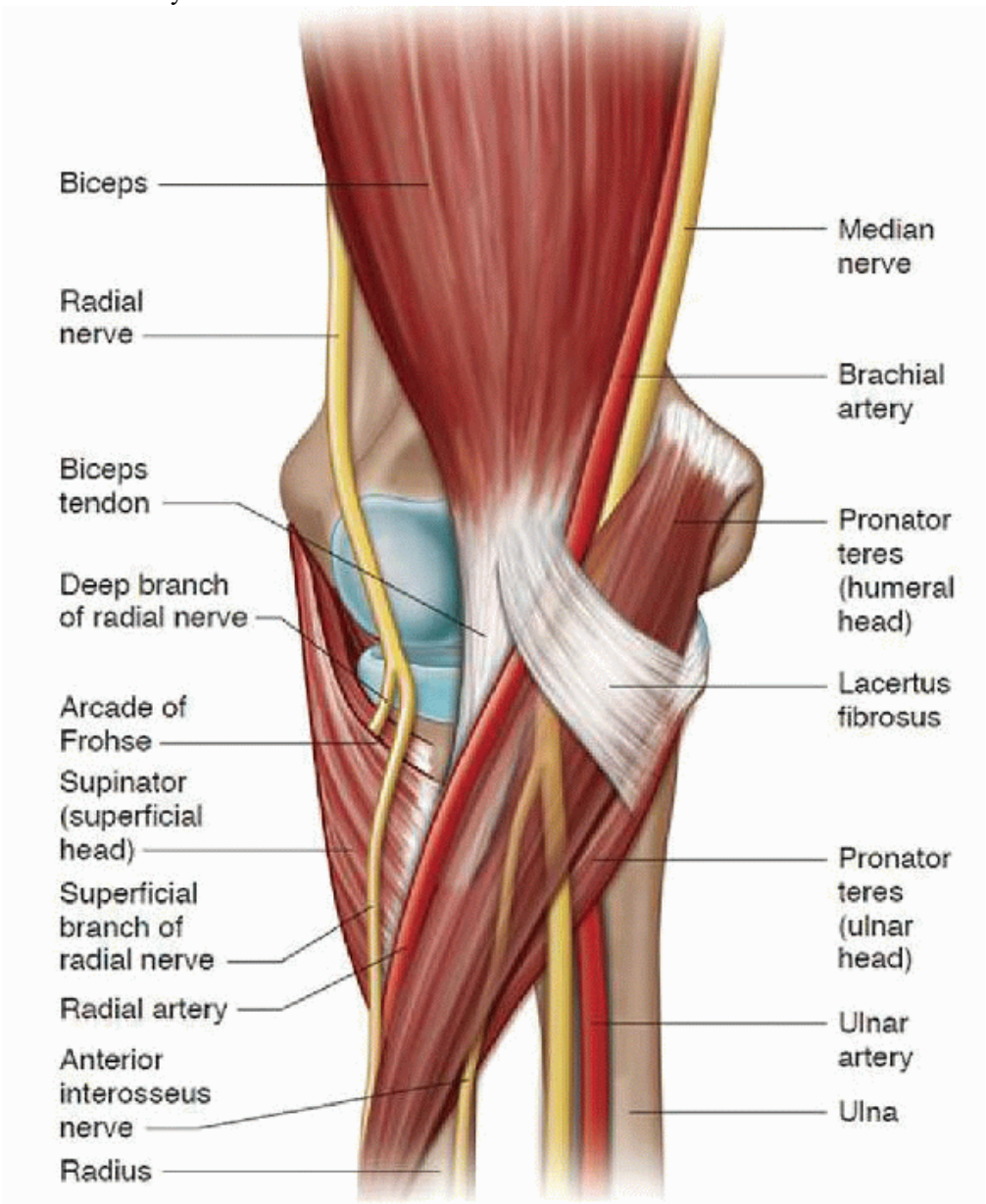

Figure 4.2. Anatomy of the anterior aspect of the elbow. In the distal arm, the biceps tendon is lateral to the brachial artery and the median nerve is medial to the brachial artery. The lacertus fibrosus (the biceps aponeurosis) extends from the common flexor mass to the distal biceps tendon. The median nerve and its anterior interosseous branch pass between the two heads of the pronator muscle. The deep branch of the radial nerve courses between the superficial and deep heads of the supinator muscle.
At the distal aspect of the radial tunnel, the deep branch pierces the supinator muscle anteriorly between the superficial and deep heads of the supinator (Figs. 4.2 and 4.5). The proximal edge of the superficial head of the supinator is called the Arcade of Frohse and is the most common site of radial nerve entrapment (Fig. 4.2). The deep branch of the radial nerve exits the posterior aspect of the supinator as the posterior interosseous nerve (PIN) and enters the posterior compartment of the forearm. At the elbow, the deep branch supplies the extensor carpi radialis brevis and the supinator. In the posterior compartment of the forearm, the deep branch, now called the PIN, supplies the extensor carpi ulnaris, the extensor digitorum communis, the extensor digiti minimi, the abductor pollicis longus, the extensor pollicis longus and brevis, and the extensor indicis proprius.[4]

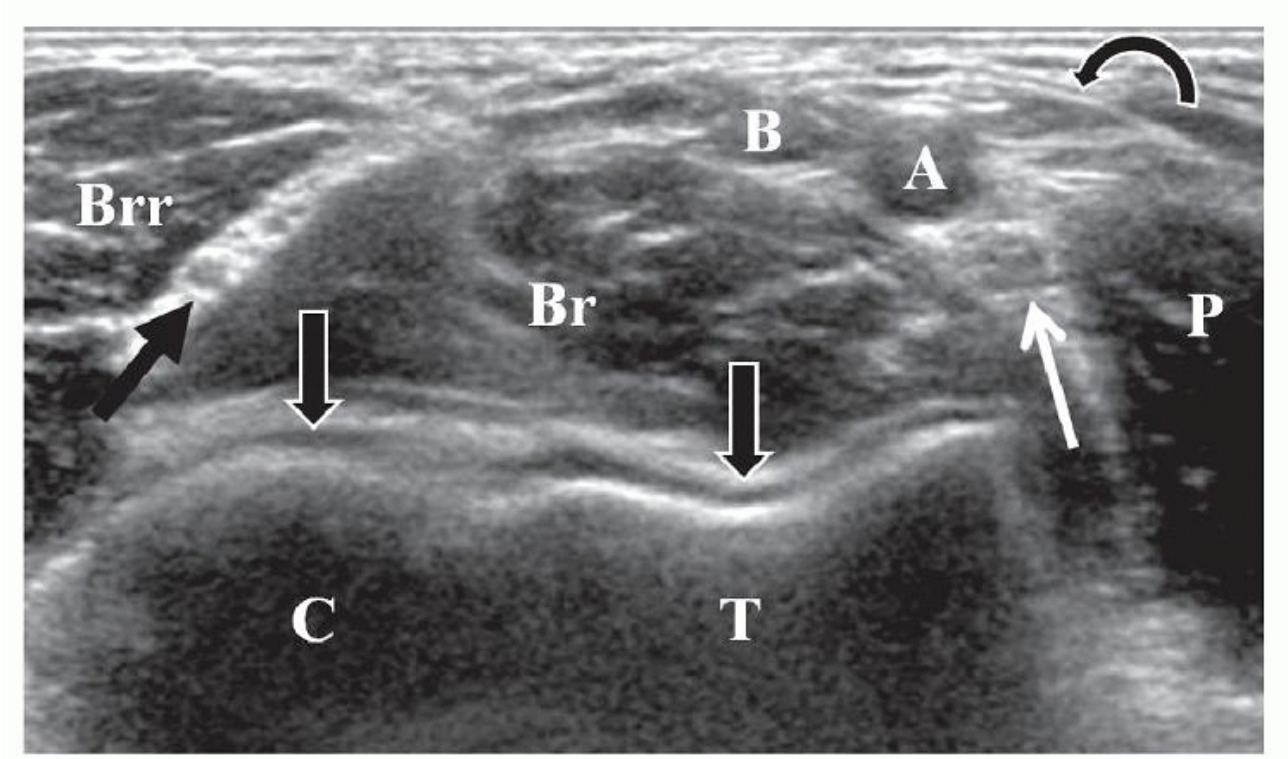

Figure 4.3. Transverse sonographic image of the antecubital fossa. The biceps tendon (B) is lateral to the brachial artery (A), and the median nerve (white arrow) is medial and deep to the brachial artery. The thin biceps aponeurosis (curved black arrow) extends from the pronator muscle (P) to the biceps tendon. The brachialis (Br) is a large muscle directly anterior to the humerus. Deep to the brachialis is the thin hypoechoic articular cartilage (straight block arrows) of the capitellum (C) and trochlea (T). The radial nerve (straight black arrow) lies between the brachialis and brachioradialis (Brr) muscles.

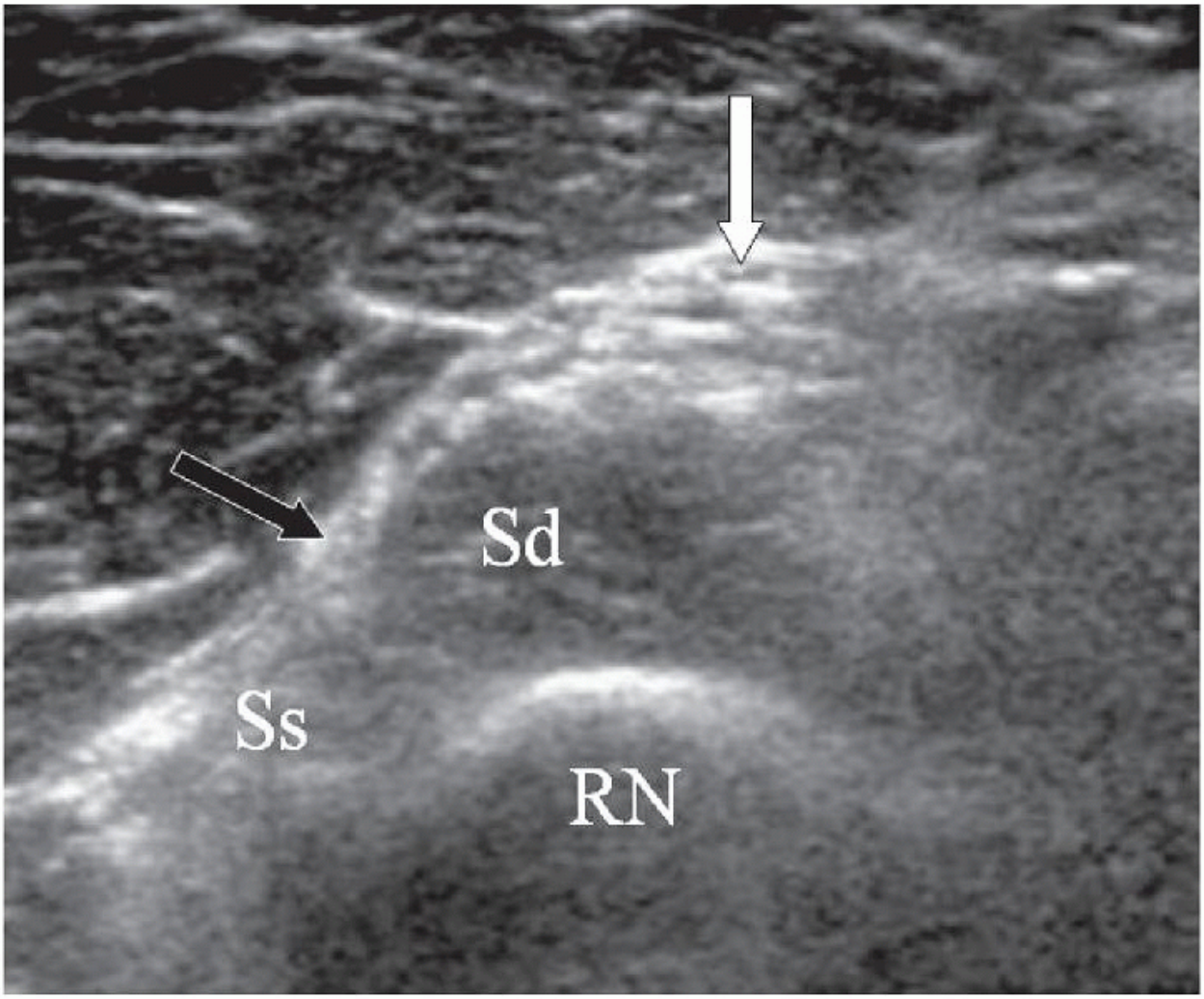

Figure 4.4. Short-axis image at the radial neck (RN) shows the superficial branch of the radial nerve (white arrow) and the deep branch (black arrow) in the proximal plane between the superficial (Ss) and deeps heads (Sd) of the supinator.
The median nerve arises from the medial and lateral cords of the brachial plexus (C6-8, T1) and courses
P. 51

alongside the brachial artery in the anterior compartment of the arm and at the elbow, passing through the antecubital fossa deep to the biceps aponeurosis (see below) and anterior to the brachialis muscle. The nerve lies between the humeral (superficial) and ulnar (deep) heads of the pronator teres muscle at the level of the elbow joint (Fig. 4.2), and enters the anterior compartment of the forearm by passing beneath the fibrous arch of the heads of the flexor digitorum superficialis (FDS)[6] (Fig. 4.6). At the elbow and proximal aspect of the forearm the median nerve supplies the pronator teres, flexor carpi radialis, palmaris longus, and FDS.[7] Within the forearm, the nerve courses between the FDS and FDP.

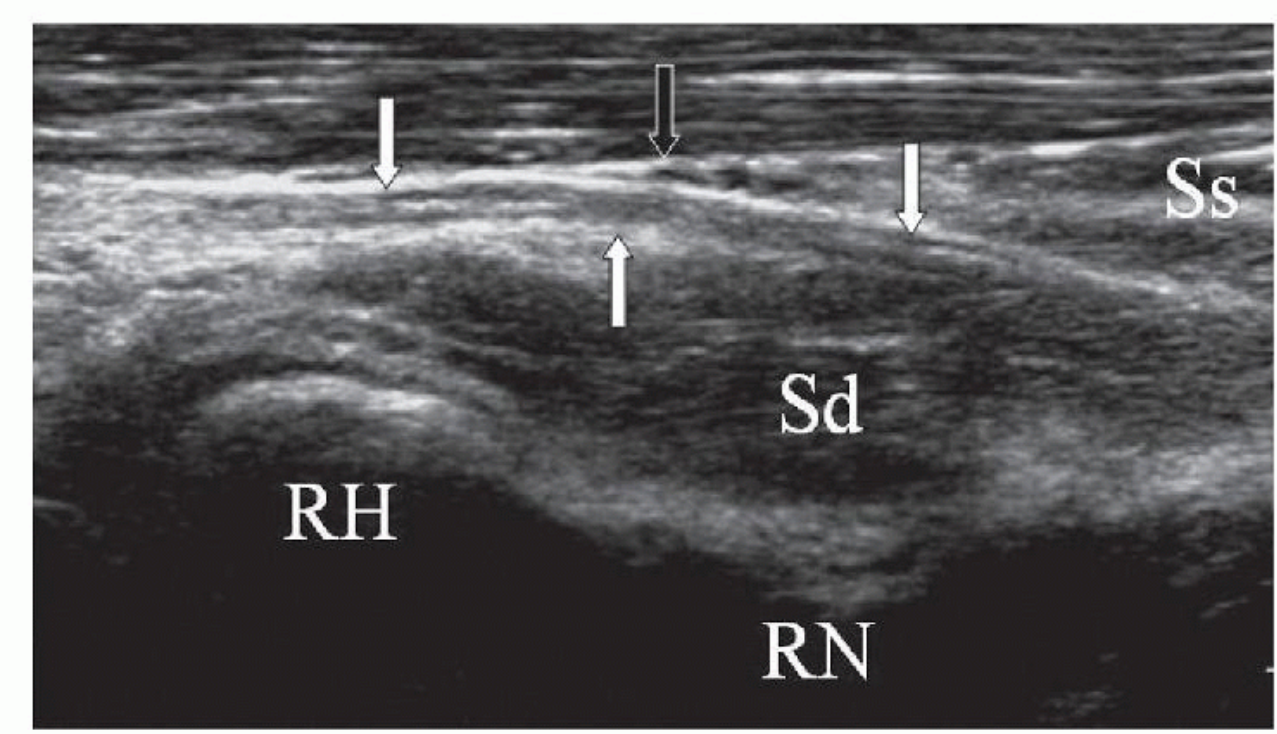

Figure 4.5. Long-axis image shows the echogenic fibrillar appearance of the deep branch of the radial nerve (white arrows) as it enters between the superficial (Ss) and deep (Sd) heads of the supinator. The proximal edge of the superficial head is the Arcade of Frohse (black arrow). RH, radial head; RN, radial neck.

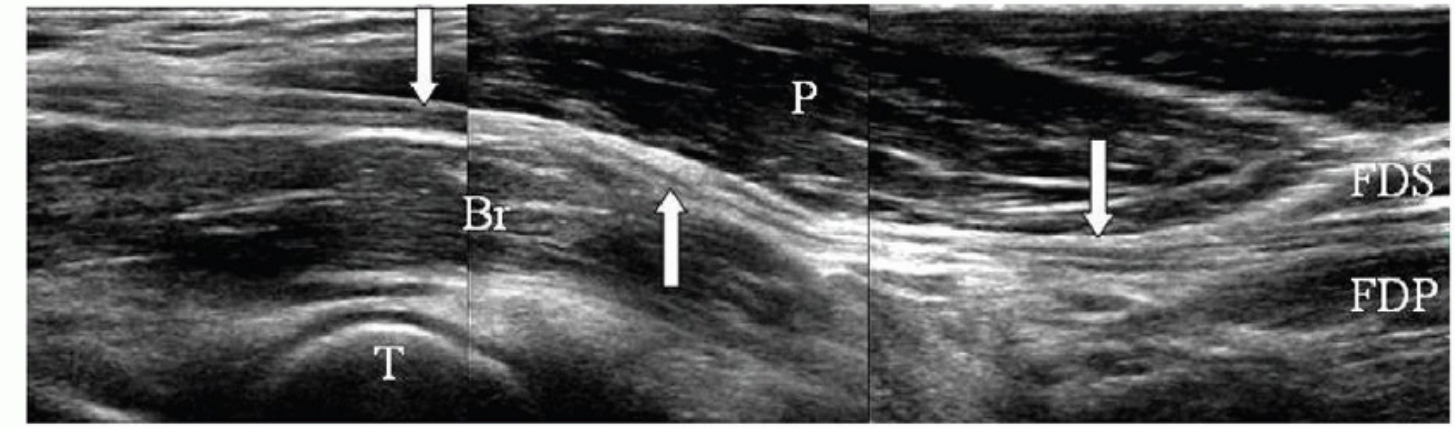

Figure 4.6. Composite long-axis image shows the median nerve (arrows) passing between the humeral head of the pronator teres (P) and the brachialis (Br) at the level of the elbow joint (T is the trochlea), and entering the forearm between the flexor digitorum superficialis (FDS) and flexor digitorum profundus (FDP). The ulnar head of the pronator teres is not visualized well in this image.

The anterior interosseous nerve (AIN) arises from the median nerve at the level of the humeral head of the pronator teres, and travels along the anterior aspect of the interosseous membrane of the forearm between the flexor pollicis longus and the flexor digitorum profundus (Fig. 4.7). The AIN is purely motor and supplies the pronator quadratus muscle, the flexor pollicis longus muscle, and the FDP muscle for the index and the middle fingers.[4,8]

Longitudinal scanning over the radiocapitellar joint shows the joint space and the thin stripe of anechoic articular cartilage of the capitellum (Fig. 4.8). Sliding the transducer medially demonstrates the coronoid fossa of the distal humerus. This is a good place to look for joint fluid and intra-articular loose bodies.

The distal biceps tendon can be challenging to image because it dives deep in the antecubital fossa to insert on the radial tuberosity and because it does not have a straight sagittal orientation. There are several techniques for scanning the distal biceps:

- Anterior approach[3,9]—With the arm extended and maximally supinated, find the tendon in short axis in the distal arm, just proximal to the elbow crease, and then rotate the transducer 90 degrees (Fig. 4.9). Alternatively, place the transducer longitudinally on the antecubital fossa, find the brachial artery, and then slide the transducer just lateral to the artery (Fig. 4.10).

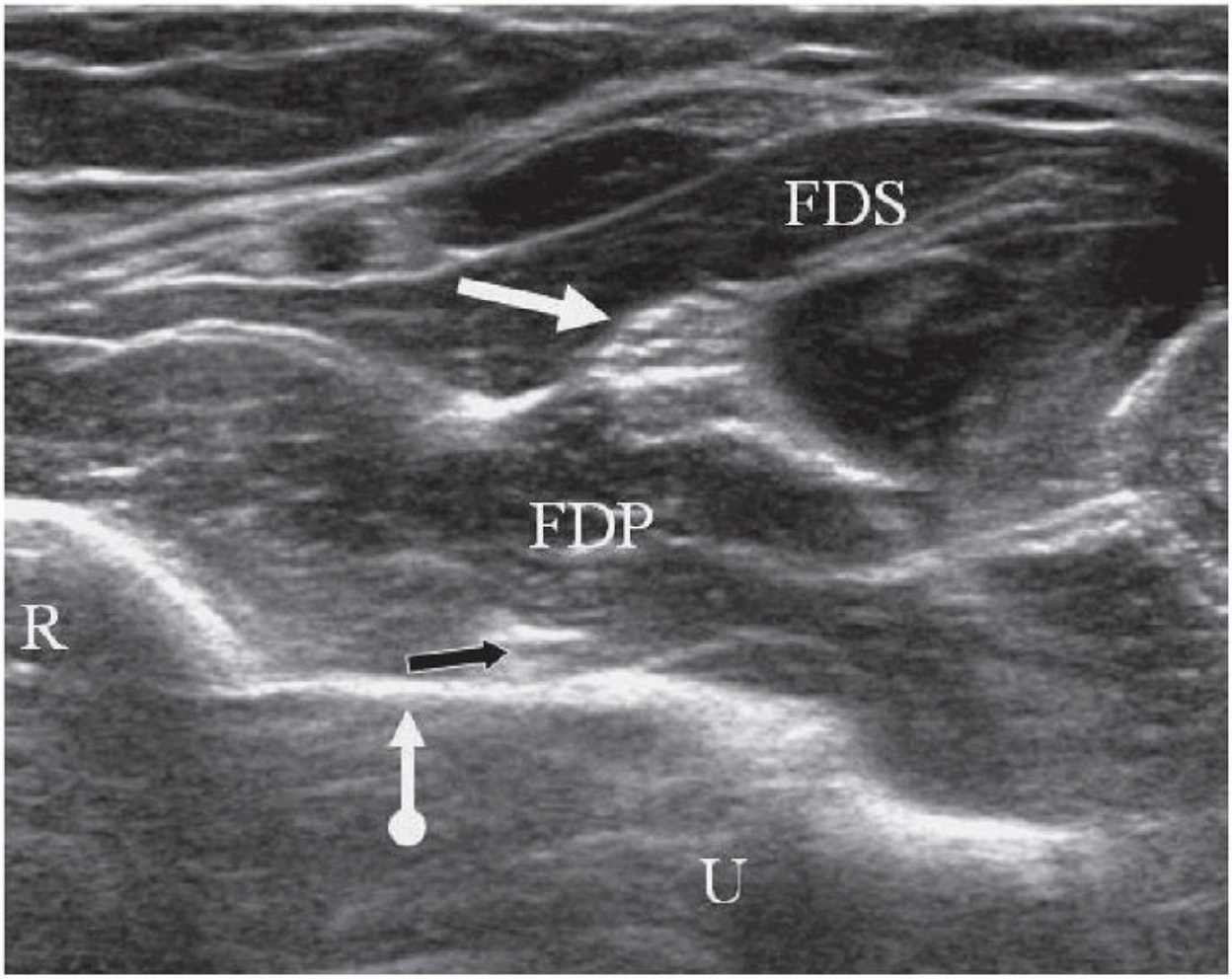

Figure 4.7. Transverse image of the proximal forearm shows the hypoechoic anterior interosseous nerve (black arrow) along the anterior surface of the echogenic interosseous membrane (round tail white arrow). The median nerve (straight white arrow) lies between the flexor digitorum superficialis (FDS) muscle and the flexor digitorum profundus (FDP) muscle. R, radius; U, ulna.

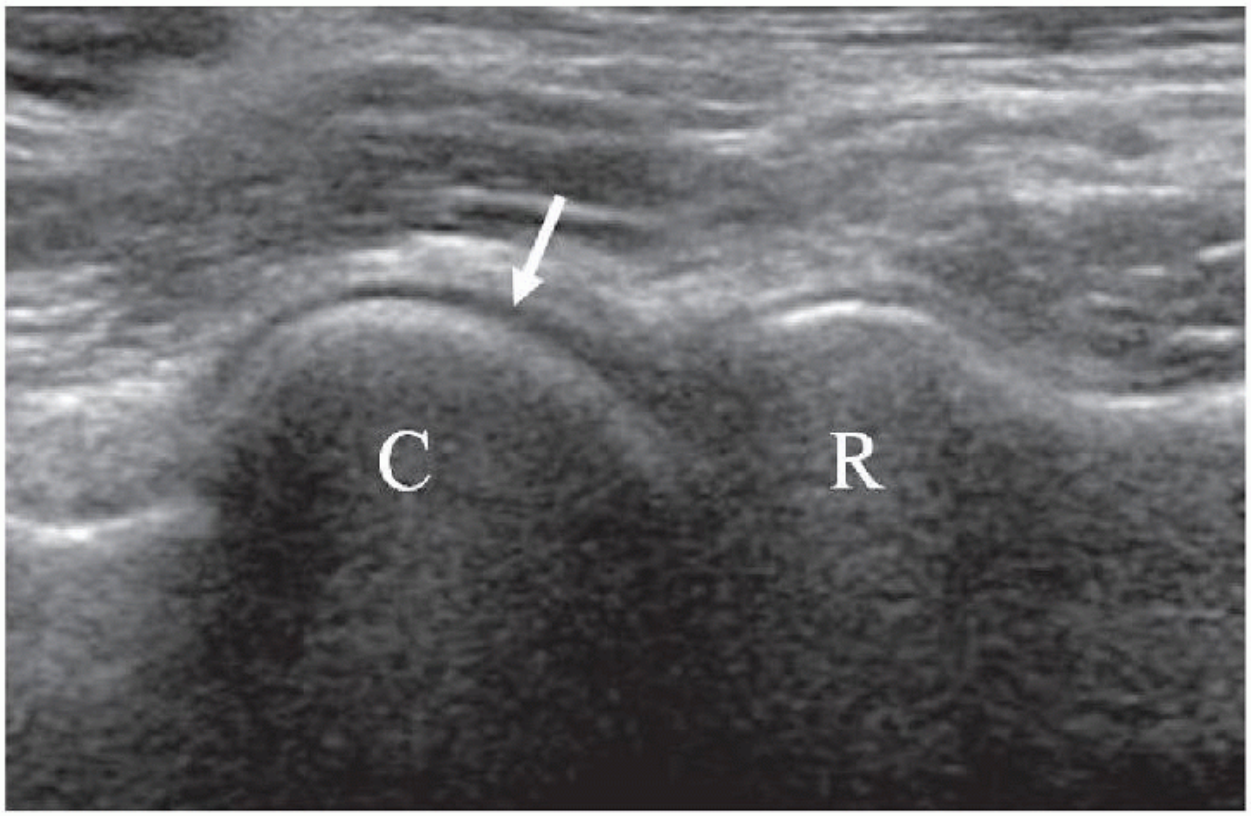

Figure 4.8. Long-axis image shows the capitellum (C), thin hypoechoic cartilage (arrow), and the radial head (R).
P. 52

Figure 4.9. Anterior approach to the biceps tendon. The transducer is long axis and pressed into the interosseous space. The forearm is maximally supinated.

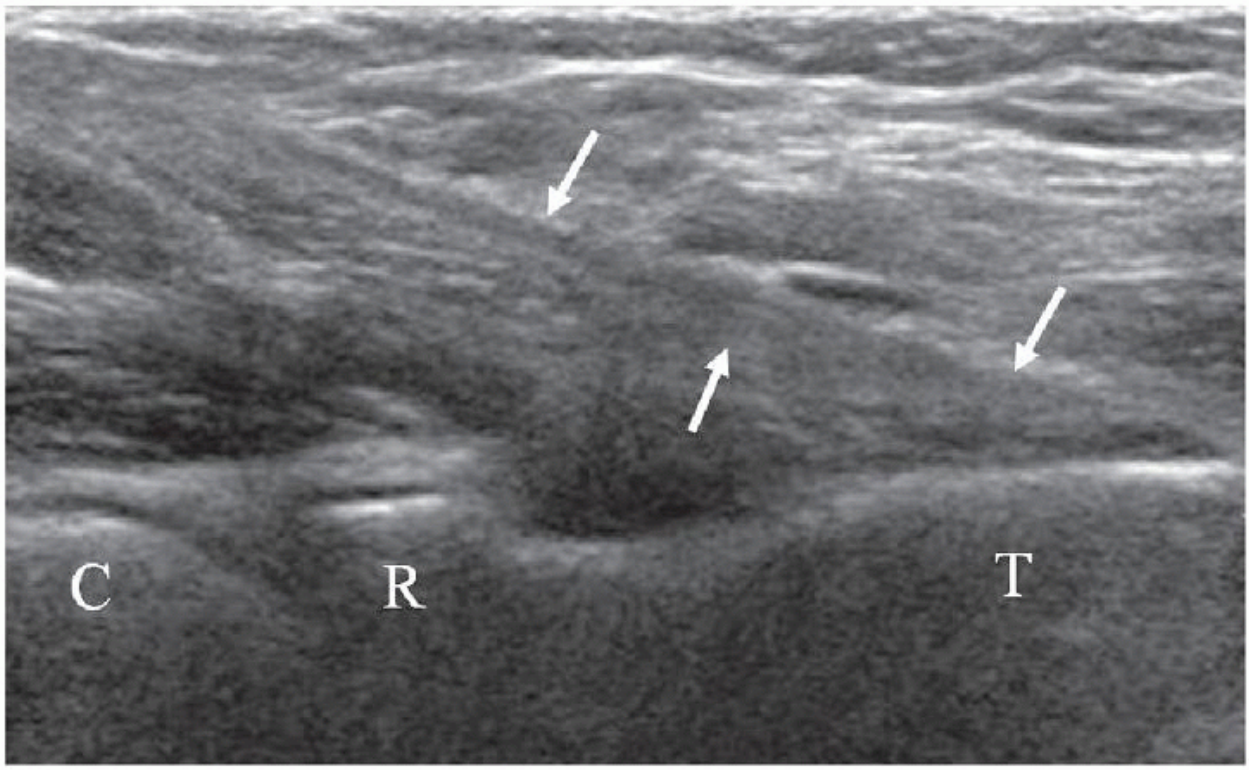

Figure 4.10. Anterior approach to the distal biceps tendon (arrows) is straight and inserts on the radial tuberosity (T). The tendon has a hypoechoic appearance because it is coursing away from the transducer. C, capitellum; R, radial head.

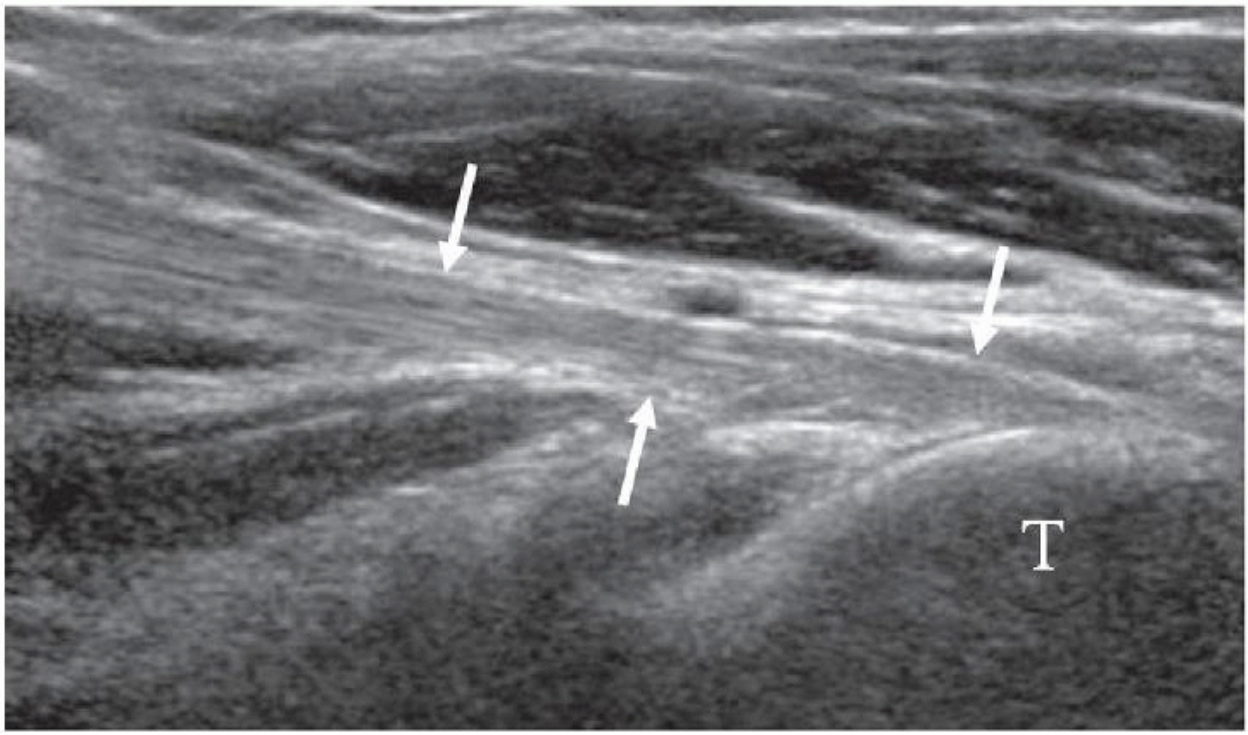

Figure 4.11. Anterior approach by pressing the distal aspect of the transducer into the forearm, the biceps tendon and transducer become more parallel, and the tendon (arrows) demonstrates a more echogenic fibrillar appearance. Radial tuberosity (T).

Figure 4.12. Lateral approach to the biceps tendon. The elbow is bent 90 degrees, the forearm is supinated, and the transducer is placed obliquely along the course of the biceps tendon.

- Lateral approach[10]—With the elbow bent 90 degrees and the forearm supinated, place the transducer longitudinally over the lateral aspect of the forearm, using the brachioradialis muscle as an acoustic window (Figs. 4.12 and 4.13).

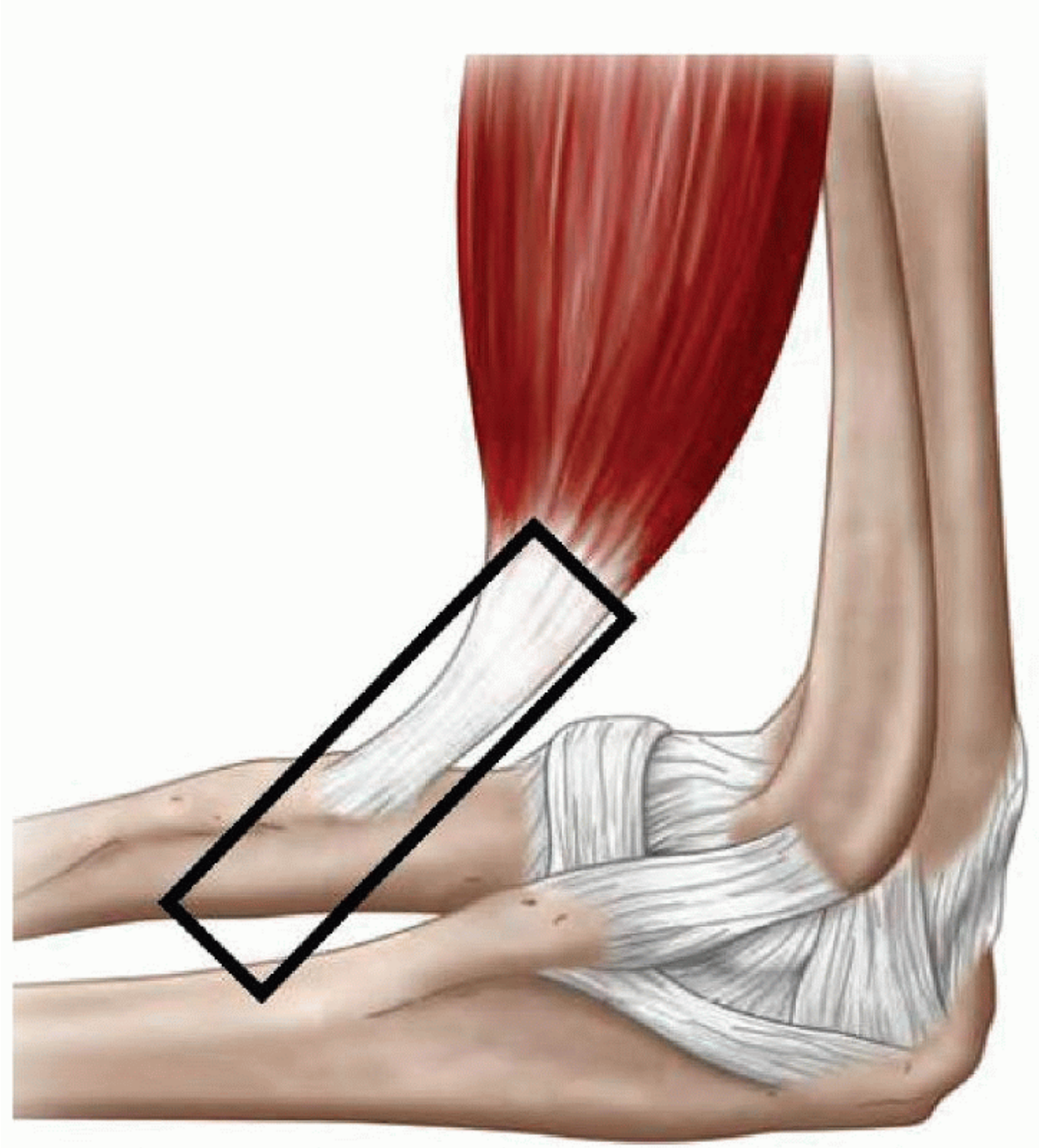

Figure 4.13. Diagram shows the course of the distal biceps tendon with the elbow bent 90 degrees. The transducer (black rectangle) is placed in the same plane as the tendon. This principle underlies both the lateral and medial approaches, and accounts for the long-axis appearance of the tendon and the short-axis appearance of the radius.
P. 53

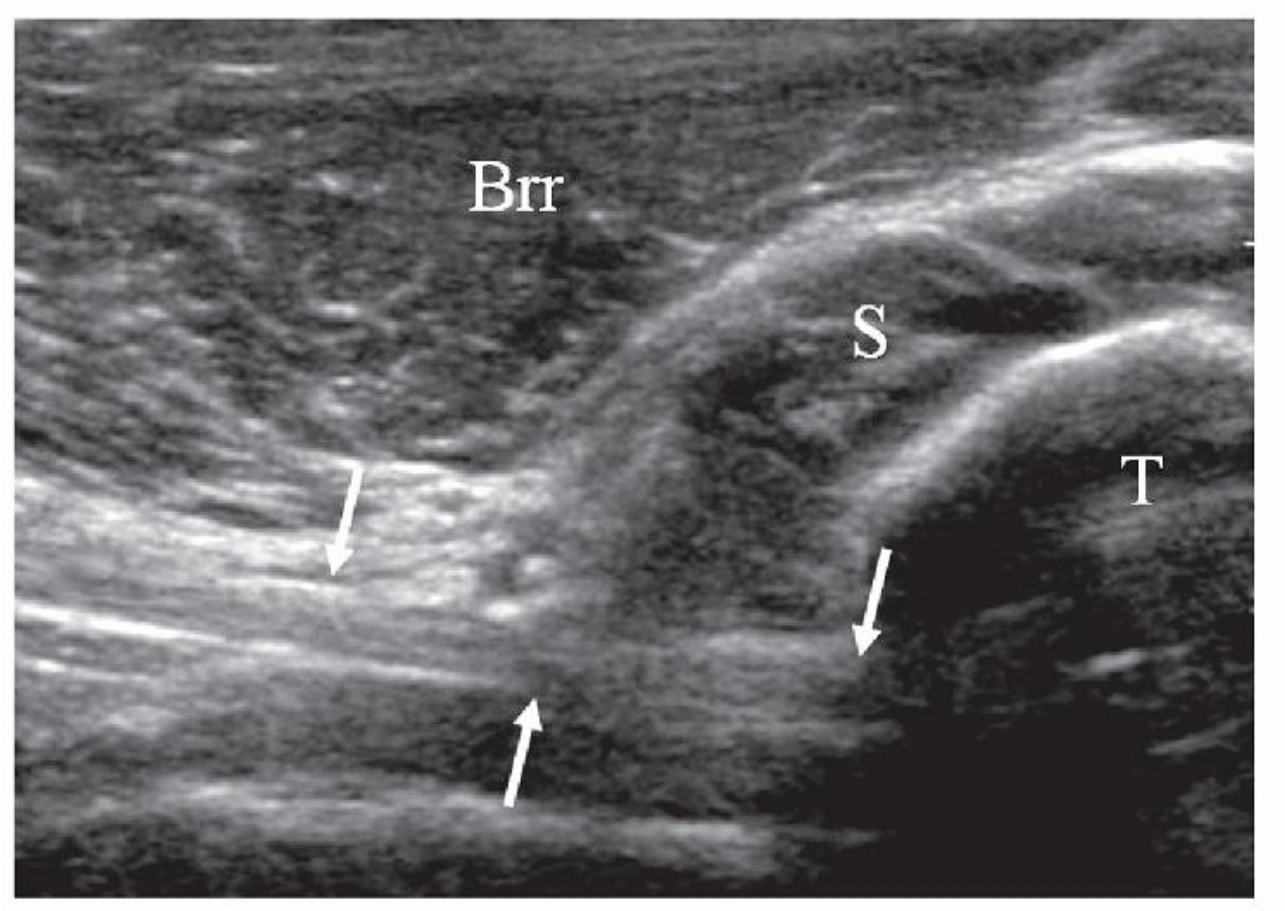

Figure 4.14. Lateral approach to the biceps tendon is seen in long axis (arrows), while the radial tuberosity (T) is seen in short axis. Brr, brachioradialis; S, supinator.

- Medial approach[11]—With the elbow bent 90 degrees and the forearm supinated, place the transducer longitudinally over the distal aspect of the arm from the medial side (Fig. 4.15). Slide the transducer anteriorly until the tendon is identified, and then slide distally, using the flexor-pronator mass as an acoustic window. The radius will be seen in short axis in this method, similar to the lateral approach (Fig. 4.16).
- Posterior approach[12]—With the elbow maximally flexed and the forearm pointing toward the ceiling, place the transducer transversely against the dorsal aspect of the proximal forearm at the level of the radial tuberosity (Fig. 4.17). As the patient supinates and pronates the forearm, the distal aspect of the biceps tendon is identified (Fig. 4.18).

Tip:
To optimally visualize the distal biceps tendon, “heel-toe” the transducer by pressing the distal aspect of the transducer footprint into the forearm and rotate the transducer toward the radius using the radial head, neck, and tuberosity as bony landmarks (Fig. 4.11).
Tip:
The radial tuberosity is visualized in short axis in this position (Fig. 4.14).

Figure 4.15. Medial approach to the biceps tendon. The elbow is bent 90 degrees and the transducer is placed parallel to the arm.

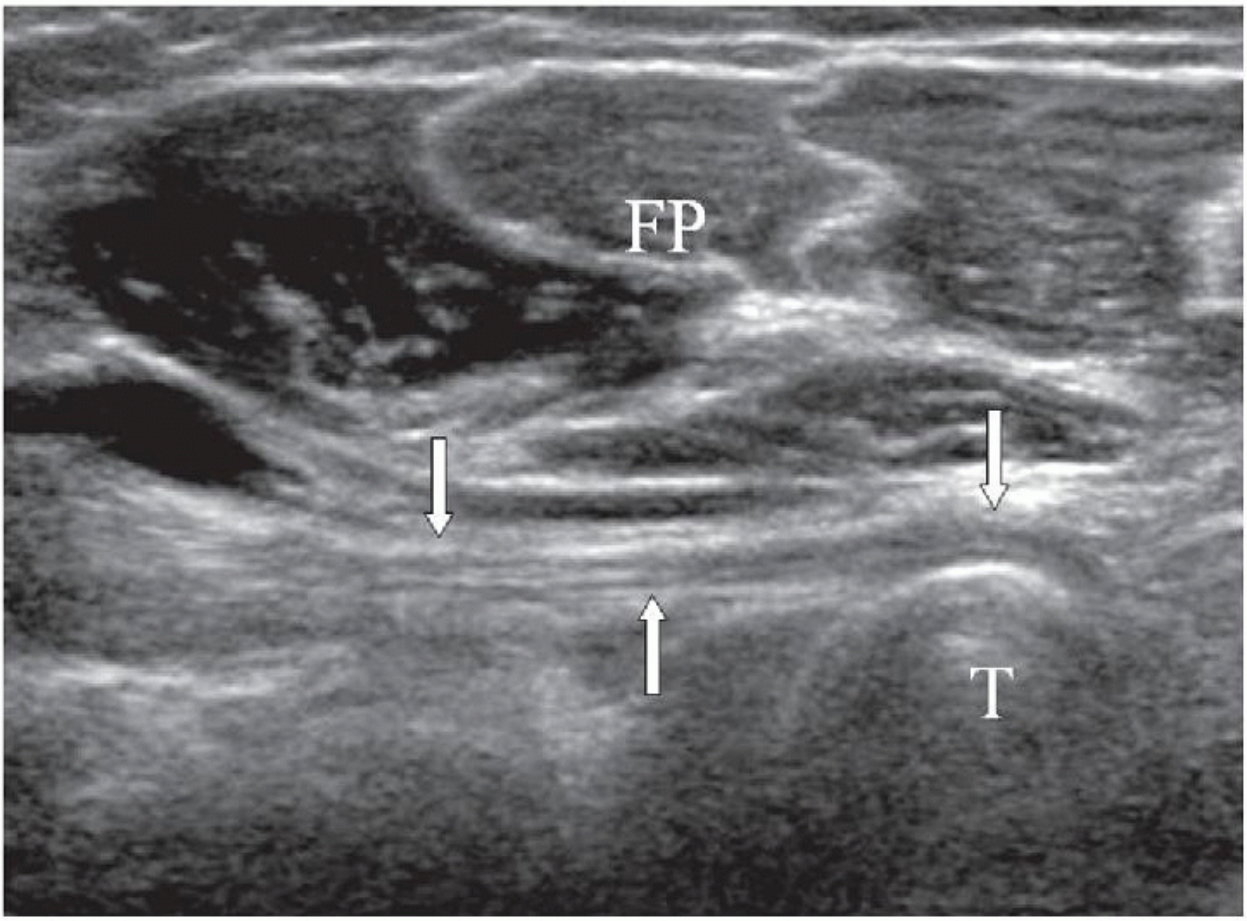

Figure 4.16. Medial approach to the biceps tendon is seen in long axis (arrows), while the radial tuberosity (T) is seen in short axis. Flexor pronator mass (FP).

In long-axis the biceps tendon is of uniform caliber and has the typical echogenic, fibrillar appearance of a tendon. It appears round and well-defined in short-axis scans. Long head and short head components of the distal biceps tendon have been described, with the long tendon being deeper and inserting on the more proximal aspect of the radial tuberosity and the short tendon being more superficial and inserting more distally,[13] but these two components are usually difficult to separate. The bicipitoradial bursa sits saddle-shaped around the

P. 54

distal biceps tendon to protect it from osseous friction during pronation of the forearm.[14] It is not normally distended.

Figure 4.17. Posterior approach to the biceps tendon. The transducer is placed transversely along the dorsal aspect of the forearm with the forearm maximally pronated to bring the biceps tendon insertion into view.

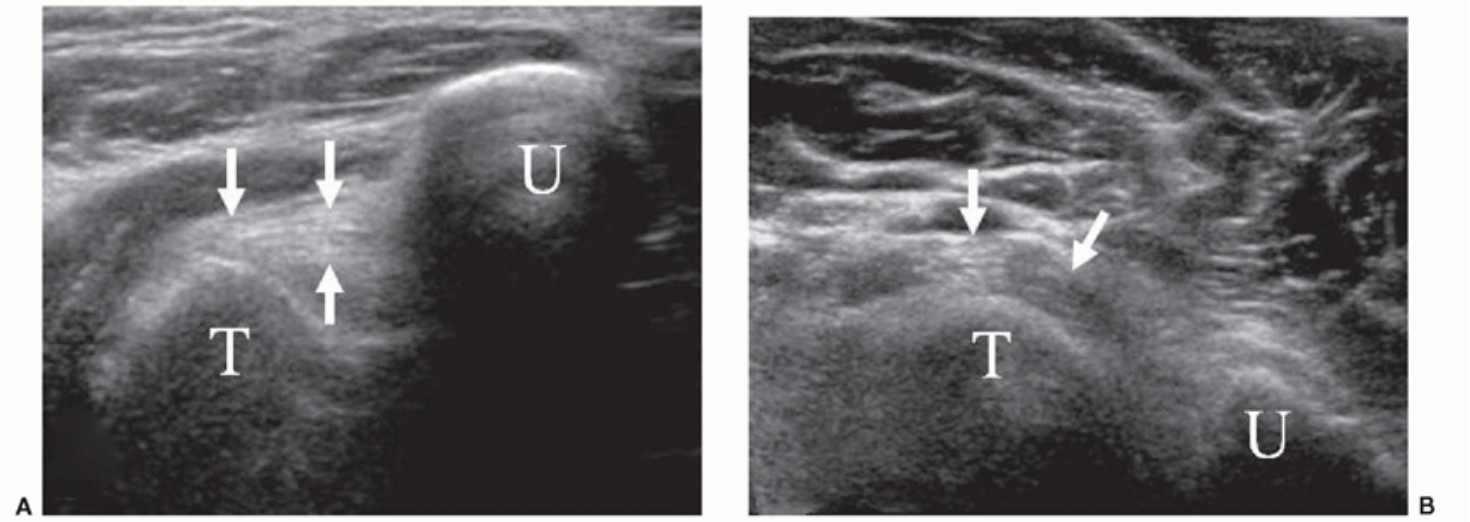

Figure 4.18. Short-axis biceps tendon insertion. A: Using the short-axis posterior approach, the distal biceps tendon (arrows) is well seen between the radial tuberosity (T) and the ulna (U). B: Using the short-axis conventional anterior approach, the distal biceps

tendon (arrows) is not as well seen attaching to the radial tuberosity (T) due to anisotropy. Ulna (U).

Lateral Quadrant

The lateral quadrant contains the lateral aspect of the radiocapitellar joint, the common extensor tendon, and the lateral collateral ligament complex that consists of the radial collateral ligament, lateral ulnar collateral ligament, and the annular ligament.[15],[16],[17] With the patient's elbow flexed 80 to 90 degrees and the forearm on the examination table, the transducer is placed longitudinally on the lateral elbow at the level of the radiocapitellar joint using the bony landmarks of the radial head and lateral epicondyle (Fig. 4.19). The common extensor tendon originates from the lateral epicondyle of the humerus and is comprised of the extensor carpi radialis brevis, extensor carpi ulnaris, extensor digitorum communis, and extensor digiti minimi (Fig. 4.20). The common tendon has a long thin echogenic fibrillar appearance (Fig. 4.21).

Figure 4.19. Scanning the lateral quadrant. The elbow is flexed, the thumb is up, and the transducer is placed long axis over the radial head.

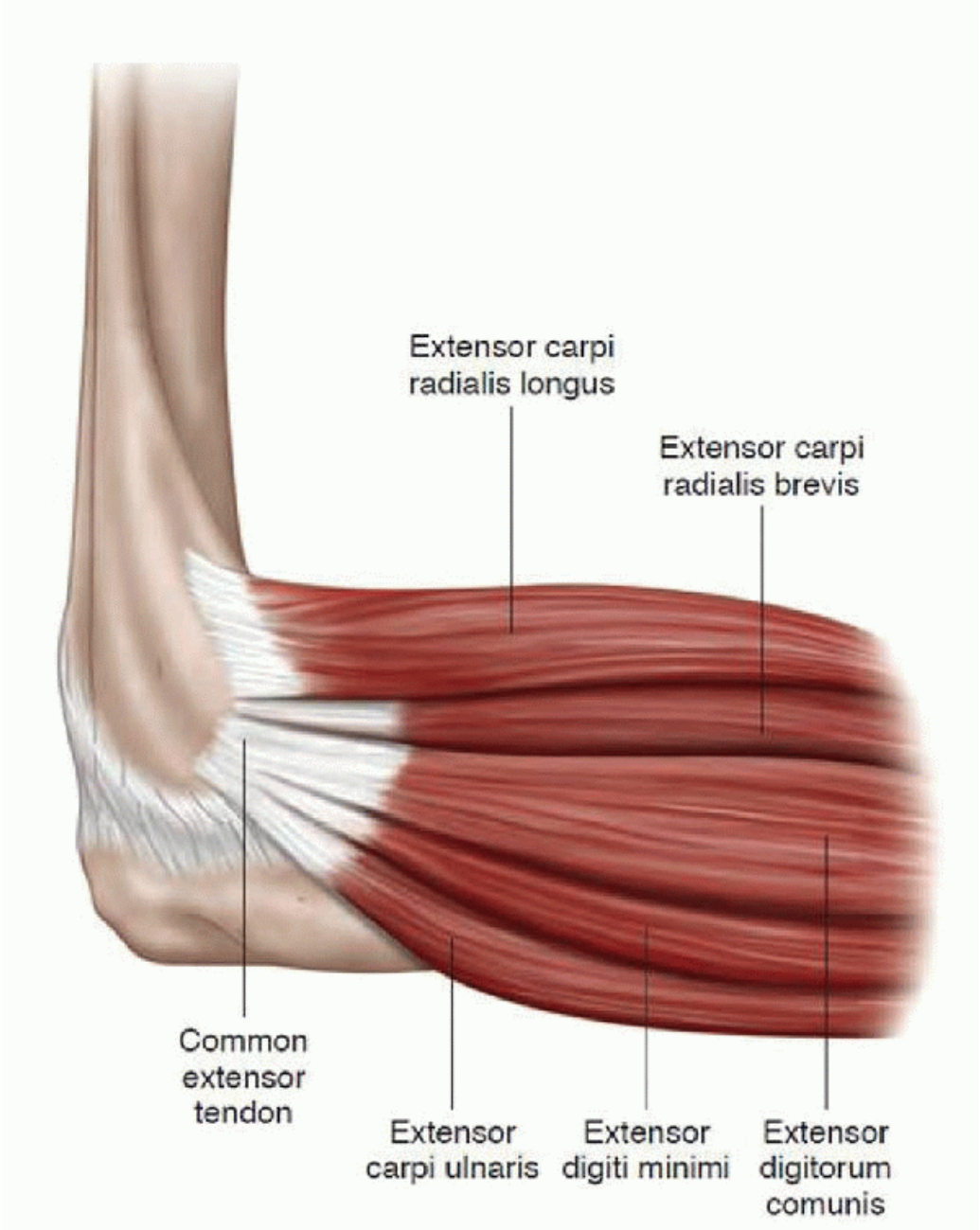

Figure 4.20. Diagram of the common extensor tendon. The extensor carpi radialis brevis component is the deep portion of the tendon and is the most commonly involved component in lateral epicondylitis. The extensor carpi radialis longus inserts more proximally, on the supracondylar ridge, and is not part of the common extensor tendon.
P. 55

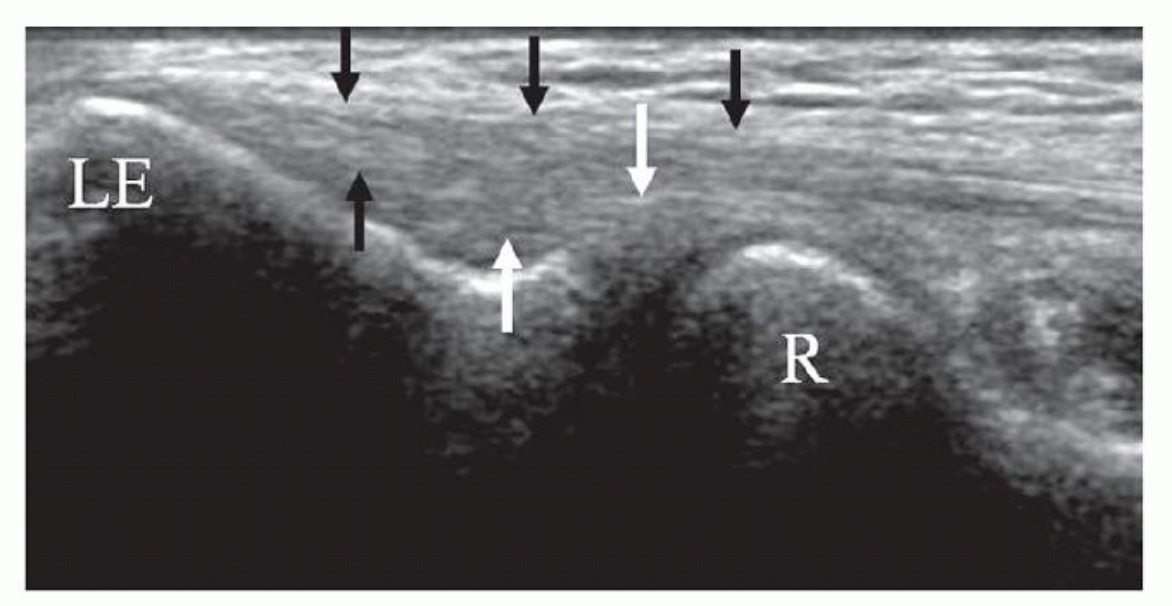

Figure 4.21. Long-axis image of the lateral quadrant shows the thin long common extensor tendon (black arrows) inserting on the lateral epicondyle (LE). The echogenic fibrillar radial collateral ligament (white arrows) extends from the radial head (R) to the LE, and is often difficult to distinguish from the overlying common extensor tendon.

The radial collateral ligament complex is composed of the radial collateral ligament, the lateral ulnar collateral ligament, and the annular ligament[15,16,17] (Fig. 4.22). The radial collateral ligament lies deep to the common extensor tendon, extending from the undersurface of the lateral epicondyle to blend with the fibers of the annular ligament. It is often difficult to distinguish the radial collateral ligament as a distinct structure from the overlying common extensor tendon (Fig. 4.21).

Short axis scanning over the radial head demonstrates the thin annular ligament. Oblique scanning is necessary to visualize the lateral ulnar collateral ligament, which extends from the undersurface of the lateral epicondyle, passes posterior to the radial head and neck, thus acting as a supporting sling, and inserts on the supinator crest of the ulna.[15,16]

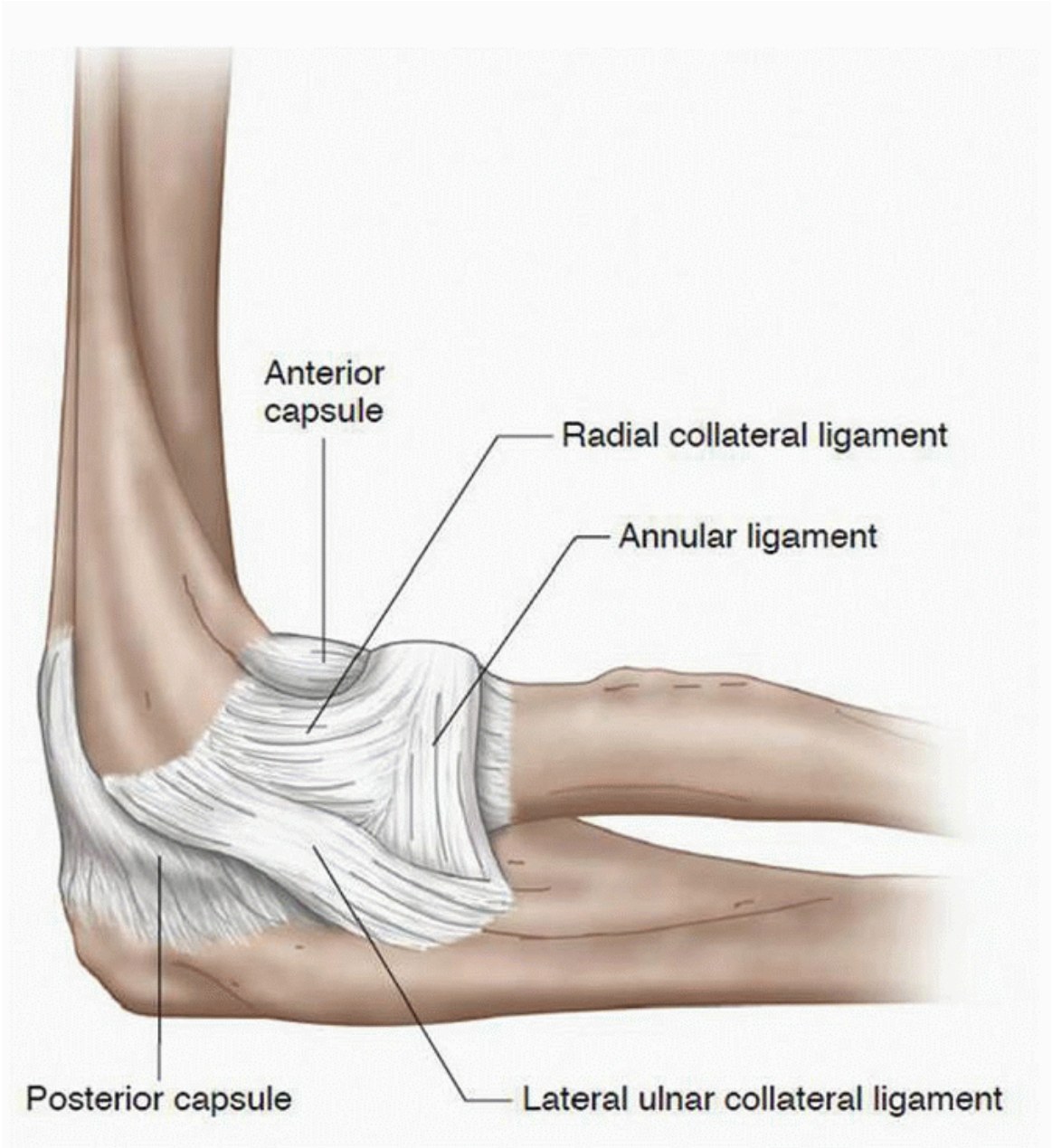

Figure 4.22. Diagram of the radial collateral ligament complex. The radial collateral ligament blends with the annular ligament. The lateral ulnar collateral ligament passes from the posterior aspect of the lateral condyle to the supinator crest of ulna, and supports the posterior aspect of the radial head.

Posterior Quadrant

The posterior quadrant contains the triceps tendon, olecranon fossa, and ulnar nerve, and it can be scanned in several ways:

- The “crawling crab” position, in which the patient’s hand is placed on the examination table with the elbow up and rotated toward the examiner (Fig. 4.23). The disadvantage of this position is that it is static.
- The elbow is flexed 90 degrees with the forearm resting on the examination couch in front of the patient (Fig. 4.24). This position is good for the triceps but is difficult for the ulnar nerve since the medial aspect of the elbow is lying against the table.
- The patient’s arm is elevated by the examiner who holds the patient’s forearm with one hand and places the transducer against the posterior aspect of the elbow with the other hand. The patient’s elbow rests against the palm of the examiner (Fig. 4.25). The advantage of this technique is that it allows dynamic scanning as the examiner flexes and extends the elbow by moving the patient’s forearm. This is particularly helpful for the evaluation of a clinically suspected

P. 56

snapping ulnar nerve. The disadvantage is that it requires a steady and experienced hand since both the patient’s elbow and the examiner’s hand are freefloating in the air.

Figure 4.23. Crawling crab position. The posterior quadrant is well accessible but the elbow is static.

Figure 4.24. The elbow is flexed 90 degrees with the forearm resting on the examination table. The ulnar nerve is difficult to assess in this position.

Figure 4.25. Posterior approach for dynamic scanning. This technique is good for assessment of a snapping ulnar nerve or triceps muscle.

The triceps tendon is a short broad structure with an echogenic fibrillar appearance composed of contributions of the long and lateral heads,[18] and inserts on the superficial aspect of the olecranon process The medial head of the triceps muscle has a separate insertion on the olecranon process, deep to the tendon (Fig. 4.26). With the elbow flexed, the olecranon fossa of the humerus is exposed and can be viewed both in short and long axis (Fig. 4.27).

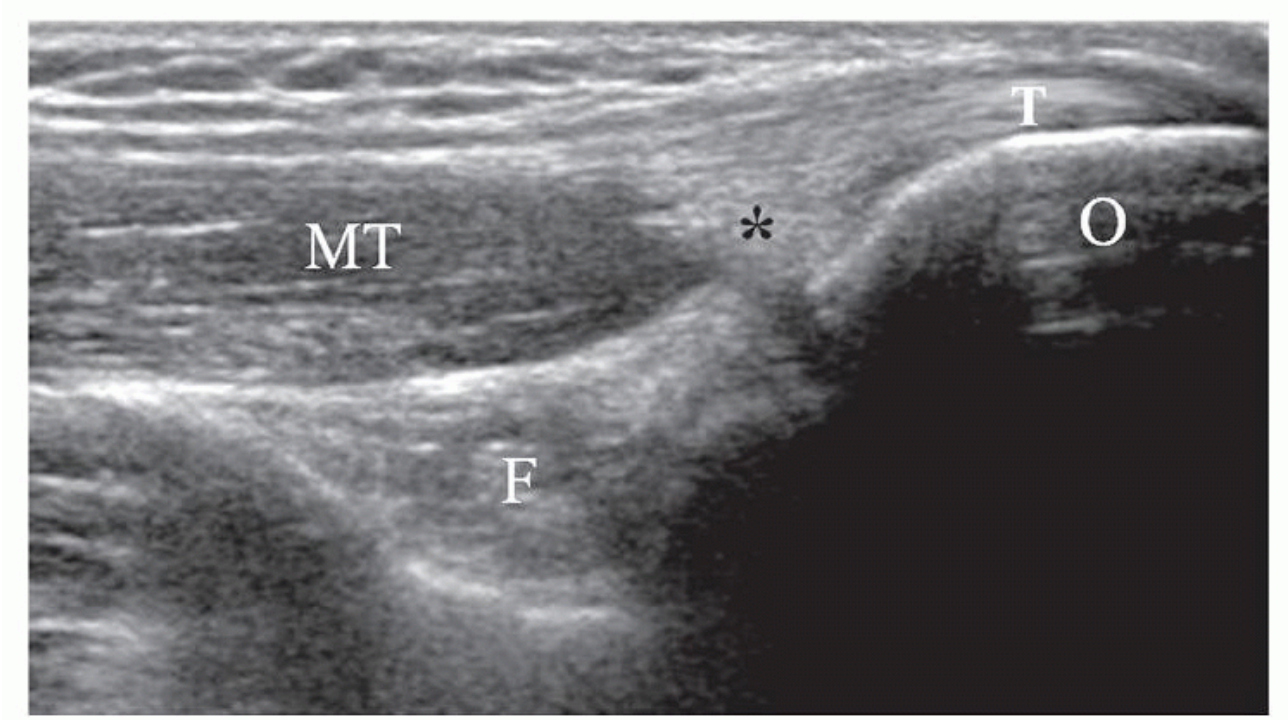

Figure 4.26. Long-axis view of the posterior quadrant. The triceps tendon (T) inserts on the olecranon process (O). The medial head of the triceps (MT) has a separate, short insertion (asterisk) deep to the tendon. By flexing the elbow, the olecranon moves distally, exposing the fossa (F).

Tip:

The olecranon fossa is a good place to look for synovitis, joint effusion, and loose bodies, and is a good target for elbow aspiration. In short axis, slide the transducer medially, posterior to the medial epicondyle to visualize the ulnar nerve. The ulnar nerve arises from the medial cord of the brachial plexus (C8, T1) and courses along the medial side of the brachial artery in the anterior compartment of the proximal arm. It then passes posterior to the medial epicondyle of the humerus in the cubital tunnel, a fibro-osseous channel formed by the olecranon process

P. 57

laterally, the posterior cortex of the medial epicondyle medially, the elbow joint capsule and posterior bundle of the medial collateral ligament (MCL) anteriorly, and the Ligament of Osborne (the cubital retinaculum) posteriorly (Fig. 4.28). The nerve exits the cubital tunnel to enter the medial aspect of the forearm between the superficial and deep heads of the flexor carpi ulnaris muscle. At the elbow, the ulnar nerve supplies the flexor carpi ulnaris and the medial half of the FDP.

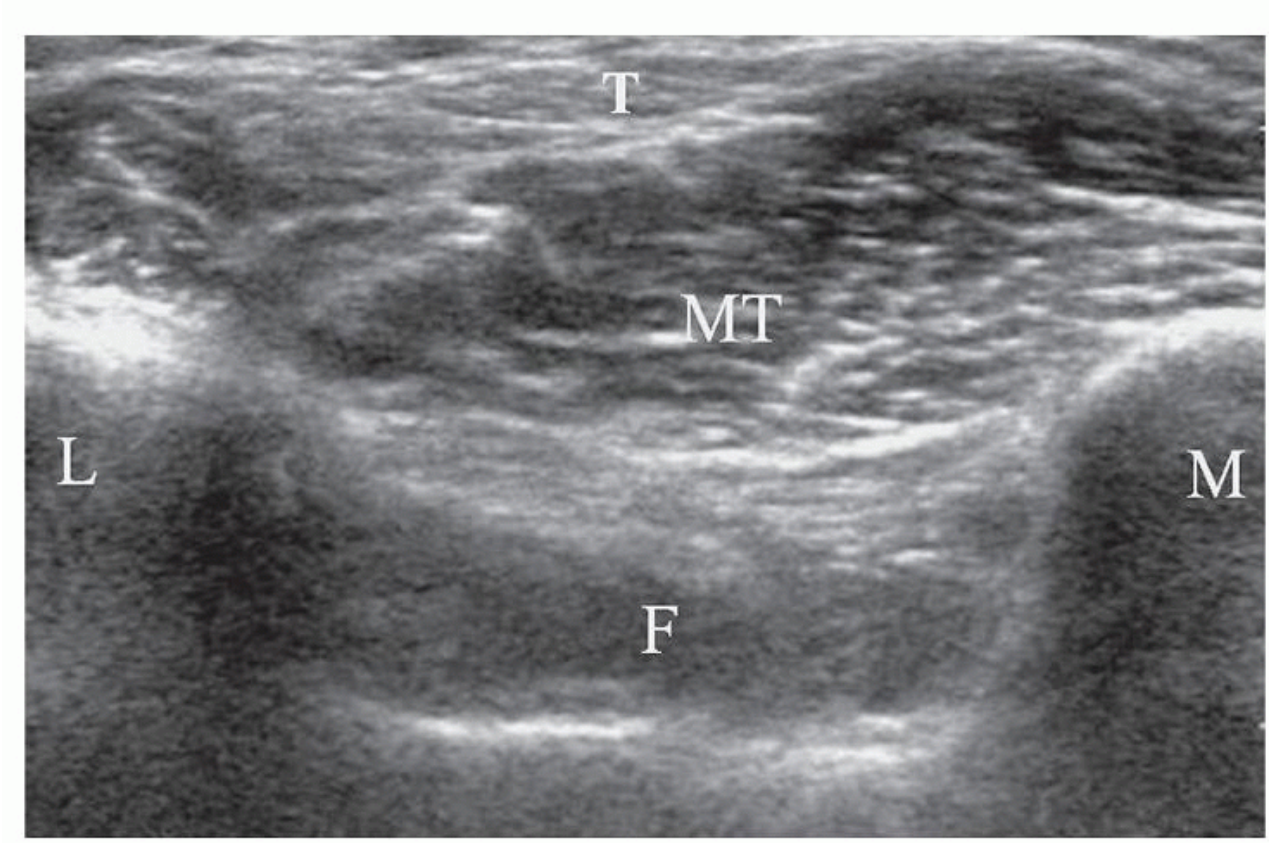

Figure 4.27. Short axis of the posterior quadrant shows the olecranon fossa (F) between the medial (M) and lateral (L) condyles of the humerus. The medial head of the triceps (MT) and the triceps tendon (T) overlie the fossa.
In the cubital tunnel, the ulnar nerve appears round and hypoechoic, surrounded by echogenic fat in transverse scans, and narrow, linear, and hypoechoic in longitudinal scans. Nerve stability is assessed while scanning transversely during flexion and extension of the elbow.

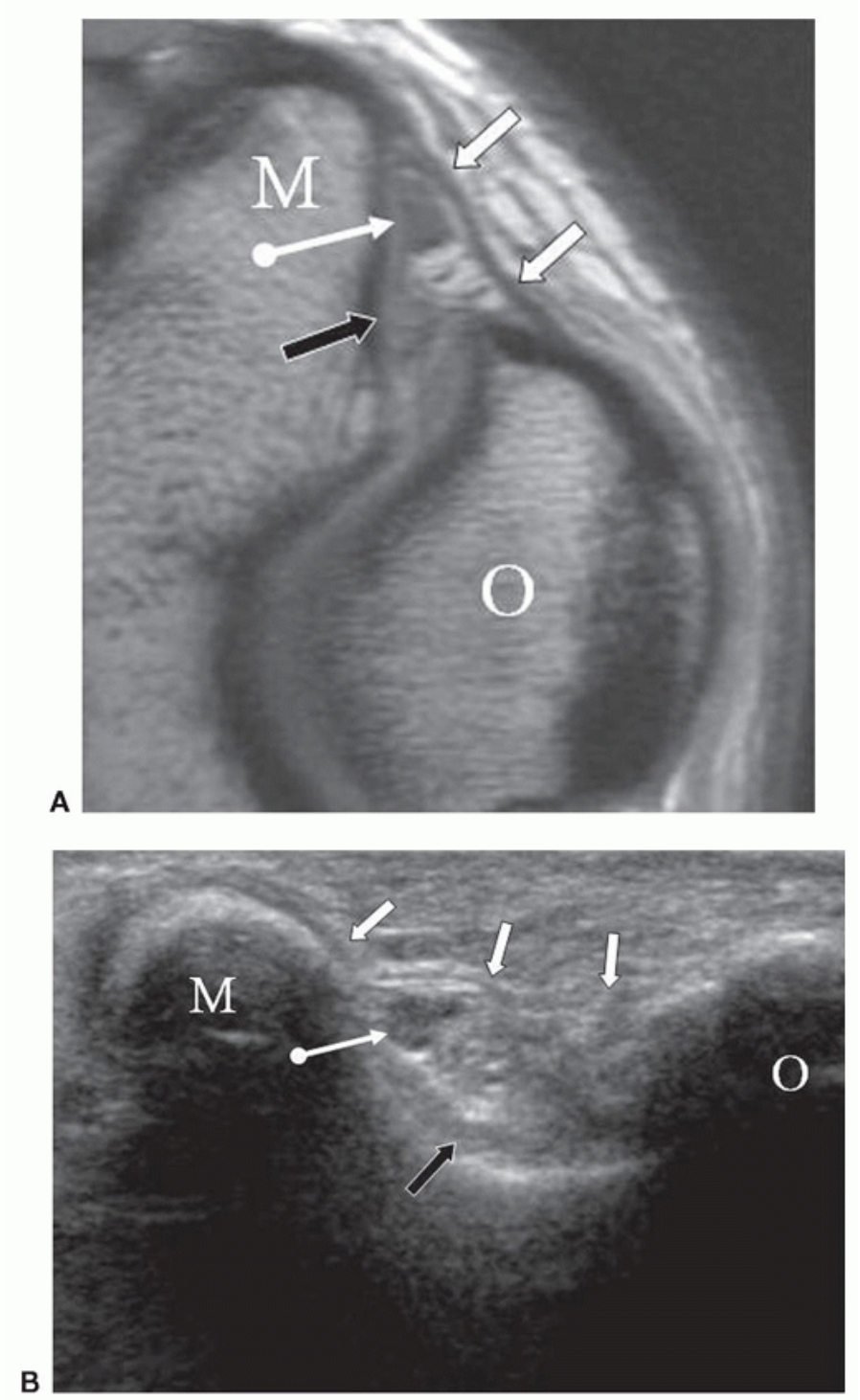

Figure 4.28. Cubital tunnel and ulnar nerve. Axial proton density MR image (A), oriented to match the sonographic image (B). The ulnar nerve (round tail arrow) is bounded by the posterior bundle of the medial collateral ligament (black arrow), the medial condyle (M), the cubital retinaculum (white arrows), and the olecranon process (O).

Figure 4.29. Scanning the medial quadrant. The elbow is extended, the forearm is supinated, and the patient may have to lean away from the examiner.

Medial Quadrant

The medial quadrant contains the common flexor tendon and MCL and is scanned with the elbow extended and the forearm supinated (Fig. 4.29). The common flexor tendon originates from the medial epicondyle of the humerus. It is composed of the flexor-pronator group of muscles: pronator teres, flexor carpi radialis, palmaris longus, and flexor carpi ulnaris (Fig. 4.30).

P. 58

The common flexor tendon is shorter and broader than the common extensor tendon, and has an echogenic fibrillar appearance as it attaches on the medial epicondyle (Fig. 4.31). It is well demonstrated by placing the transducer longitudinally over the medial joint line.

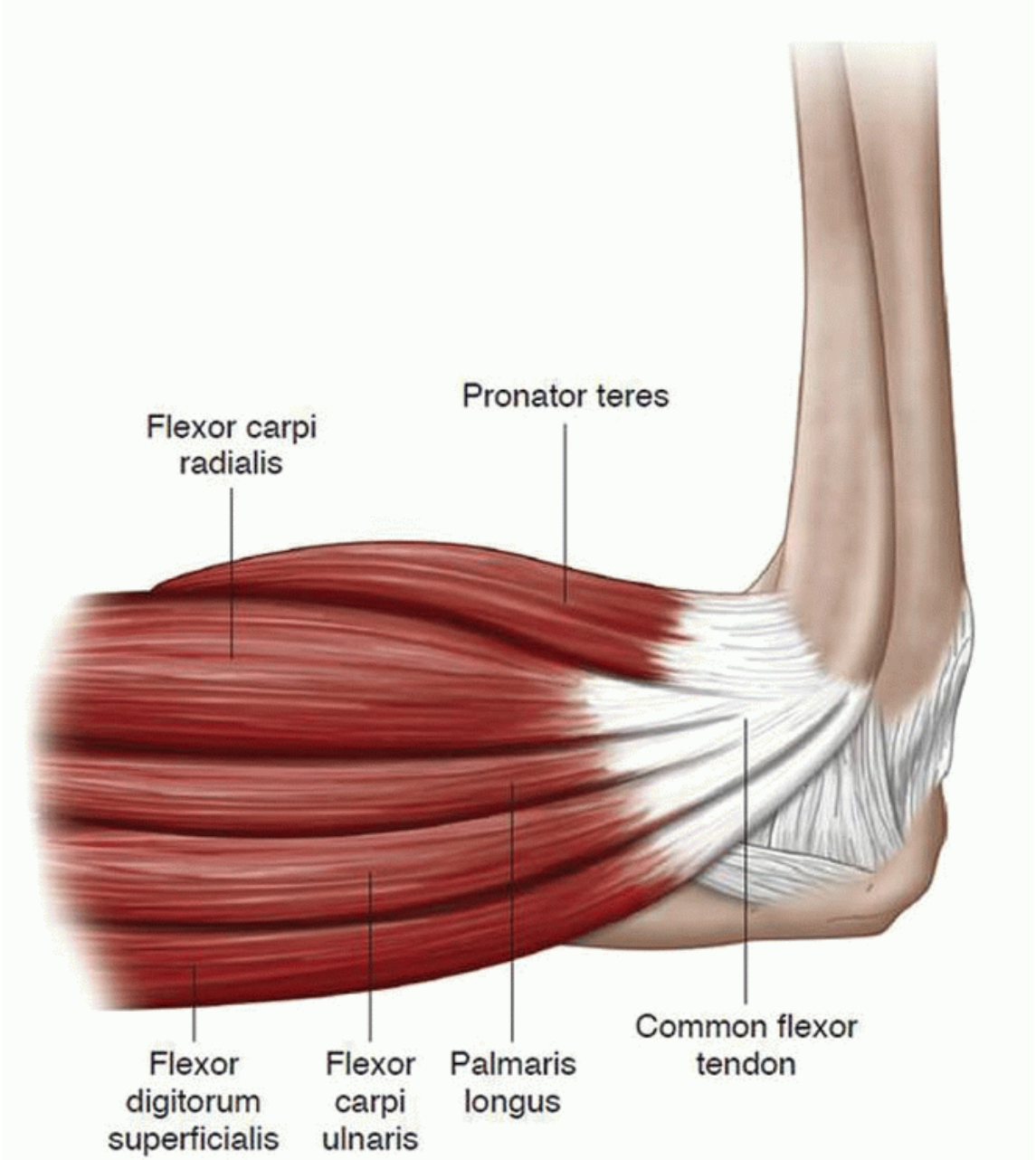

Figure 4.30. Diagram of the flexor pronator group, forming the common flexor tendon. The pronator teres and flexor carpi radialis components are most commonly involved in medial epicondylitis.

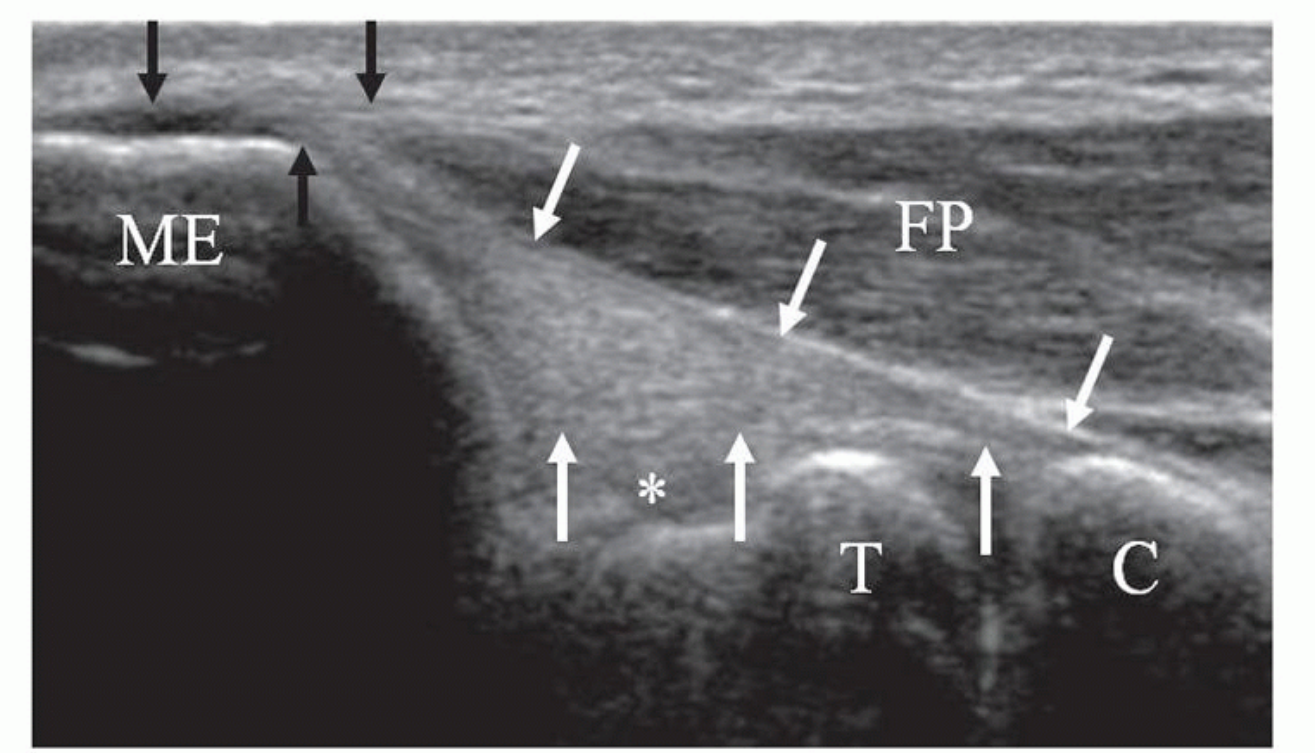

Figure 4.31. Long-axis image of the medial side of the elbow shows the short common flexor tendon (black arrows) of the flexor-pronator (FP) muscle group, with hypoechoic anisotropy at its attachment on the medial epicondyle (ME). The anterior bundle of the MCL (white arrows) has a fan shape, with a broad origin on the medial condyle and a tapered insertion on the sublime tubercle of the coronoid process (C) of the ulna. The ligament crosses the joint space between the coronoid process and trochlea (T) of the humerus, and has echogenic fibrofatty material (asterisk) between it and the humerus.

Deep to the common flexor tendon is the anterior bundle of the MCL. The MCL is also composed of a posterior bundle and a transverse bundle, but the anterior bundle is the primary restraint to valgus stress, is the bundle that is usually of clinical concern, and is most visible at imaging (Fig. 4.32). The anterior bundle has a fan shape, with a broad origin on the undersurface of the medial condyle and a thin insertion on the sublime tubercle of the coronoid process of the ulna (Fig. 4.31).

Tip:

The anterior bundle of the MCL may have a hypoechoic appearance because of its oblique course distally. Press the distal aspect of the transducer into the forearm to make the ligament more echogenic.

TENDON PATHOLOGY

Epicondylitis

Lateral epicondylitis (“tennis elbow”) is the term used for pain over the lateral epicondyle and proximal lateral forearm during wrist extension and supination. It is an overuse injury typically affecting the extensor carpi radialis brevis component of the common extensor tendon,[19] and got the name “tennis elbow” because of its association with poor backhand technique in amateur players,[20] but most cases are not due to tennis, and it may be encountered in the lead elbow of professional golfers[21] and activities that require repetitive extension and supination of the wrist.[19] Lateral epicondylitis and radial nerve neuropathy may have similar clinical presentations, and imaging plays an important role in distinguishing the two conditions.[22]

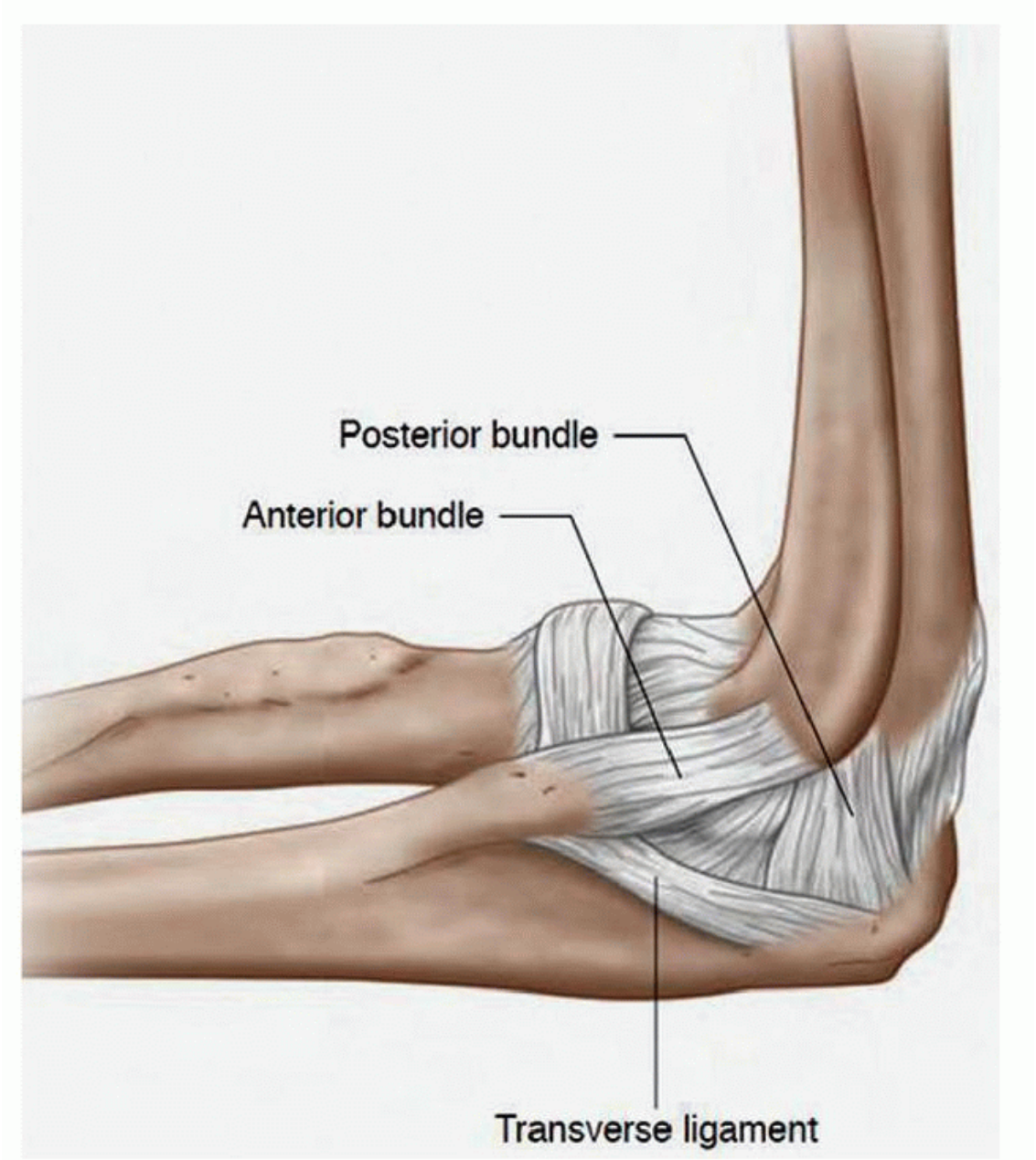

Figure 4.32. Diagram of the medial collateral ligament, showing the anterior and posterior bundles and the transverse ligament component.

Medial epicondylitis is the term used for pain over the medial epicondyle with wrist and finger flexion and wrist pronation. It is less common than lateral epicondylitis. Medial epicondylitis is also called “golfer’s elbow”, affecting the trail arm as a result of poor swing technique in amateur golfers,[21] but most cases are not due to golf. Weight lifting, bowling, and throwing are all associated with medial epicondylitis due to the valgus stress that accompanies these activities.[23] The pronator teres and flexor carpi radialis components are predominantly affected.[24] Patients with medial epicondylitis may also have ulnar neuritis due to tensile and valgus compressive loads that produce medial epicondylitis.

The term “epicondylitis” is a misnomer, since histologically there is no acute inflammatory process.[25],[26],[27] Rather, it is a degenerative process due to repetitive microtrauma of the common extensor or flexor tendons, with micro tearing of the fibers leading to mucoid degeneration, angiofibroblastic proliferation, and eventual macro tearing if the offending activity continues. Sonographically, the process looks similar regardless of the side affected. In the early stages the tendon may be hypoechoic and/or thickened (Fig. 4.33).

P. 59

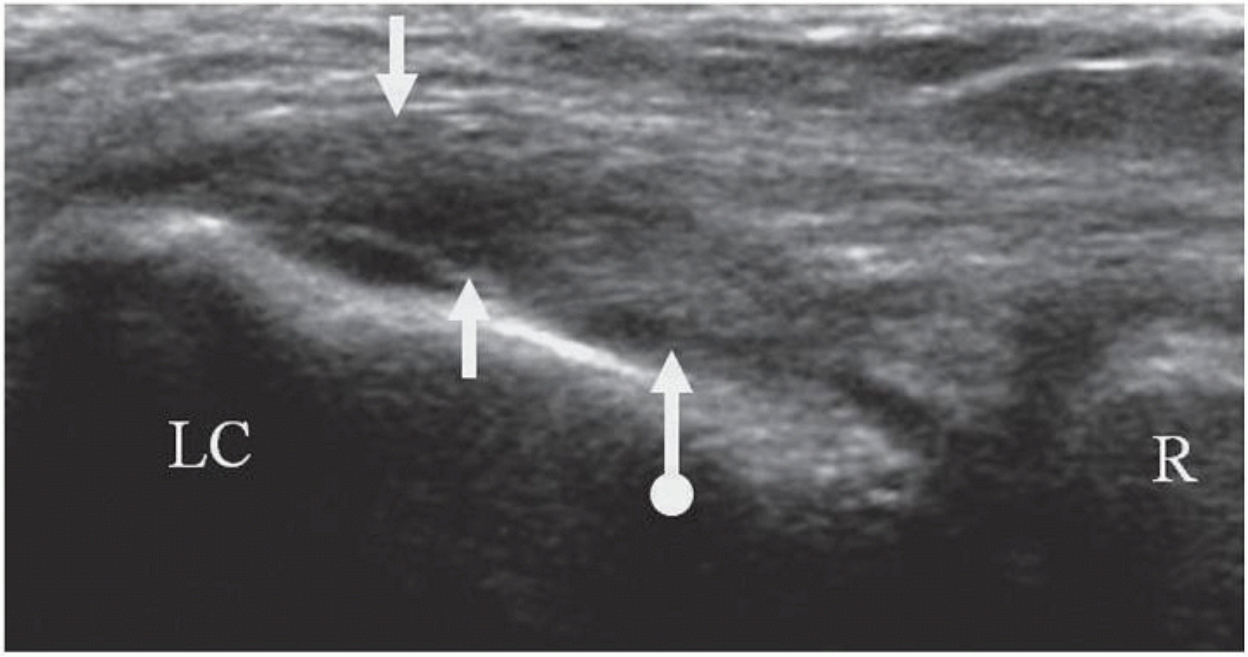

Figure 4.33. Long-axis image shows a thickened and hypoechoic common extensor tendon (straight white arrows). The radial collateral ligament, deep to the tendon, is also degenerated hypoechoic (round tail arrow). LC, lateral condyle; R, radial head.

Tip:

Rock the transducer to eliminate anisotropy as an artifactual cause of decreased echogenicity.

Occasionally, calcium hydroxyapatite is deposited in the degenerated tendon, giving a patchy echogenic appearance (Fig. 4.34). More severe disease may show linear hypoechoic clefts in the tendon or partial tearing of the deep surface at its condylar attachment, and scanning in the short axis helps to confirm a partial tear (Fig. 4.35). Hyperemia due to angiofibroblastic proliferation may be demonstrated using color or power Doppler[24,28,29] (Fig. 4.36) but is not always present. Enthesophytes may be present at the apex of the epicondyle in long-standing cases. Sonoelastography may demonstrate softening of the tendon.[30] The underlying radial collateral and medial collateral ligaments may also be degenerated or torn as a result of the overlying tendon abnormality and should be examined when scanning for epicondylitis.

Sonography has variable sensitivity and specificity for detecting epicondylitis. Miller et al. reported sensitivities ranging from 64% to 82% and specificities of 67% to 100%,[29] whereas Levin reported sensitivities of 80% to 92% but specificities of only 41% to 59%.[31] Struijs reported positive predictive values of 78% to 82%.[32] Lee et al. found that more than 4.2 mm of thickening of the common extensor tendon had 78% sensitivity and 95% specificity for lateral epicondylitis,[33] but their overall sensitivity and specificity were only 76.5% and 76%, respectively. On the other hand, Park et al. reported 95% sensitivity and 92% specificity for the sonographic diagnosis of medial epicondylitis.[34]

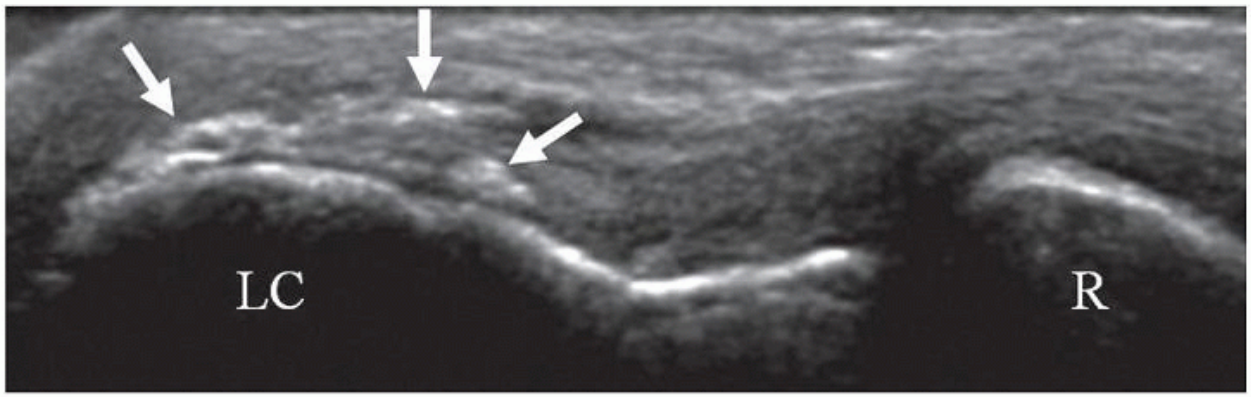

Figure 4.34. Long-axis image of common extensor origin shows focal areas of speckled echogenic calcification (arrows). LC, lateral condyle; R, radial head.

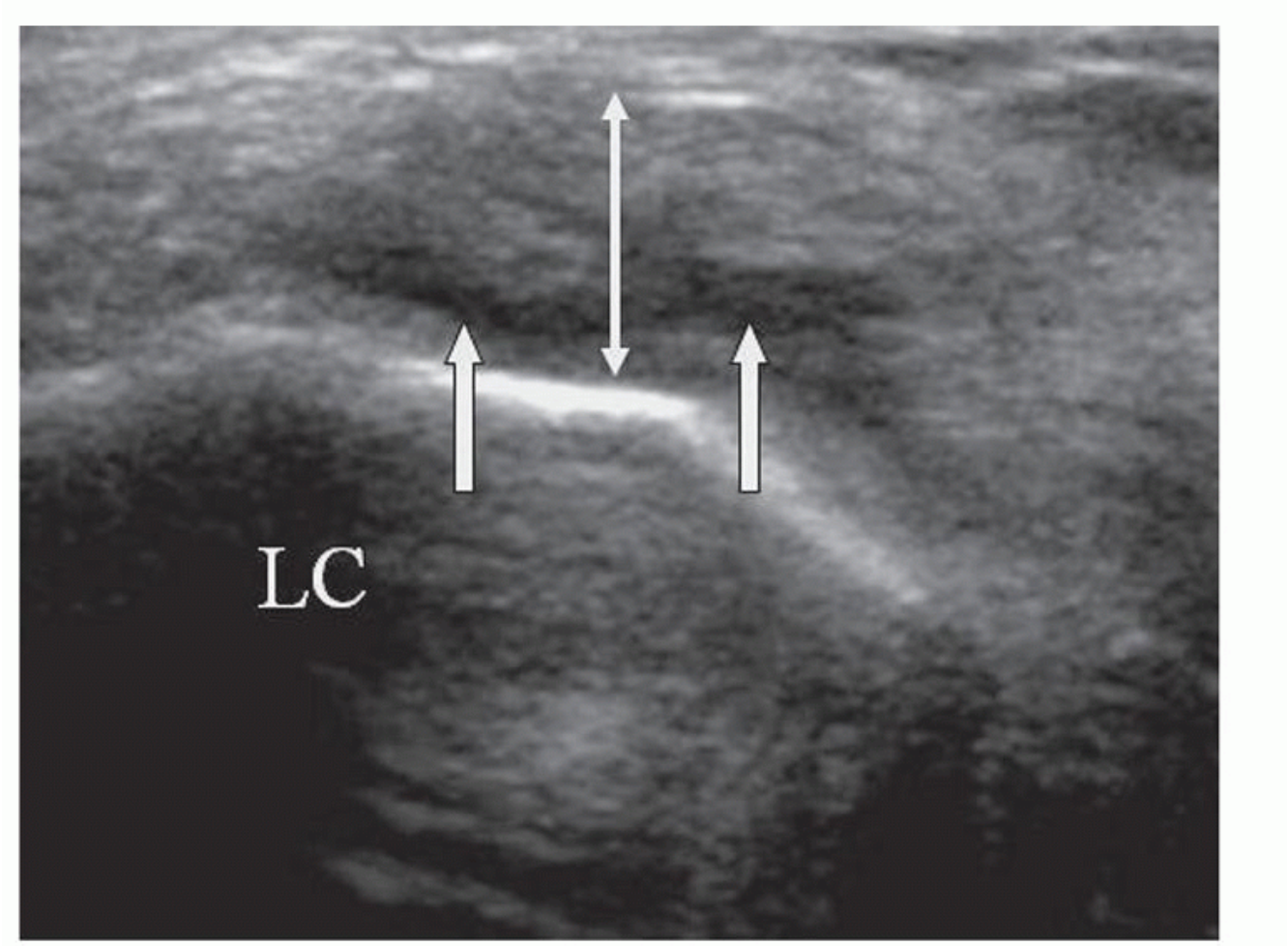

Figure 4.35. Short-axis image shows a tear (arrows) of the common extensor tendon. Note the thickening of the tendon (double-headed arrow). LC, lateral condyle.

Epicondylitis may be treated with ultrasound-guided needle techniques such as fenestration,[35] steroid injection,[36] lavage of hydroxyapatite, and platelet-rich plasma (PRP) or autologous blood injections.[37] Regardless of the procedure, the needle technique is the same, using a long- or short-axis approach, whichever gives better access to the abnormal tissue. As with other ultrasound-guided techniques, success depends on keeping the transducer in plane with the needle. There is no scientific evidence regarding the most effective needle size for fenestration, nor how many fenestrations are needed to stimulate healing. Typically, the needle sizes range from 20G to 25G. Similarly, there is no evidence regarding efficacy of any particular corticosteroid. A typical injectate consists of 0.5 mL of 1% lidocaine, 0.5 mL of 0.25% bupivacaine, and 1 mL of betamethasone (Celestone
P. 60

Soluspan 6 mg/mL). Betamethasone is less likely to cause skin depigmentation and atrophy of subcutaneous fat than long-acting depot preparations, which is a particular issue in such a visible joint as the elbow. Fenestration is always performed as part of a steroid injection. Fenestration of the tendon is performed first, followed by injection of the anesthetic-steroid mixture around the tendon. Steroid is not directly injected into the tendon so as to minimize the risk of tendon rupture. On the other hand, autologous blood or PRP are injected directly into the tendon after fenestration, and will occasionally demonstrate intrasubstance tears that were not otherwise visible. Various commercially available kits are used to produce PRP from the patient's autologous blood. Typically, 3 mL of PRP are obtained after spinning 20 mL of the patient's blood, and all 3 mL are injected into the degenerated or torn tendon after fenestration.

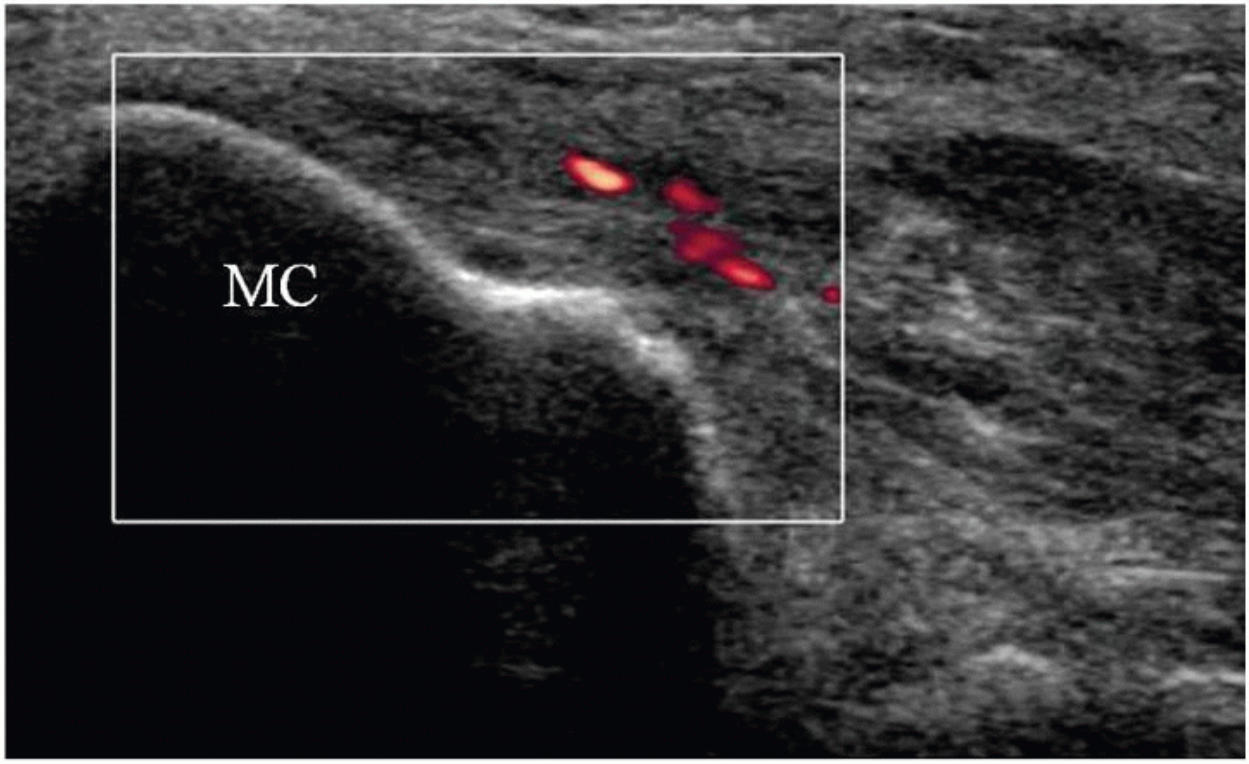

Figure 4.36. Power Doppler long-axis image shows hyperemia within a degenerated common flexor tendon. MC, medial condyle.

Distal Biceps Tendon

Degeneration of the distal biceps is the result of repetitive microtrauma from exercise or manual labor, but large partial tears or complete rupture are usually the result of a single episode affecting a degenerated tendon. The mechanism of injury is an eccentric contraction of the tendon (i.e., the elbow is forcibly extended during active flexion) such as grabbing a banister while falling down steps, jerking an object that is too heavy to lift, or doing “negatives” as part of a biceps curl exercise. Weight lifting and anabolic steroid abuse are risk factors.[38]

The patient may experience sudden pain in the antecubital fossa, and may demonstrate the “Popeye” sign of the retracted muscle and tendon on physical examination. Retraction of the tendon is limited if the biceps aponeurosis (the lacertus fibrosus) remains intact and this may make the diagnosis more difficult. The aponeurosis is a thin fascial layer that extends from the superficial surface of the common flexor muscle mass of the medial side of the forearm to blend with the fibers of the distal biceps tendon. If it remains intact, the biceps does not usually retract beyond the radiocapitellar joint. Clinically, the patient with a ruptured biceps tendon has weak but not absent flexion and supination, since other supinators and flexors remain intact (e.g., the supinator and brachialis muscles, respectively). The examiner may be able to palpate a defect in the antecubital fossa.

Sonographically, biceps tendinosis or low-grade partial tearing demonstrates thickening or thinning, irregular contour, and hypoechogenicity of the tendon, and there may be distension of the adjacent bicipitoradial bursa[9,39] (Fig. 4.37).

Tip:

Scanning from the extensor surface of the forearm while the patient supinates and pronates can be helpful.

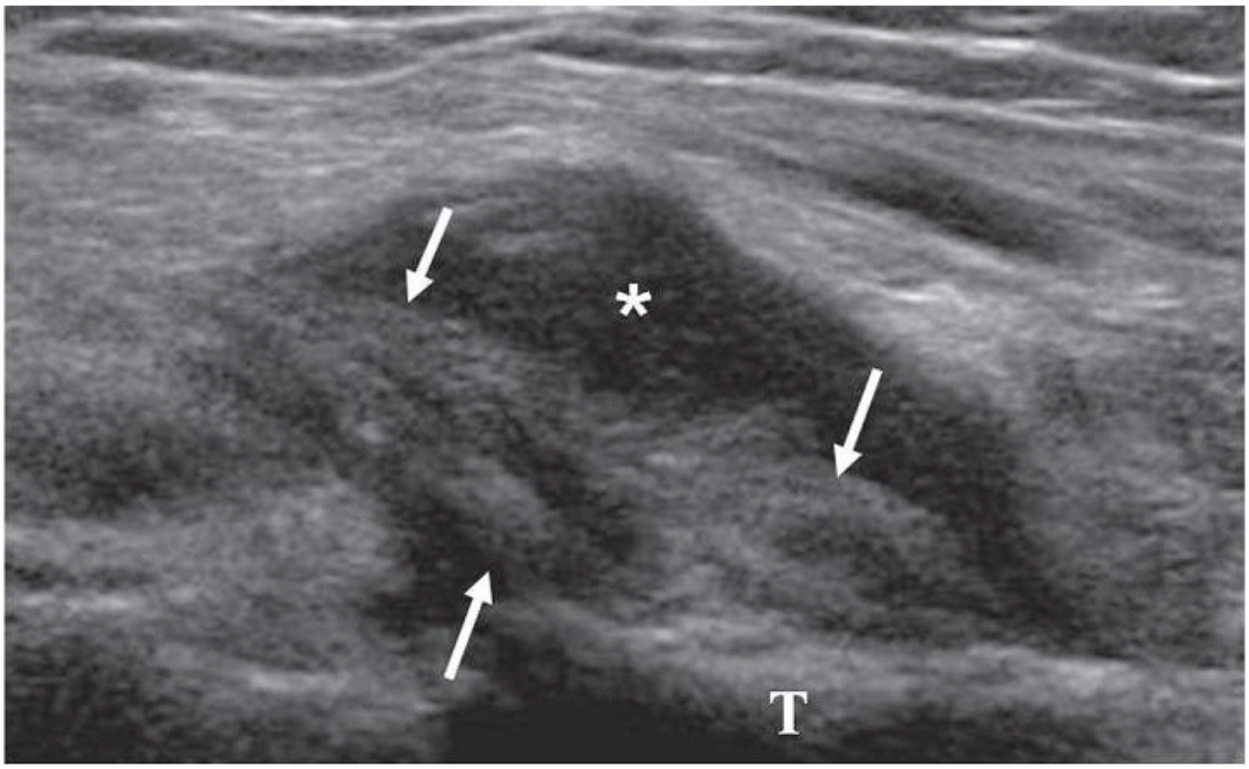

Figure 4.37. Long-axis image of distal biceps tendinosis and partial tearing shows a thickened tendon (arrows) with intrasubstance hypoechoic clefts, and distension of the bicipitoradial bursa (asterisk). Radial tuberosity (T).

Complete rupture results in discontinuity and variable retraction of the tendon (Fig. 4.38). The extent of retraction is important as it will assist the surgeon in planning the surgical repair and the level of incisions. It is also important to evaluate the torn tendon ends to determine the tissue quality: A frayed end suggests poor tissue quality. Heterogeneous hypoechoic edema/hematoma may be present in the tendon gap or in the bicipitoradial bursa.

Da Gama Lobo et al. reported 95% sensitivity, 71% specificity, and 91% accuracy for the diagnosis of complete versus partial tears of the distal biceps tendon, and found that posterior acoustic shadowing emanating from the ruptured tendon edge had 98% accuracy for distinguishing a ruptured tendon from normal, and 91%

P. 61

accuracy for distinguishing a ruptured tendon from a partially torn tendon.[40]

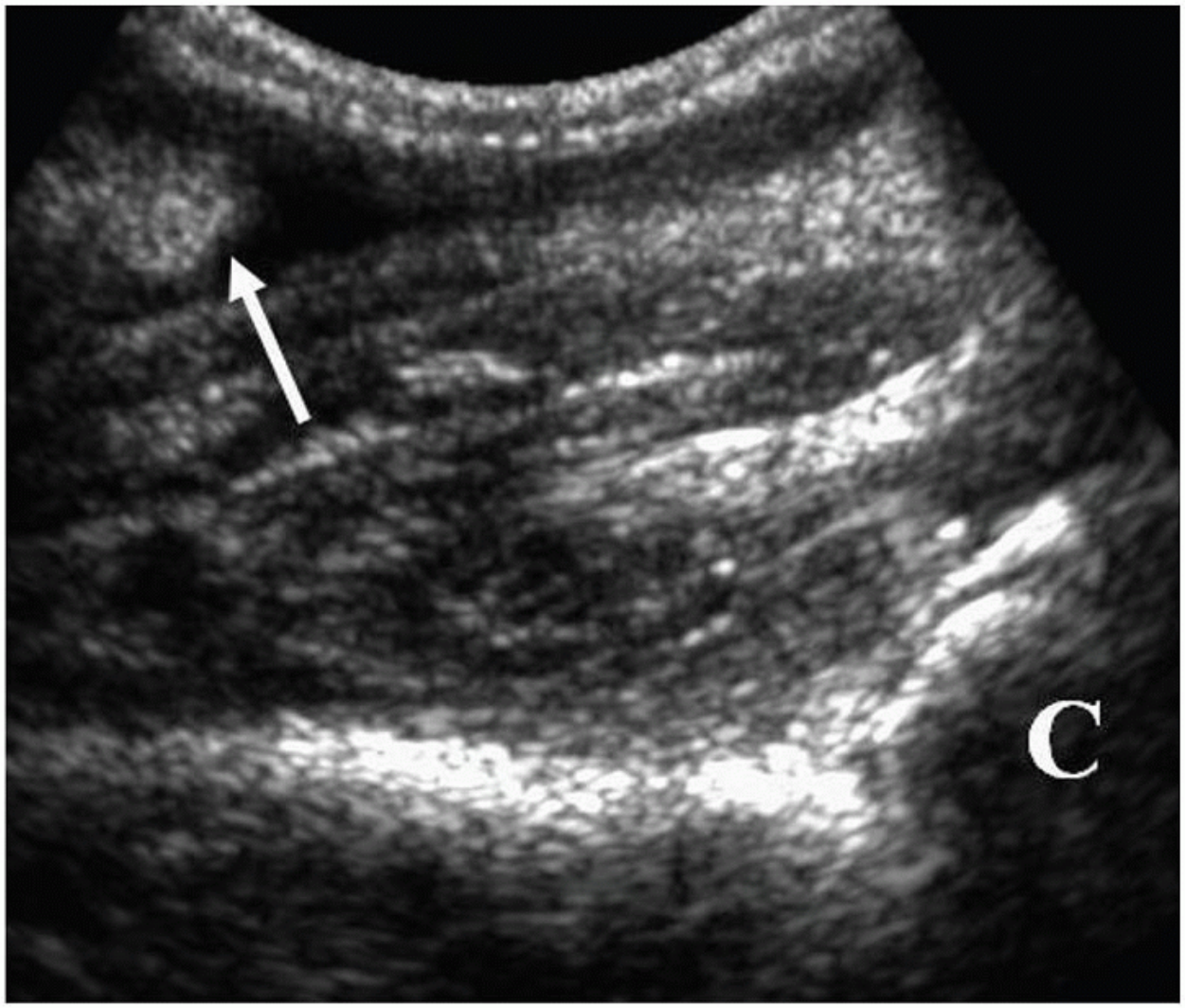

Figure 4.38. Long-axis image shows a ruptured biceps tendon, with its torn edge (arrow) retracted several centimeters proximal to the capitellum (C).

Distal Triceps Tendon

Distal triceps tendon injuries occur as a result of repetitive extension, such as in bench press exercises, or a fall on an outstretched arm with resultant concentric contraction, but triceps tendon injuries in general are rare.[18] Chronic systemic diseases, such as rheumatoid arthritis, diabetes, renal failure, and steroid use may weaken the tendon and predispose to injury.[18] The patient usually complains of pain during resisted elbow extension, with or without weakness depending on the severity of tendon injury. Degeneration results in a thickened hypoechoic tendon, and partial tears produce clefts or gaps in the tendon[41,42] (Fig. 4.39). Rupture of the tendon can occur but actually represents a delamination type of injury since the medial head insertion on the olecranon remains intact[41,42] (Fig. 4.40).

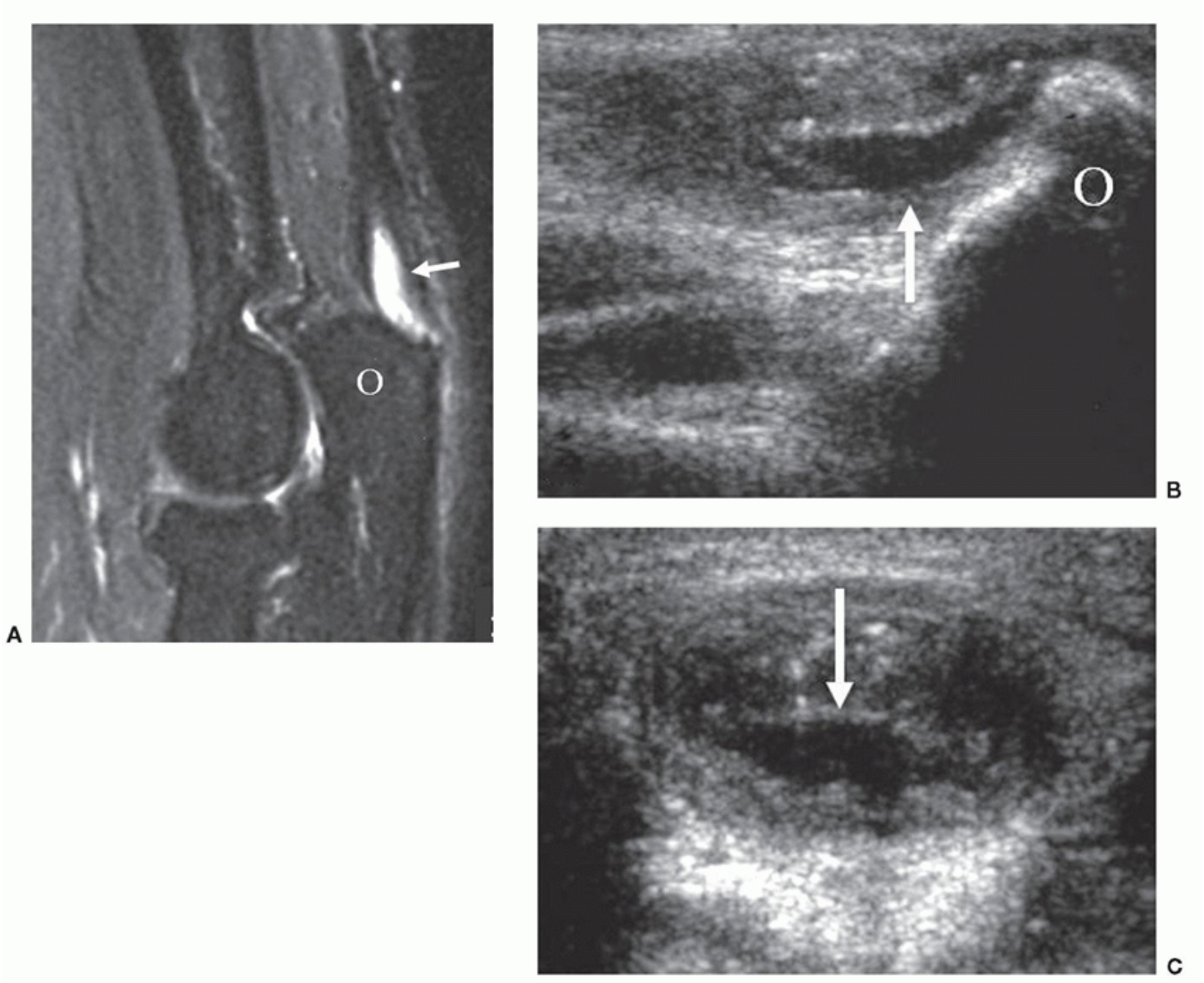

Figure 4.39. Partial tear of triceps tendon. A: Sagittal fat-suppressed T2-weighted MR image shows a large high-signal intensity tear (arrow) within a thickened distal triceps tendon. Olecranon (O). B: Long-axis sonographic image shows the hypoechoic tear (arrow) in the thickened tendon, inserting on the olecranon (O). C: Short-axis sonographic image shows the intrasubstance tear (arrow).

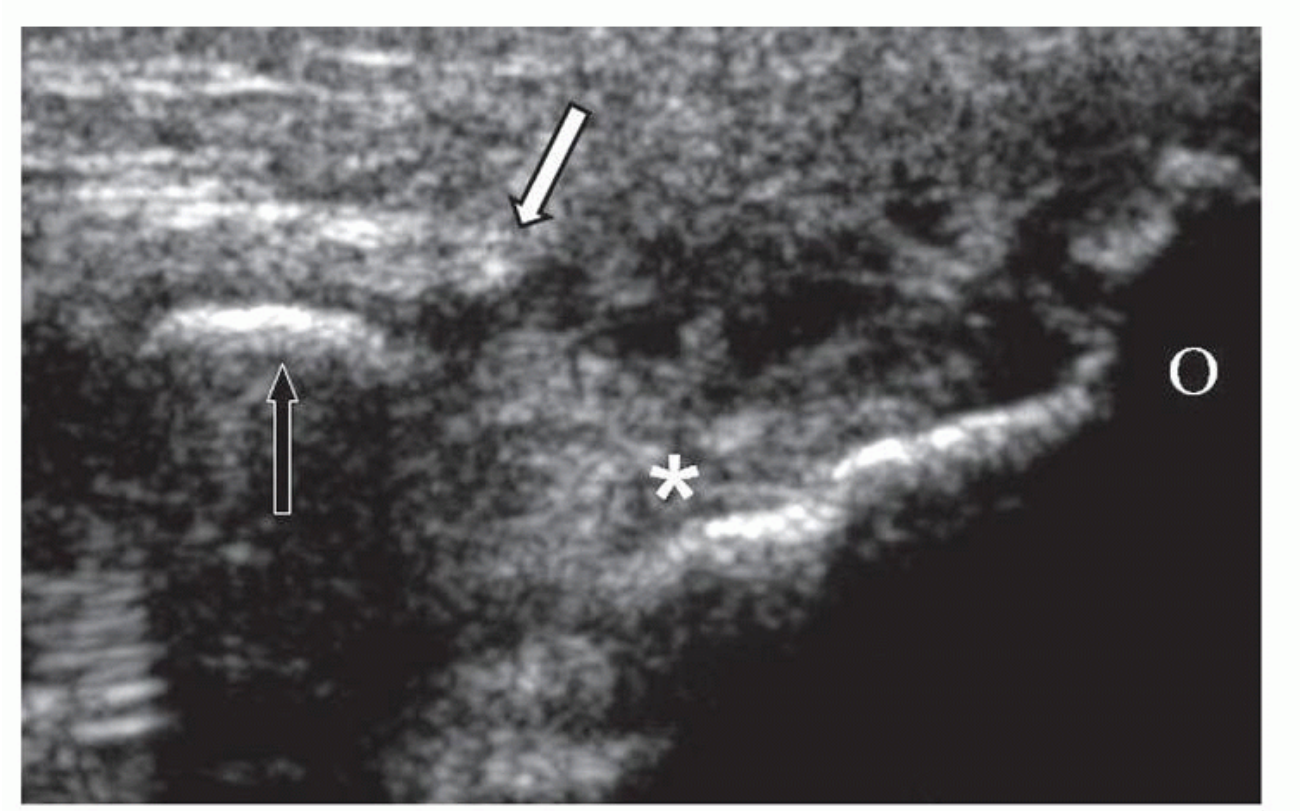

Figure 4.40. Long-axis image shows a torn and retracted triceps tendon (white arrow) with heterogeneous blood between it and the olecranon (O). The attachment of the medial head of the triceps is degenerated but intact (asterisk). A large focus of dystrophic ossification with posterior shadowing is present in the retracted tendon (black arrow), indicating chronic degeneration of the tendon.
P. 62

Another triceps abnormality is the snapping medial head during elbow flexion, usually associated with a snapping ulnar nerve. During elbow flexion, both the ulnar nerve and medial head of the triceps can be seen to dislocate anteriorly, snapping over the medial epicondyle. Usually the nerve and triceps dislocate simultaneously, producing a single snapping sensation, but occasionally they are temporally separated and the patient reports a double snap sensation.[43]

LIGAMENT PATHOLOGY

Medial Collateral Ligament

The anterior bundle of the MCL, the primary restraint against valgus stress, is composed of anterior and posterior bands that are reciprocally taut as the elbow flexes.[44,45] Consequently, the anterior bundle is usually injured by repetitive valgus loads in throwing activities such as baseball, javelin, and volleyball spiking.[46] In the late cocking-early acceleration phase of baseball throwing, the tensile force across the flexed elbow is as much as 120 N-m,[47] with an angular velocity of over 3,000 degrees/second.[48] Less commonly, injury to the MCL is the result of a fall or posterior dislocation of the elbow. The posterior bundle of the MCL, which forms the floor of the cubital tunnel, is a secondary restraint to valgus load of the flexed elbow, and the transverse bundle has no known mechanical function.[44,49]

The normal MCL adapts to repetitive stress. Studies on asymptomatic baseball and handball players have shown that the MCL of the dominant (throwing) arm is thicker than the nondominant arm (Fig. 4.41), and that the medial joint line may gap by 1 to 2 mm more in the dominant than nondominant arm with valgus stress[50,51,52] (Fig. 4.42). Valgus stress can be achieved in the sonography suite by having the patient lie supine and hang the flexed elbow over the edge of the couch, or, with the patient sitting or standing with the elbow flexed, by placing the supinated forearm against the examiner's side while the examiner pushes against the lateral side of the elbow (Fig. 4.43).

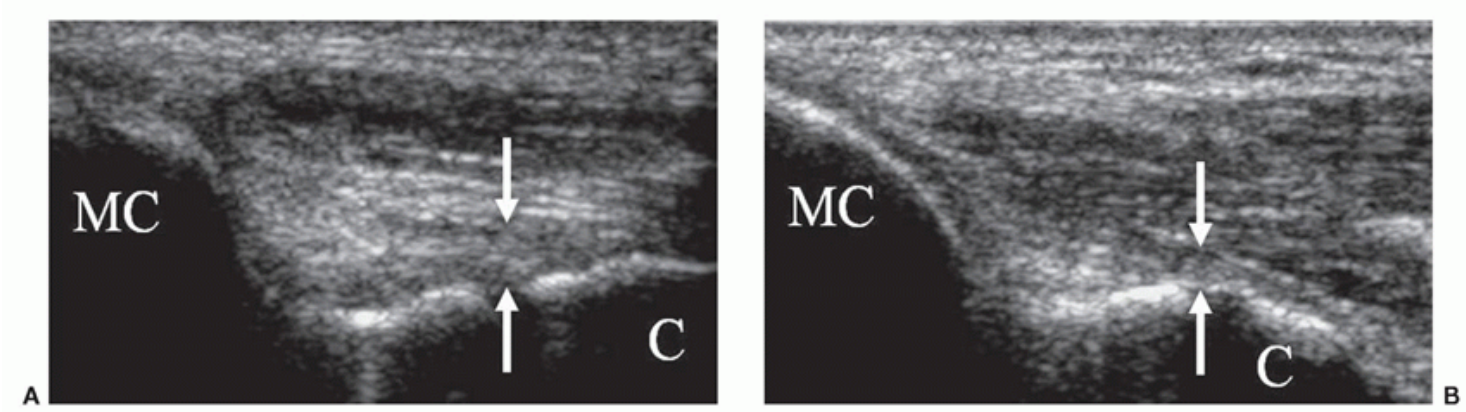

Figure 4.41. Thick MCL. A: Long-axis image of the dominant elbow shows a thickened distal aspect of the MCL (arrows). B: Long-axis image of the patient's nondominant arm shows normal thickness of the MCL (arrows). C, coronoid process of the ulna; MC, medial condyle.

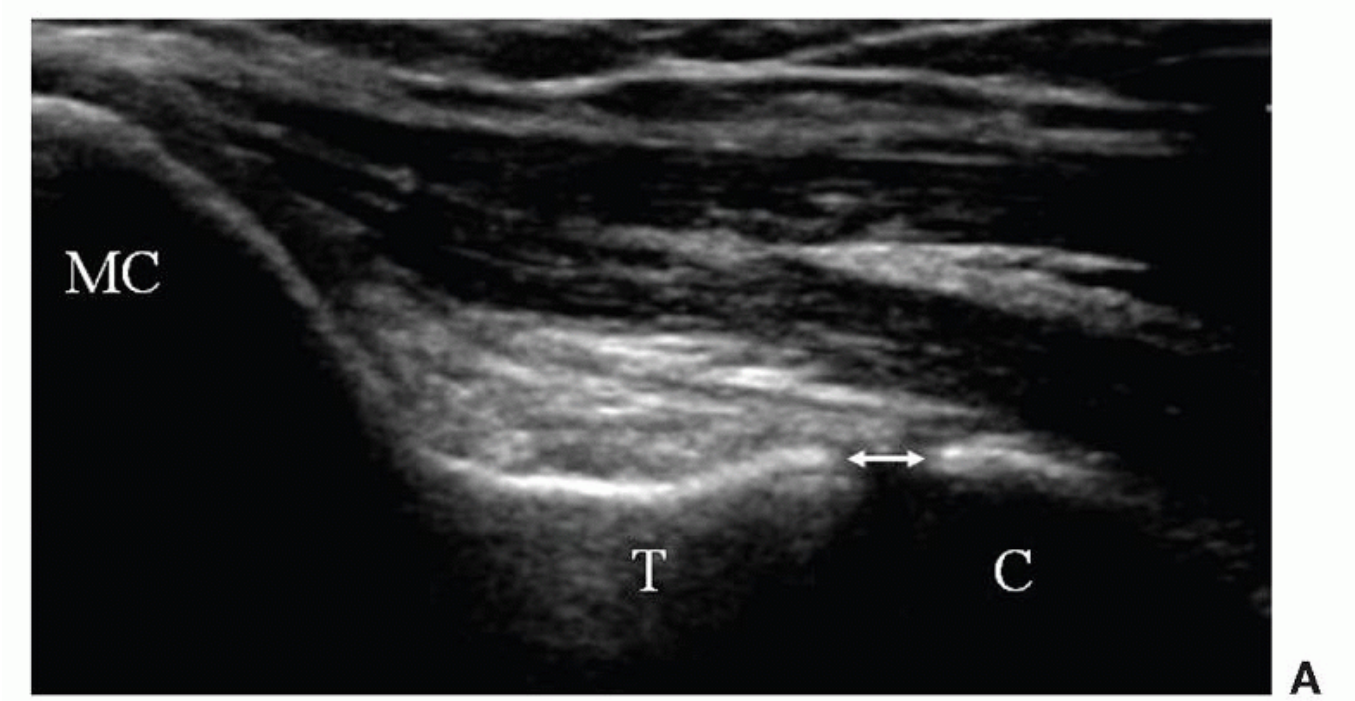

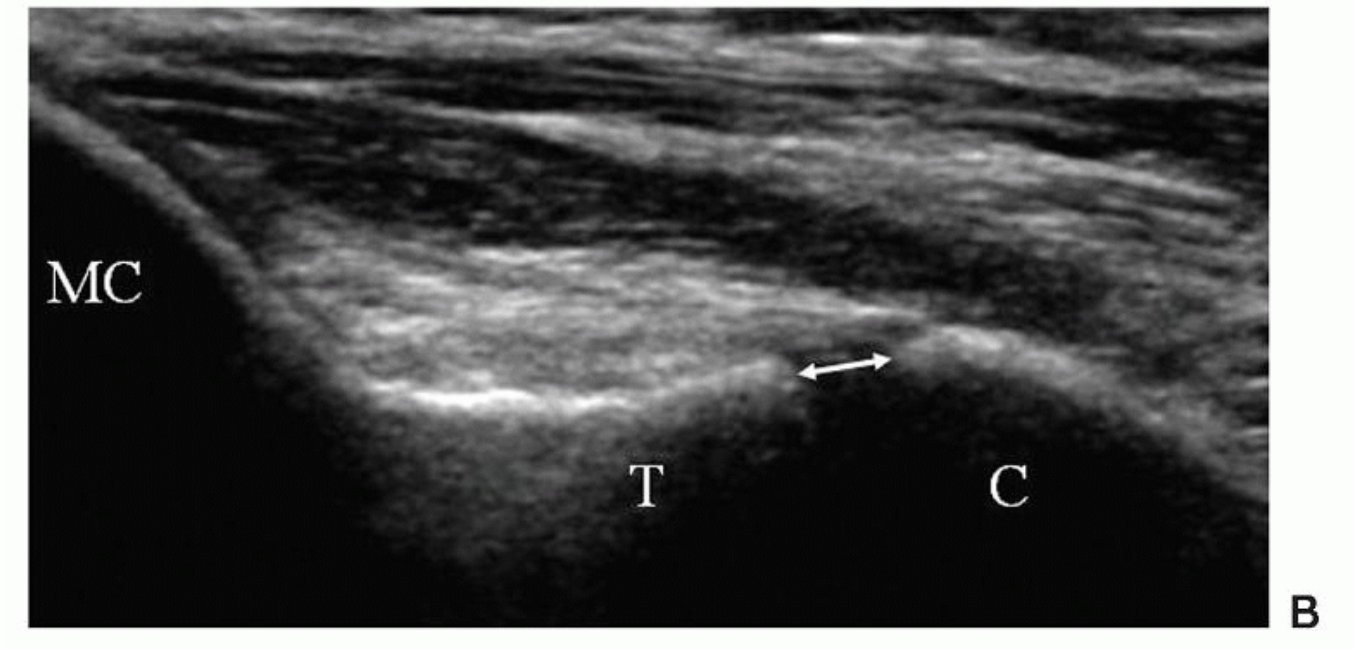

Figure 4.42. Widening of the medial joint line. A: Long-axis image at rest shows the joint line (double headed arrow) between the coronoid process of the ulna (C) and the trochlea (T). B: Long-axis image with valgus stress shows widening of the joint line (double headed arrow) between the coronoid process of the ulna (C) and the trochlea (T). MC, medial condyle.

Tip:

The elbow must be flexed at least 30 degrees when testing valgus stress so as to unlock the osseous stability provided by the olecranon process within the olecranon fossa.

P. 63

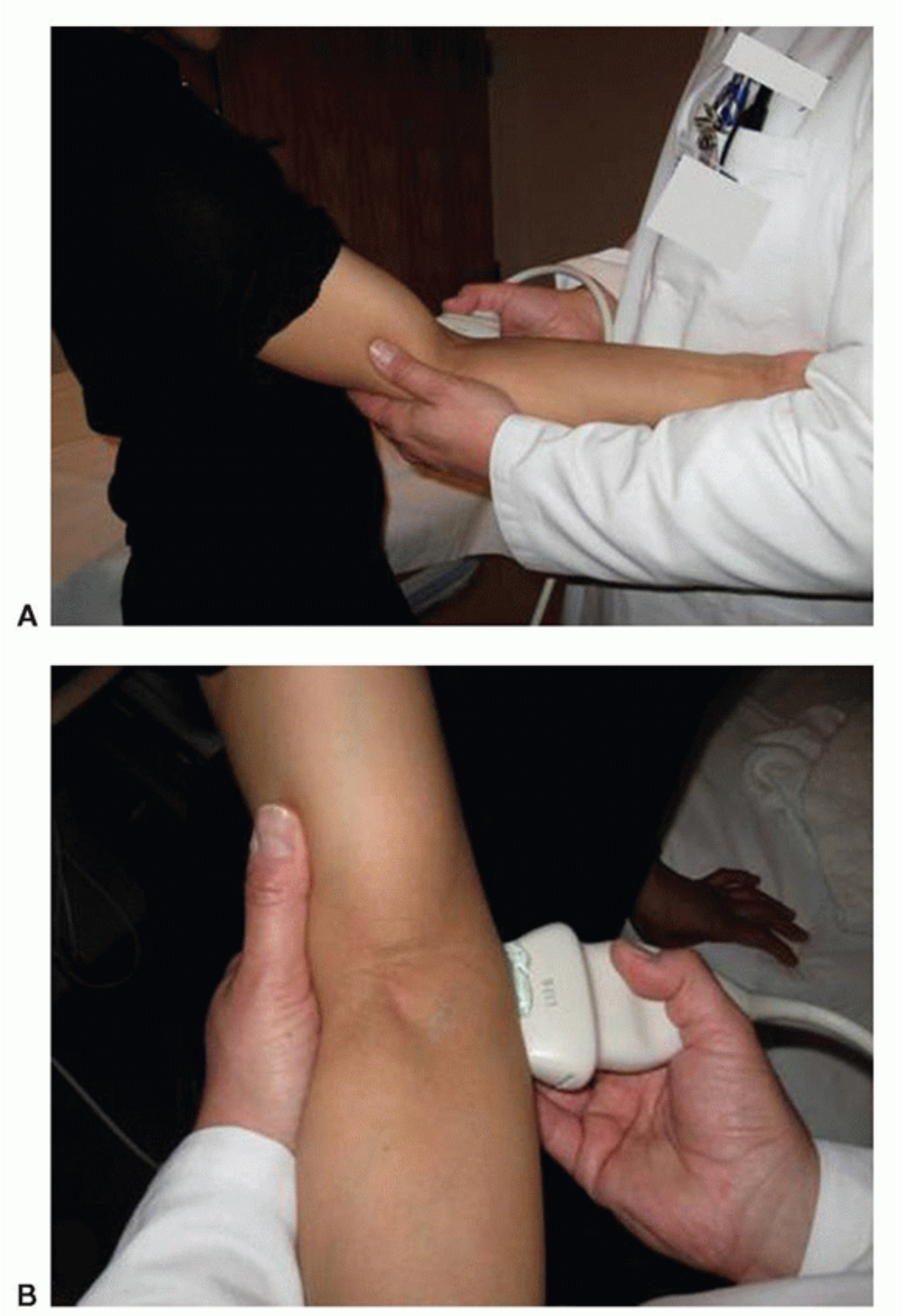

Figure 4.43. Valgus stress testing. A: Side view shows the patient's forearm supinated and tucked under the examiner's arm. The patient's elbow is flexed at least 30 degrees. B: Frontal view shows the transducer against the medial side of the elbow while the examiner pushes the elbow toward the transducer with his/her other hand.

In throwers, MCL injury may be an isolated event or part of the larger spectrum of the "valgus extension overload" syndrome. This syndrome represents a constellation of findings that results from valgus stress on the medial side of the elbow and resultant compressive forces on the radiocapitellar joint[53,54,55]:

- MCL injury.
- Medial epicondylitis or strain of the common flexor mass.
- Ulnar neuritis
- Osteochondral injury of the capitellum.
- Stress reactions or fracture of the olecranon process.
- Osteophytes along the medial margins of the olecranon and olecranon fossa.

When the MCL is injured, the patient complains of medial elbow pain during valgus loads. Throwers will also complain of decreased velocity of the throw and inability to control the pitch. Mild sprains may be difficult to detect sonographically as the only clue may be subtle hypoechoic edema around the ligament.[56] High-grade partial tears demonstrate thickening, thinning, or contour irregularity, and ruptures can be diagnosed by discontinuity or non-visualization of the ligament[56] (Fig. 4.44).

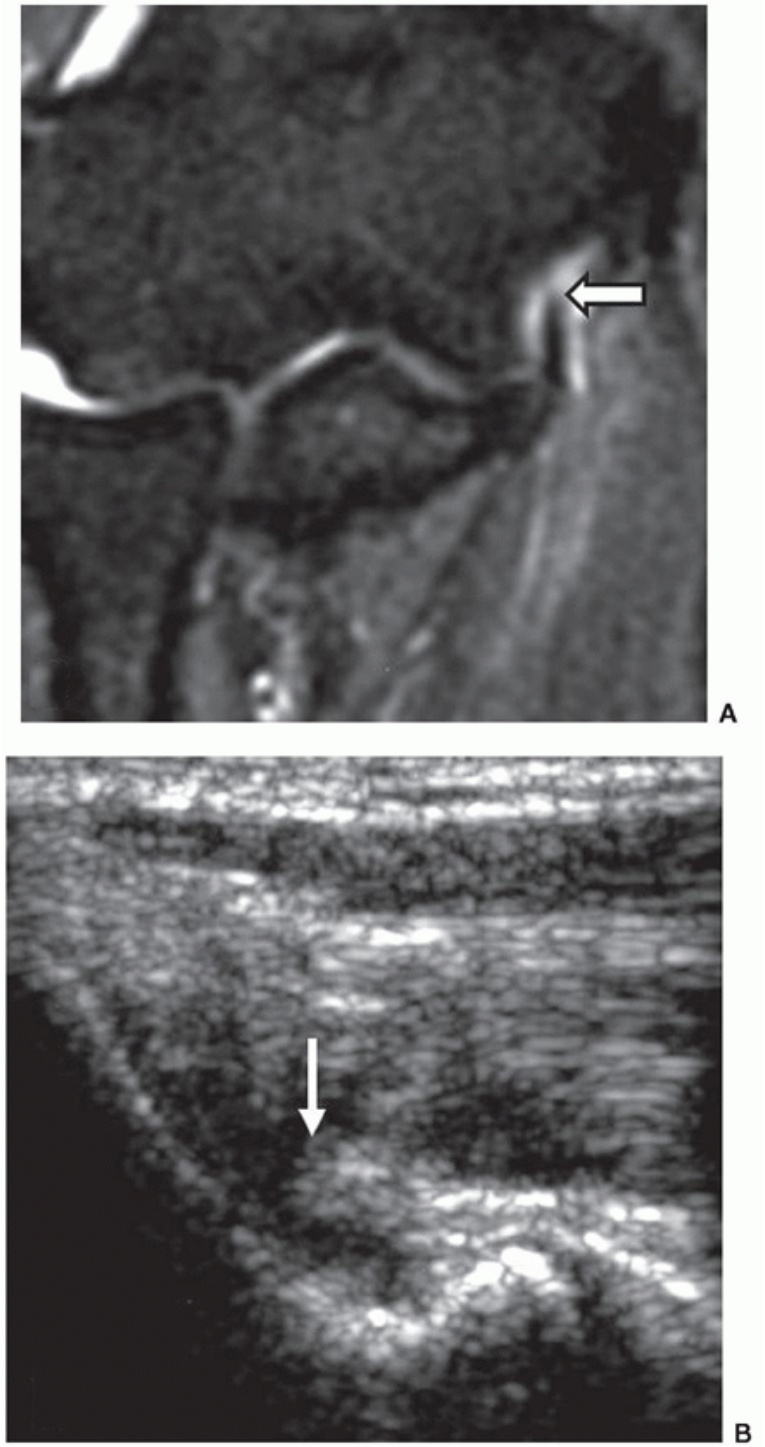

Figure 4.44. Ruptured MCL. A: Coronal fat-suppressed T2-weighted image of the elbow in a collegiate baseball player shows a ruptured MCL proximally (arrow). B: Corresponding long-axis sonographic image of the same patient shows the discontinuity of the ruptured ligament (arrow).
P. 64

A particular type of partial tear occurs at the deep surface of the distal aspect of the ligament due to focal stripping of the deep fibers. On MR-arthrography and CT-arthrography, contrast insinuates into the space between the MCL and sublime tubercle of the coronoid process, producing the "T-sign" on coronal images.[57] Such a deep surface distal tear can also be visualized on sonography, although the sensitivity and specificity of ultrasound is currently unknown.

In the skeletally immature thrower, the growth plate of the medial epicondylar apophysis is the weakest portion of the ligament-bone and tendon-bone units, and the tensile load placed on the apophysis by the MCL and common flexor tendon can occasionally avulse the apophysis ("little leaguer's elbow") instead of tearing the ligament or common flexor tendon.[58,59] Thus, little leaguer's elbow is a Salter I injury, and is treated conservatively if the apophysis is displaced less than 5 mm. Sonographically, the hypoechoic apophysis will be displaced (Fig. 4.45).

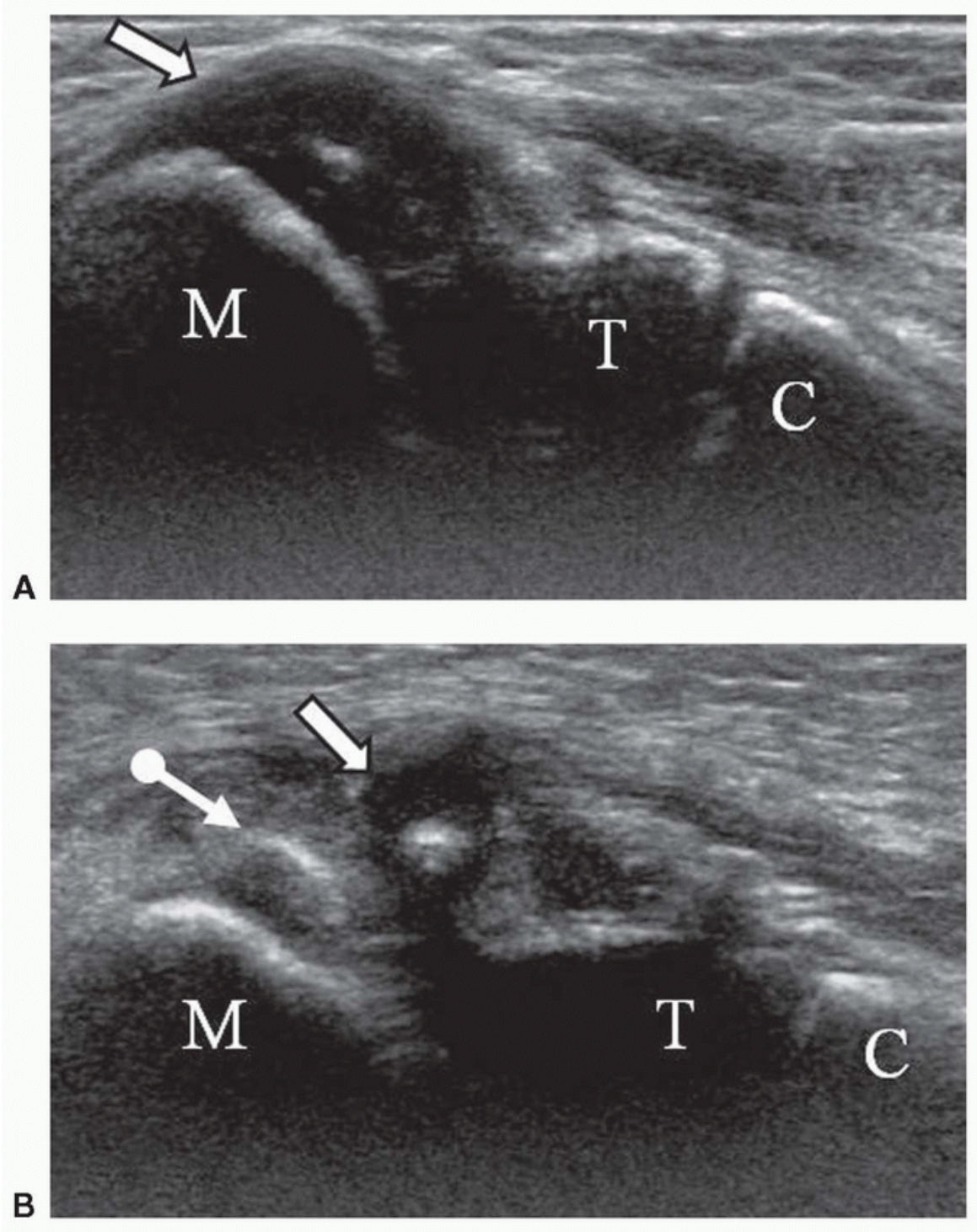

Figure 4.45. Little leaguer's elbow. A: Long-axis image of the patient's contralateral normal elbow shows the hypoechoic medial epicondylar apophysis (arrow) with an early echogenic ossification center, located immediately adjacent to the medial condyle (M). T, trochlea; C, coronoid process of ulna. B: Long-axis image of the injured elbow in the same patient shows the displaced apophysis (straight arrow) and a separate fragment of growth plate (round tail arrow). M, medial condyle; T, trochlea; C, coronoid process of ulna.

Tip:
Comparison with the patient's normal contralateral side can be helpful.

Radial Collateral Ligament Complex

The radial collateral ligament is the primary restraint to varus stress, and the lateral ulnar collateral ligament is the primary restraint to posterolateral stress. The annular ligament maintains the proximal radioulnar joint by restraining the radial head against the sigmoid notch of the proximal ulna.

The radial collateral and lateral ulnar collateral ligaments are usually injured as a result of a fall, either leading to a varus load or a posterior dislocation. Ligament injury as a result of elbow dislocation occurs in a predictable fashion dependent on the force of injury, beginning with the radial collateral and lateral ulnar collateral ligaments, followed by the joint capsule with continued injury, and lastly by the MCL.[60] The annular ligament remains intact. Rupture of the lateral ulnar collateral ligament leads to posterolateral instability of the elbow.[17,60,61] Although the lateral ulnar collateral ligament can be visualized sonographically, patients with instability after dislocation are best assessed with MRI.

The radial collateral ligament and lateral ulnar collateral ligament may also be affected in cases of lateral epicondylitis, and it is important to look at these ligaments when scanning for abnormalities of the common extensor tendon[62] (Figs. 4.33 and 4.46). In addition, the lateral ulnar collateral ligament may be iatrogenically injured during surgical debridement of lateral epicondylitis.

The annular ligament is not often injured. In young children, the radial head may be pulled out of the annular ligament by a forceful yank on the forearm, usually by

P. 65

an aggravated adult ("nursemaid's elbow"), and can be diagnosed sonographically by a widened radiocapitellar space compared to the contralateral side[63,64] (Fig. 4.47).

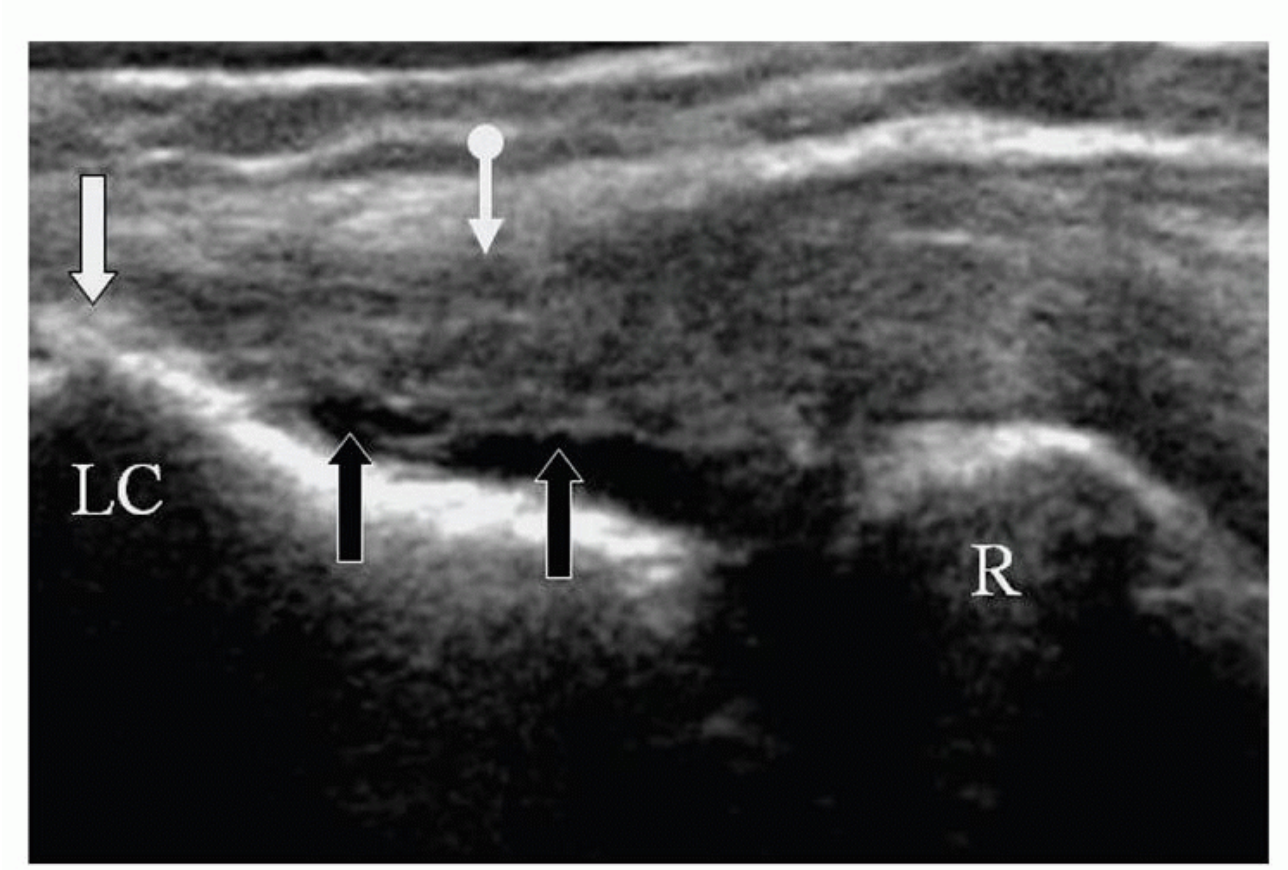

Figure 4.46. Long-axis image shows a high-grade partial tear of the radial collateral ligament (black arrows), associated with lateral epicondylitis, seen as a thickened and hypoechoic common extensor tendon (round tail arrow) with an epicondylar enthesophyte (straight white arrow). LC, lateral epicondyle; R, radial head.

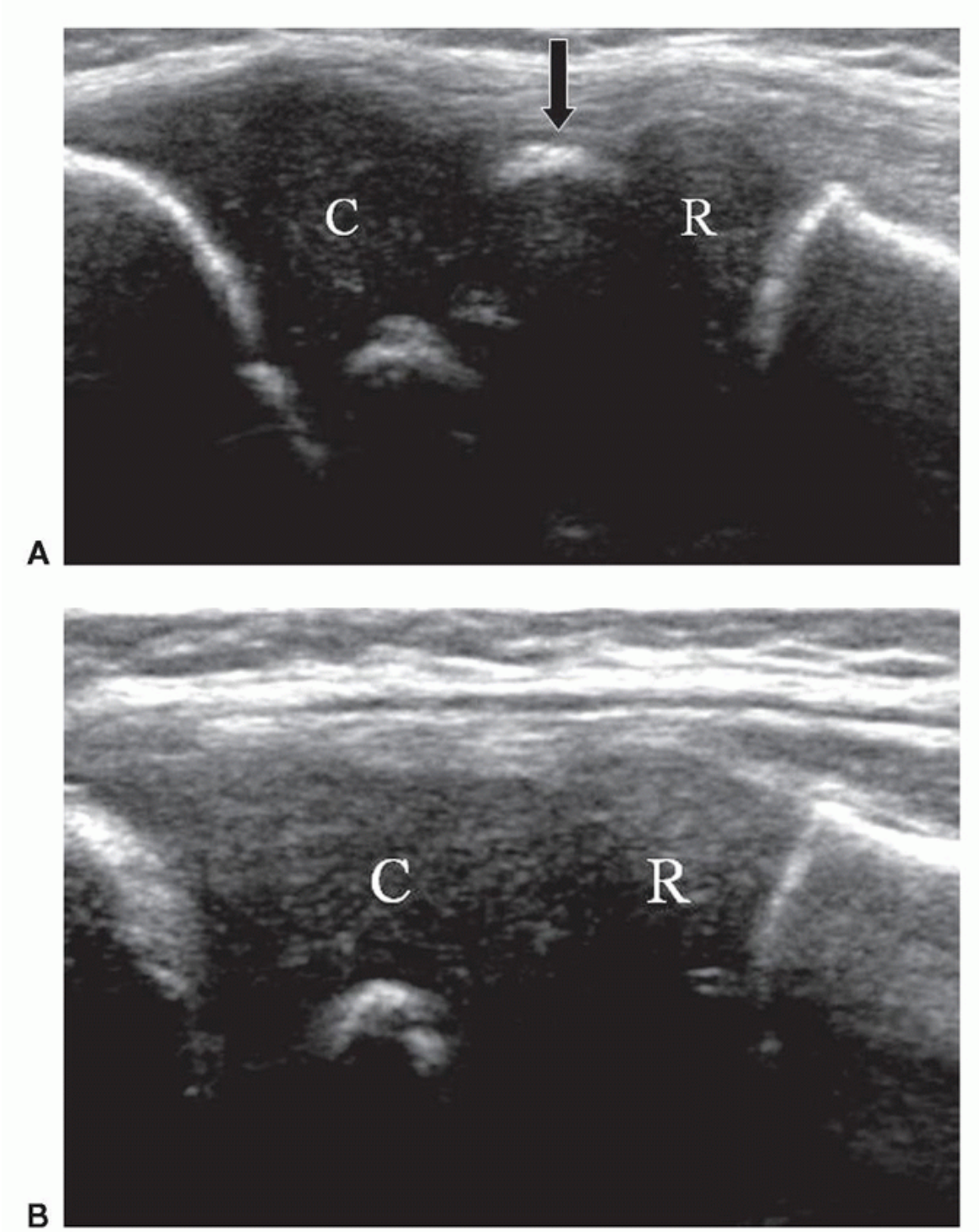

Figure 4.47. Nursemaid's elbow. A: Long-axis image over the radiocapitellar joint shows interposition of the displaced annular ligament (arrow) between the hypoechoic cartilaginous capitellum (C) and radial head (R). B: Long-axis image of the patient's contralateral elbow shows the capitellum (C) directly against the radial head (R).

Tip:

Scan the radiocapitellar joint longitudinally along the lateral joint line to detect widening of the radiocapitellar joint in "nursemaid's elbow". Comparison with the contralateral elbow can be helpful.

The echogenic annular ligament can sometimes be seen interposed between the hypoechoic cartilaginous epiphyses of the capitellum and radial head.

NERVES

The nerves of interest at the elbow are the ulnar nerve, the radial nerve and its deep branch that becomes the posterior interosseous nerve, and the median nerve and its branch, the AIN.

Ulnar Nerve

Ulnar nerve compression at the elbow is the second most common nerve entrapment of the upper extremity after carpal tunnel syndrome, with an estimated annual incidence of 21 to 25 cases per 100,000.[65,66] There is no agreement on risk factors, although physical labor is commonly reported.[65,66] Flexion of the elbow causes increased tensile load on the ulnar nerve and increases the

pressure in the cubital tunnel up to 20 times the pressure at rest.[67,68] Populations at risk for flexion-induced ulnar neuropathy include truck drivers who lean the flexed elbow against the open window of the truck[69] and constant cell phone users.[68] Baseball pitchers are also at risk due to the valgus stress that is induced in the late cocking and early acceleration phases of throwing.[70] Patients with ulnar neuropathy complain of pain, paresthesia, and weakness in the little finger and ulnar side of the ring finger, and numbness in the dorsal ulnar aspect of the hand and fingers.[67] Chronic compression may lead to claw deformities of the ring and little fingers and loss of grip.[68]

Compression of the ulnar nerve may occur at four different locations at the elbow from proximal to distal[67]:

- At the intermuscular septum in the medial aspect of the mid arm.
- Posterior to the medial epicondyle at the entrance to the cubital tunnel.
- Within the cubital tunnel.
- At the flexor-pronator aponeurosis between the heads of the flexor carpi ulnaris as the nerve enters the forearm.

The cubital tunnel is the most common location of ulnar nerve compression, and the most common structural abnormality in the cubital tunnel is the anconeus epitrochlearis muscle. This is an anomalous muscle reported in 23% of asymptomatic elbows on MR imaging and in up to 34% of the population in anatomic dissections.[71] Located along the posterior aspect of the cubital tunnel, the anconeus epitrochlearis muscle may compress the ulnar nerve against the medial epicondyle or olecranon. Osteophytes may also compress the ulnar nerve in the cubital tunnel.[72]

Ulnar neuritis is demonstrated sonographically by nerve enlargement[73,74] (Fig. 4.48). Comparison of the nerve with the contralateral asymptomatic nerve[73] or comparison of the cross-sectional area at the site of maximal nerve swelling with the cross-sectional area at a nonswollen location[74] can be helpful.

Tip:

When scanning the contralateral elbow or other locations in the ipsilateral elbow, make sure that images are obtained in same degree of elbow flexion as the cross-sectional area of the nerve decreases with increased flexion.[67]

P. 66

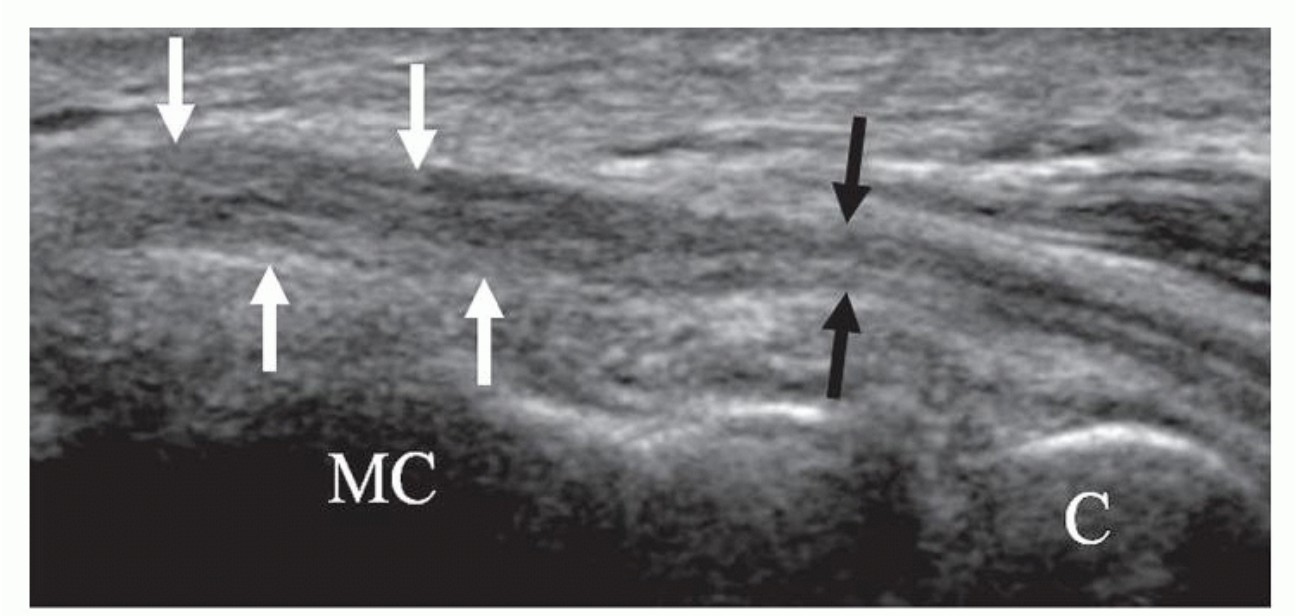

Figure 4.48. Long-axis image of the ulnar nerve shows proximal enlargement (white arrows) compared to more distal fibers (black arrows). MC, medial condyle; C, coronoid process.

If the nerve is bifid or trifid, the separate moieties must be evaluated additively[75] (Fig. 4.49).

Another group at risk for ulnar neuropathy are people with recurrent anterior dislocation of the ulnar nerve that occurs asymptomatically in 16% to 20% of the population.[76,77] Risk factors for ulnar nerve dislocation include cubitus varus deformity, absent or lax ligament of Osborne (the fascia that forms the roof of the cubital tunnel), hypertrophic medial head of triceps, or an accessory head of triceps.[43,78,79,80] The dislocation may be associated with activities that involve resisted elbow extension such as the early acceleration phase of throwing and bench press.[78] The abnormal movement of the nerve may be felt as a snap by the patient during elbow flexion, but the snapping may also include the medial head of the triceps or an accessory triceps muscle; in these instances the patient may report a double-snap sensation.[78,79] The repetitive translation of the nerve over the bony prominence of the epicondyle as it dislocates in flexion and reduces in extension can cause frictional neuritis,[76] and patients can present with a spectrum of clinical abnormalities such as medial elbow pain, snapping, ulnar neuropathy, or combinations thereof.[78,79]

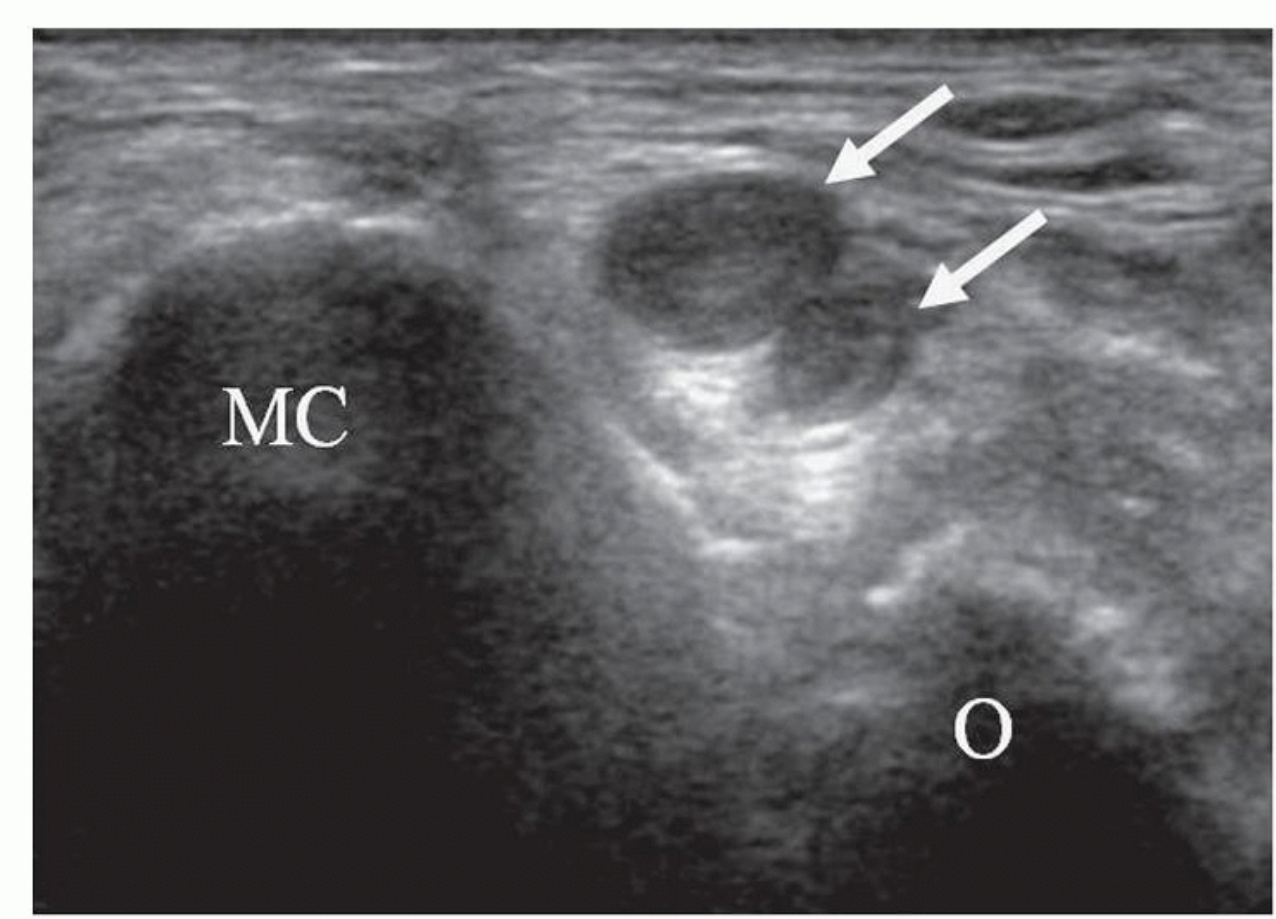

Figure 4.49. Short-axis image through the cubital tunnel shows enlargement of both portions of a bifid ulnar nerve (arrows). MC, medial condyle; O, olecranon process.

Sonographic imaging during flexion and extension is a real-time method of evaluating ulnar nerve dislocation. Transverse scans over the cubital tunnel demonstrate both the nerve and medial head of the triceps[43] (Fig. 4.50). Scanning during resisted extension and flexion may be needed to demonstrate the abnormal movement.[79] Recognition of concomitant triceps dislocation is crucial to correct treatment, since surgical anterior transposition of the nerve without correction of the snapping triceps will lead to persistent symptoms.[78,79,81]

Radial Nerve

Compression of the deep branch of the radial nerve may occur at five different locations at the elbow from proximal to distal[4]:

- At the level of the radial head by fibrous bands between the brachioradialis muscle and joint capsule.
- Distal to the radial head by the “Leash of Henry,” an arcade of anastomosing branches of the radial recurrent artery.
- At the level of the tendinous edge of the overlying extensor carpi radialis brevis muscle.
- At the “arcade of Frohse” along the proximal aspect of the supinator muscle.
- At the distal aspect of the supinator muscle.

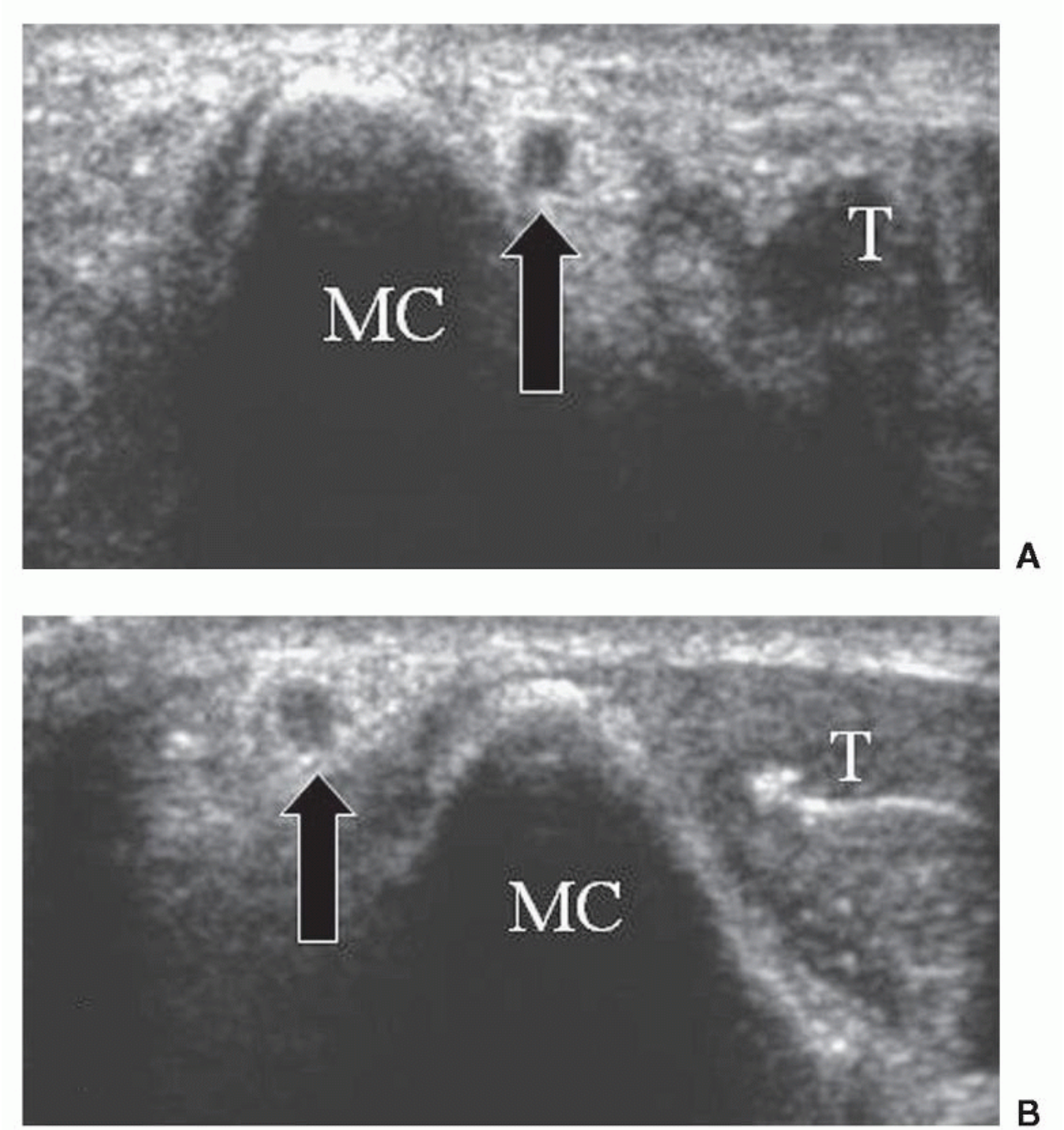

Figure 4.50. Snapping ulnar nerve. A: Short-axis image through the cubital tunnel in elbow extension shows normal location of the nerve (arrow), posterior to the medial condyle (MC). T, medial head of triceps. B: Short-axis image in elbow flexion shows dislocation of the nerve (arrow) anterior to the medial condyle (MC), with the medial head of the triceps muscle (T) now filling the cubital tunnel.
P. 67

The arcade of Frohse is the most common site of compression and represents a thickened tendinous proximal edge of the superficial head of the supinator. The normal edge is thin and membranous. The tendinous thickening is most likely due to repetitive pronation/supination.[82] Deep branch radial nerve compression can lead to either “radial tunnel syndrome” or “posterior interosseous nerve syndrome” (also called “supinator syndrome”), although it is not known why in any individual one syndrome occurs and not the other.[4] Radial tunnel syndrome leads to a burning sensation along the lateral aspect of the forearm mimicking lateral epicondylitis, whereas posterior interosseous nerve syndrome presents with weakness of the extensor muscles of the forearm.
Lateral epicondylitis and deep branch radial nerve compression may coexist, often due to irritation or compression of the nerve by the degenerated or torn extensor carpi radialis brevis tendon. The two clinical entities are also difficult to distinguish on physical examination,[4] and electrodiagnostic tests are usually normal in radial tunnel syndrome.[82] Compression of the lateral antebrachial

cutaneous nerve can also cause burning pain in the lateral aspect of the forearm, mimicking both lateral epicondylitis and radial tunnel syndrome, but compression of this nerve is rare.[4]

Caution must be exercised in interpreting structural changes in patients without symptoms of nerve compression; for example, a hypertrophic leash of Henry, arbitrarily defined as more than six vessels, was present in 9 of 60 asymptomatic elbows.[71]

Patients with PIN syndrome may have a hypoechoic swollen deep branch, with a mean diameter of 4.2 mm, as well as hyperemia of the nerve on color Doppler imaging.[83]

The sonographic appearances of radial nerve abnormalities include compression within the radial tunnel, as described above (Fig. 4.51), compression by masses such as ganglion cysts, or intrinsic abnormalities of the nerve such as a nerve sheath tumor (Fig. 4.52).

Tip:

The deep branch of the radial nerve may normally have an angulated course at the arcade of Frohse if scanned with the forearm pronated,[84] and this should not be misinterpreted as entrapment.

Median Nerve

The median nerve can be trapped at four locations around the elbow:

- In the distal humerus by the ligament of Struthers, a fibrous vestigial remnant, present in up to 2.7% of the population that extends from the anteromedial aspect of the distal humerus to the medial epicondyle.[6,7,85] It is the rarest cause of median nerve compression.[6] The ligament takes its origin from a supracondylar spur on the distal humerus that is present in approximately 1% of the population.[86]

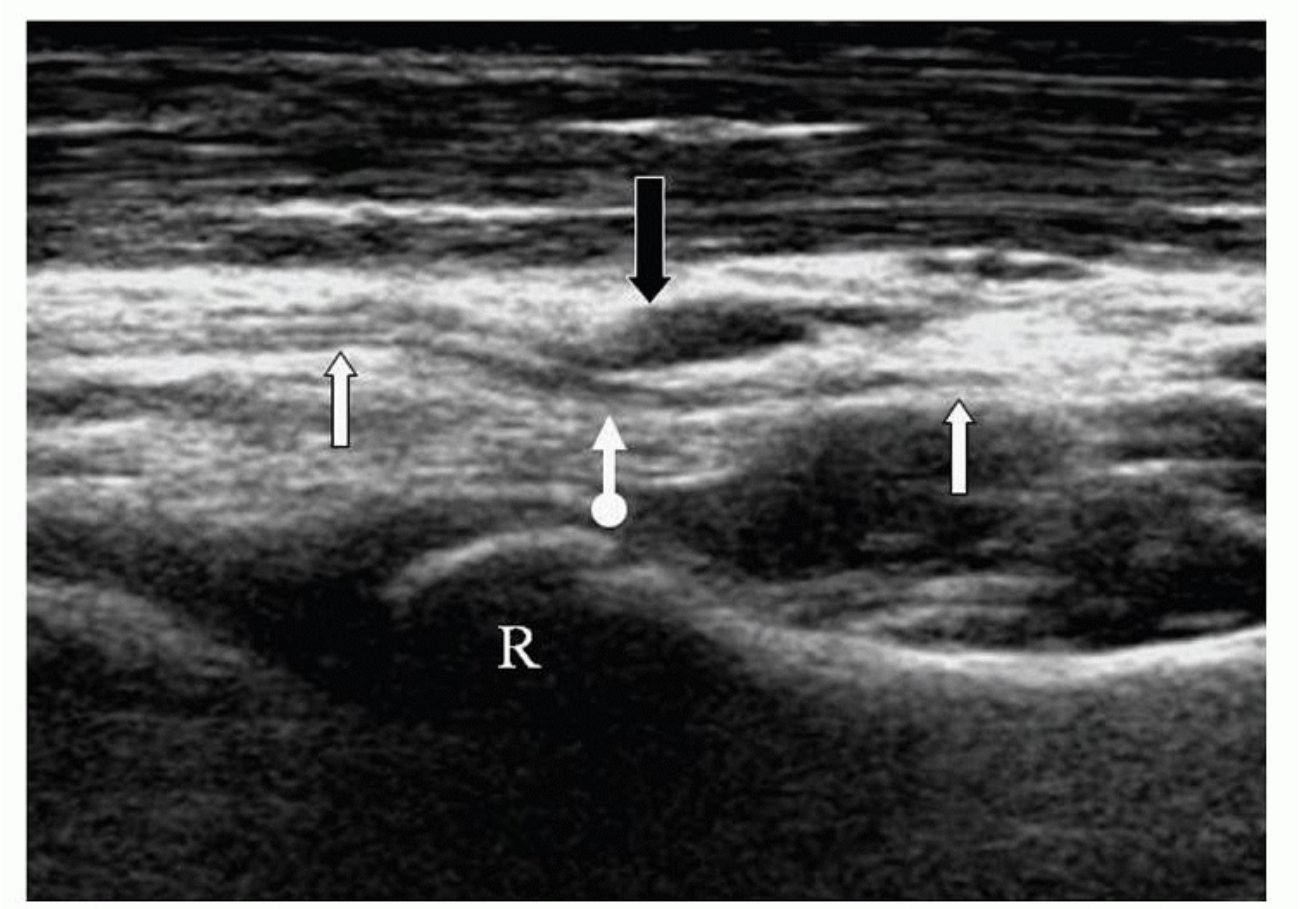

Figure 4.51. Long-axis image shows focal deviation (round tail arrow) of the radial nerve (white arrows) by a prominent vessel (black arrow) at the Leash of Henry. R, radial head.

- At the proximal elbow by a thickened biceps aponeurosis.
- At the elbow joint between the superficial and deep heads of the pronator teres, which is the most common cause of median nerve compression.
- At the proximal forearm by a thickened proximal edge of the FDS.[4,6,7,87]

The AIN may be compressed by the pronator teres and by the proximal edge of the FDS,[4,7] and can be dynamically compressed by repetitive elbow flexion or forearm pronation.[4,88]

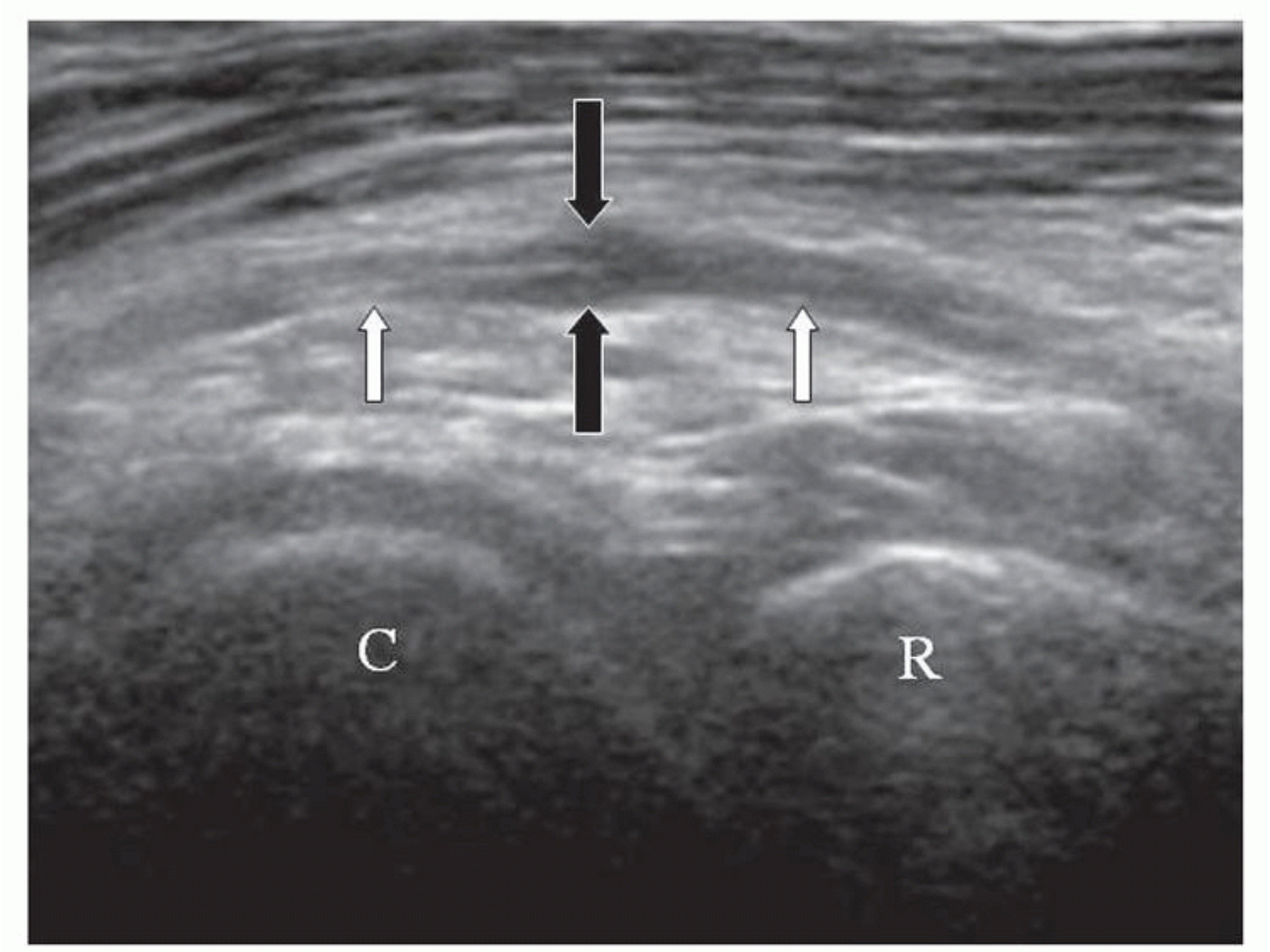

Figure 4.52. Long-axis image of the radial nerve (white arrows) at the level of the radio (R)-capitellar (C) joint shows a focal neurofibroma (black arrows).
P. 68

Similar to radial nerve compression, compression of the median nerve has two presentations: “pronator syndrome” and “AIN syndrome”.
Patients with pronator syndrome have pain and paresthesia in the volar aspects of the elbow and forearm and in the hand affecting the thumb, the index and long fingers, and the lateral half of the ring finger.[4,7] The hand symptoms are similar to those of carpal tunnel syndrome. Both syndromes may be aggravated by overuse, but pronator syndrome may also have associated numbness of the palm due to compression of the palmar cutaneous nerve, whereas symptoms that wake the patient at night are more common with carpal tunnel syndrome.[4,88] Tinel’s sign should be positive over the wrist in patients with carpal tunnel syndrome and is positive over the elbow and proximal forearm in pronator syndrome.[4,88] Symptom reproduction during resisted forearm pronation suggests median nerve compression by the pronator teres, and symptom reproduction during resisted elbow flexion and supination suggests the biceps aponeurosis as the cause of compression.[4]
Patients with AIN syndrome, also called the “Kiloh-Nevin syndrome”,[89] have motor weakness typically manifested by weakened ability to pinch the thumb and index finger together, tested by asking the patient to make an “ok” sign, reflecting the palsy of the flexor pollicis longus muscle and FDP muscle to the index finger.[4,7,88] A non-mechanical cause of AIN syndrome is Parsonage-Turner syndrome (acute brachial neuritis), which can affect the AIN and cause symptoms of AIN syndrome following a transient period of shoulder pain.[4,90]
MR imaging of patients with AIN syndrome shows denervation edema in the muscles supplied by the nerve, or fatty atrophy in chronic cases. The pronator quadratus muscle is always involved, followed by the FDP muscle, and flexor pollicis longus.[8,91] Ultrasound shows increased echogenicity and decreased bulk of the three muscles, suggesting atrophy.[92]
Perineural injection of the ulnar, radial, or median nerves or their branches can be performed as either diagnostic (anesthetic only) or therapeutic (anesthetic and cortisone) procedures. The technique is the same regardless of which nerve is injected: The nerve is identified sonographically in short axis, and a 25G hypodermic needle is placed in-plane with the transducer adjacent to the nerve (Fig. 4.53). For a diagnostic injection, use 0.5 mL of 1% lidocaine and 0.5 mL of 0.25% marcaine, and for therapeutic injections add 1 mL of either triamcinolone (40 mg/mL) or betamethasone (6 mg/mL) to the anesthetics.
BURSAE

The two bursae of clinical concern are the olecranon bursa posteriorly, and the bicipitoradial bursa in the antecubital fossa. The olecranon bursa is subcutaneous and overlies the posterior aspect of the olecranon. It is usually distended as a result of systemic diseases such as rheumatoid arthritis and gout, but can be inflamed due to mechanical irritation. Sonography shows a distended bursa with irregular synovial thickening and hypoechoic or anechoic fluid (Fig. 4.54). Power Doppler may demonstrate hyperemia.[93]

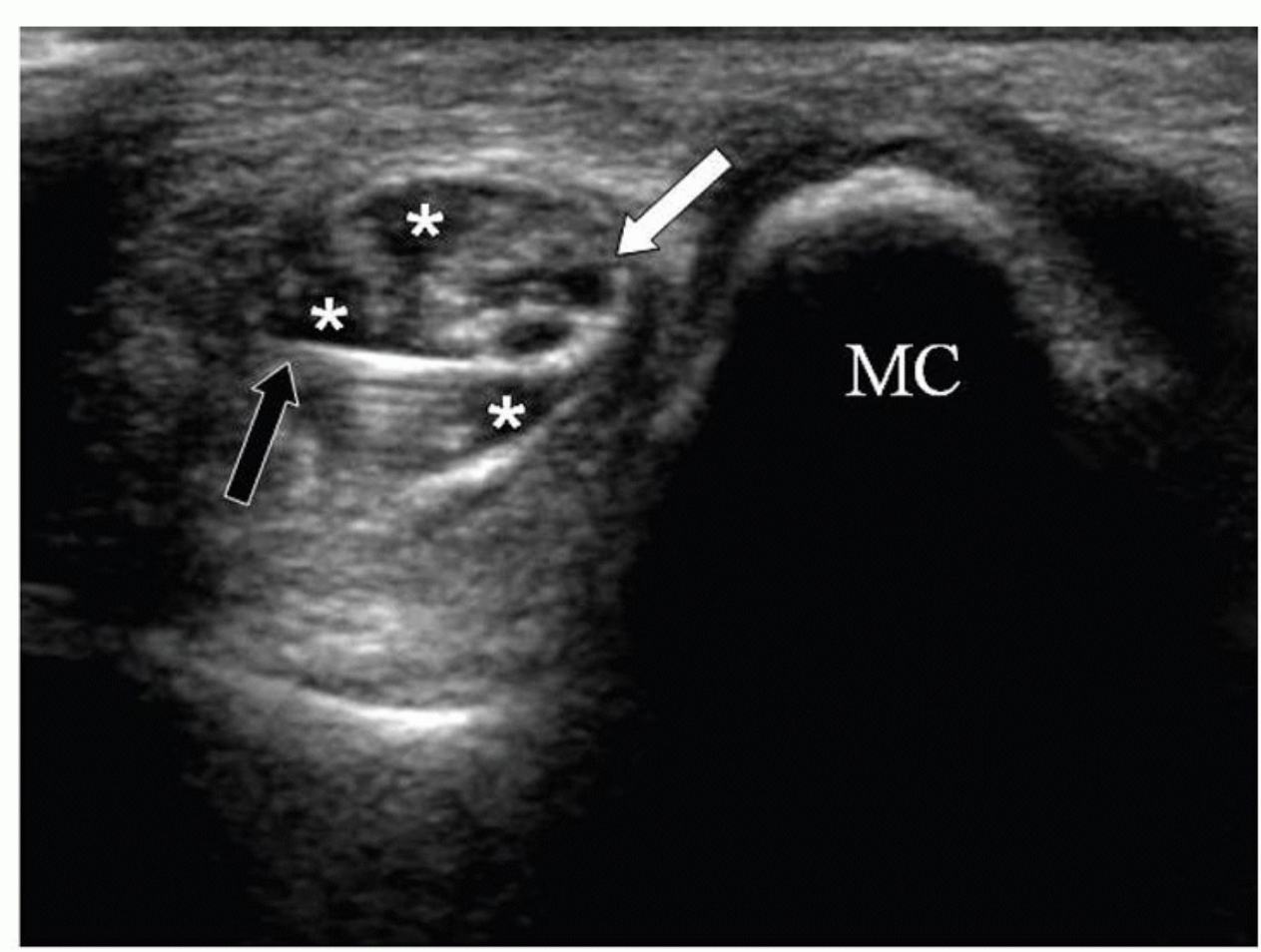

Figure 4.53. Short-axis image during a sonographically guided ulnar nerve injection shows the needle (black arrow), with reverberation artifact, adjacent to the ulnar nerve, which has a fascicular appearance (white arrow). The hypoechoic injectate (asterisks) surrounds the nerve. MC, medial condyle.

The bicipitoradial bursa is adjacent to the distal biceps tendon insertion, and acts to cushion the tendon during forearm pronation as the tendon is pulled into the interosseous space.[14] It can be inflamed due to mechanical irritation or inflammatory arthritis and is often distended

P. 69

when the distal biceps tendon is torn. The distended bursa is usually wrapped around the distal biceps tendon simulating tenosynovitis, but the distal biceps tendon does not have a sheath. The appearance of the distended bursa is variable; it can have a thin or thick and irregular wall (Fig. 4.37), may be complex, and may be hyperemic on Doppler.[94,95]

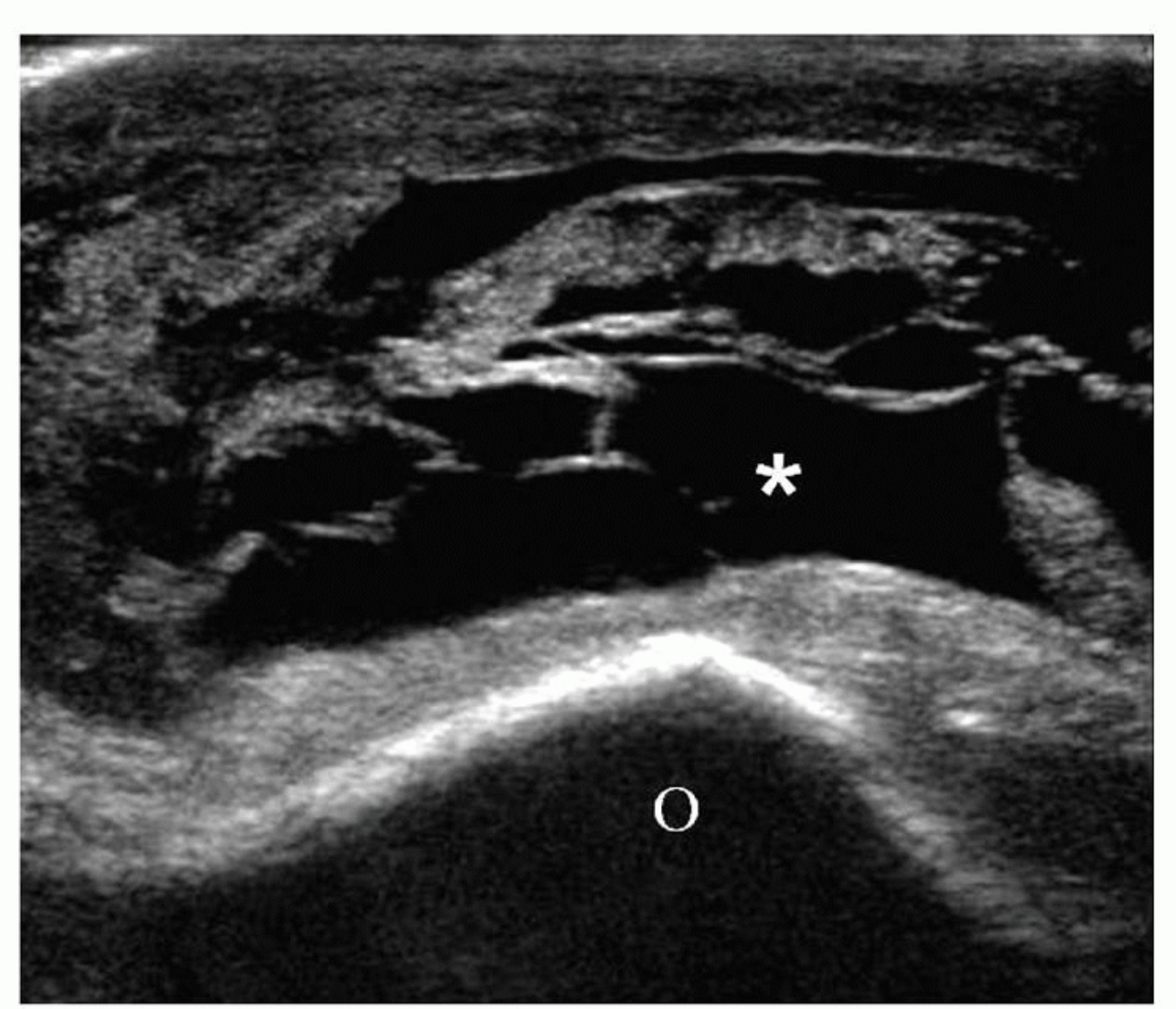

Figure 4.54. Long-axis sonographic image shows a distended olecranon bursa (asterisk) with irregular walls adjacent to the olecranon process (O).

JOINT SPACE

Joint fluid tends to pool in the recesses of the joint, and the most useful places to look for an effusion are the olecranon fossa, the coronoid fossa, and the annular recess of the radiocapitellar joint.

Tip:

Flex the elbow to move the olecranon process out of the olecranon fossa to show joint fluid (Fig. 4.55).

Effusions are usually hypoechoic or anechoic. In infection or active inflammatory arthritis, the synovium is thickened and irregular, and power Doppler may show hyperemia (Fig. 4.55). In chronic cases, the synovium may be thickened without hyperemia. Aspiration of joint fluid may be required in suspected infection or to look for crystals, and is easily accomplished under ultrasound guidance using a short-axis approach to the olecranon fossa with an 18G or 20G hypodermic needle and the elbow flexed 90 degrees. Alternatively, the needle can be placed short axis to the radiocapitellar joint if fluid is visualized in this location with the elbow bent. Both the olecranon fossa and radiocapitellar joint are also easily accessible sites for injecting anesthetics and steroids into the joint, using a 25G hypodermic needle.

Loose bodies can be detected sonographically as hypoechoic or echogenic, depending on their mineralization, and they tend to collect in areas of capsular laxity, such as the olecranon and coronoid fossae and the annular recess, but the donor site of the loose body is not always visible sonographically.[96,97] The presence of an effusion may make intra-articular bodies more conspicuous.[98] Purely cartilaginous bodies are hypoechoic and visualized only if they cause a contour deformity of the adjacent joint capsule. In the presence of an effusion they may be masked by the low echogenicity of the surrounding fluid. Calcified or ossified bodies have an echogenic surface and posterior shadowing (Fig. 4.56).

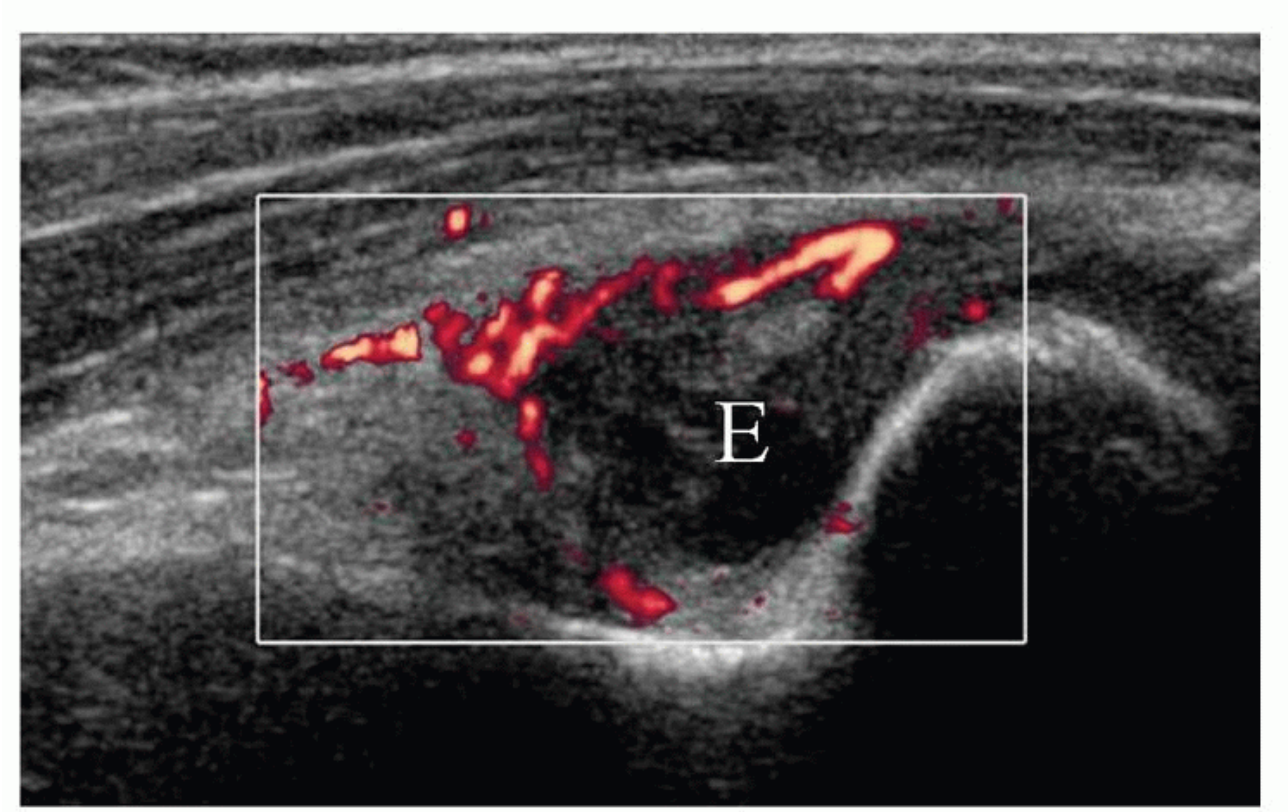

Figure 4.55. Power Doppler long-axis image shows a large effusion (E) in the olecranon fossa with marked surrounding hyperemia. The elbow has been flexed to move the olecranon process out of the way.

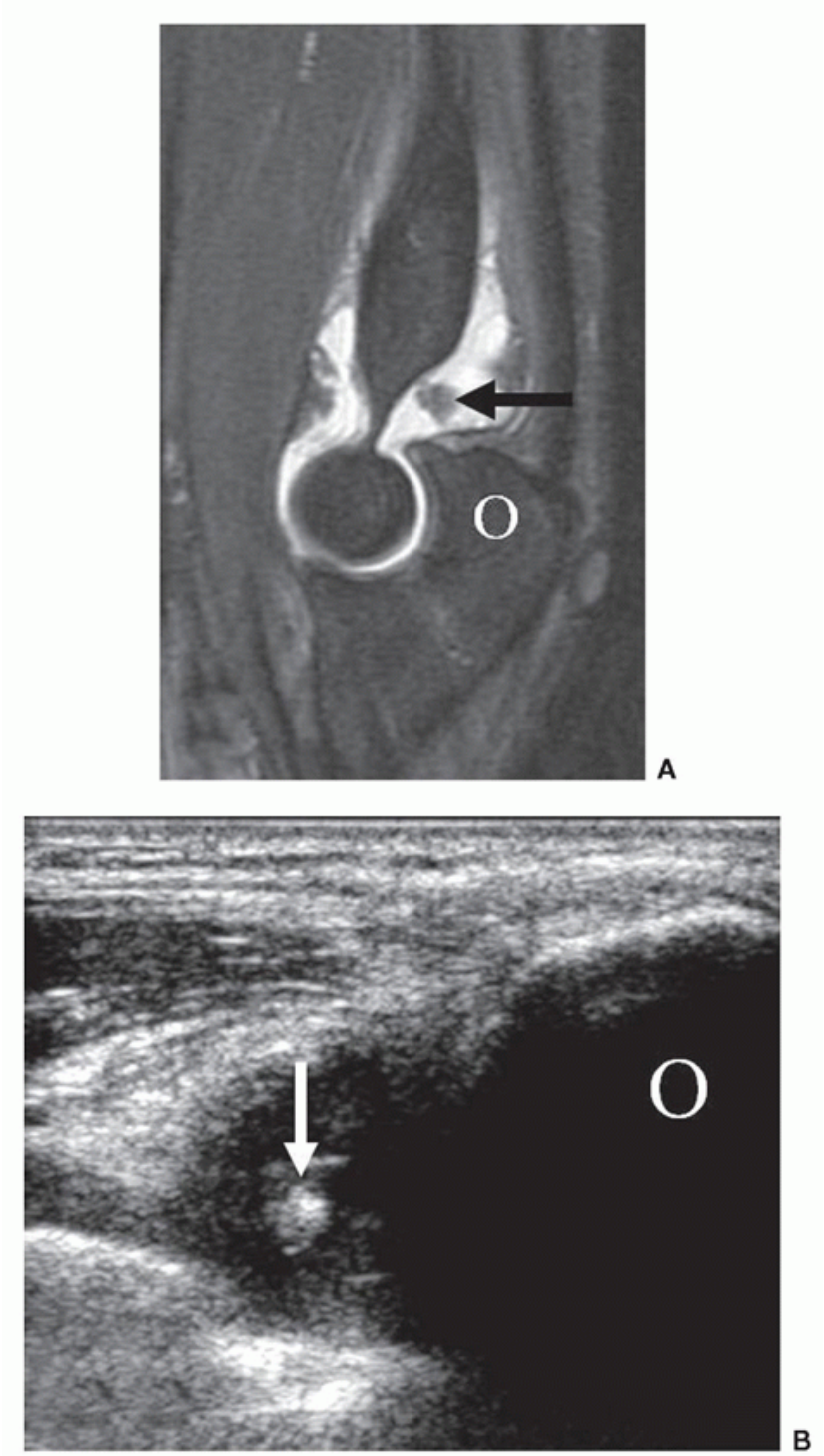

Figure 4.56. Loose body. A: Sagittal fat-suppressed T2-weighted MR image shows a low signal intensity loose body (arrow) in the olecranon fossa with a large effusion. B: Corresponding long-axis sonographic image in the same patient shows the echogenic body (arrow) in the large hypoechoic effusion. O, olecranon.
P. 70

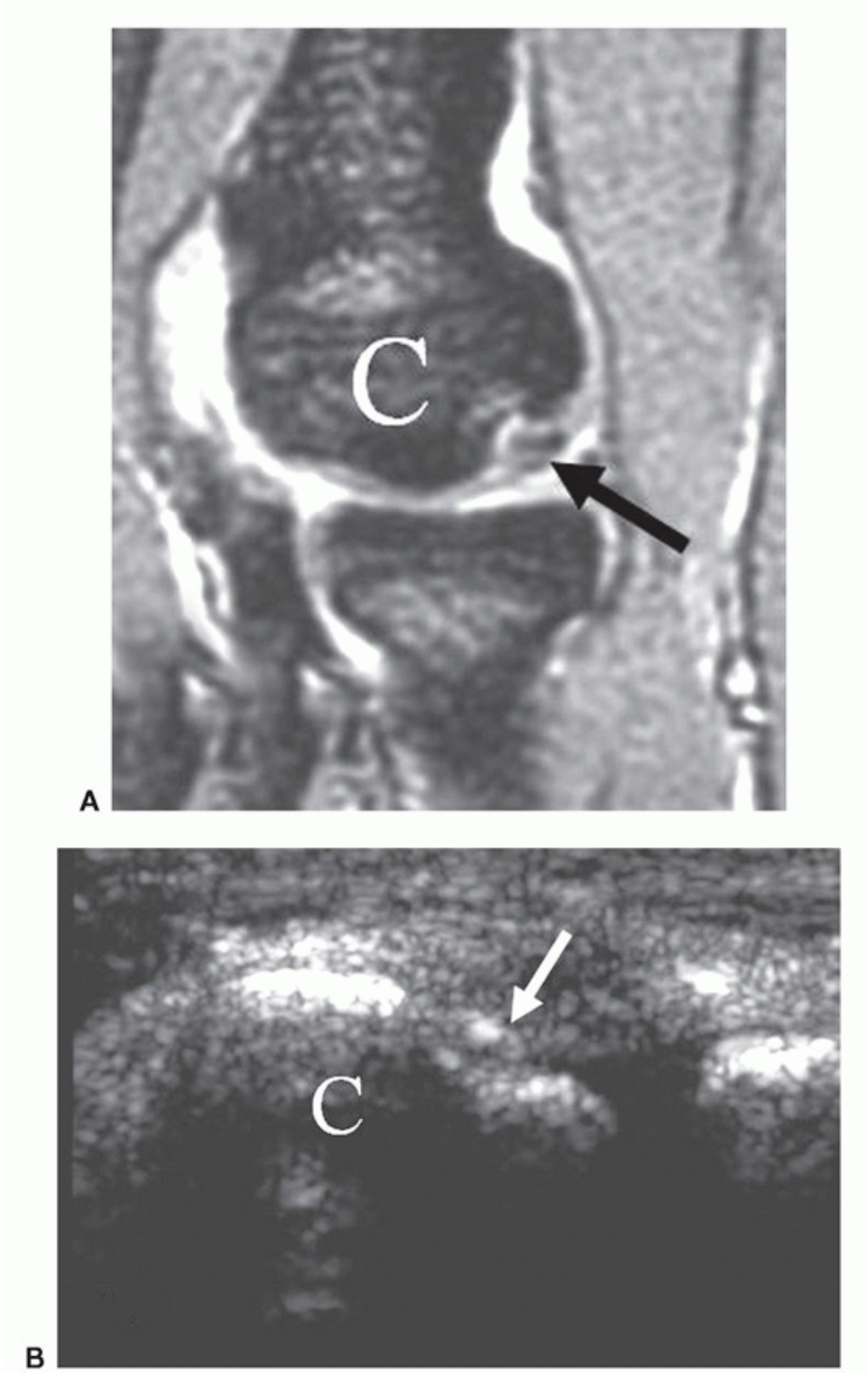

Figure 4.57. Osteochondral injury. A: Sagittal gradient-echo MR image shows an in situ osteochondral fracture (arrow) of the capitellum (C). B: Corresponding long-axis sonographic image in the same patient shows the in situ fragment (arrow) of the capitellum (C).

Osteochondral injuries of the elbow usually occur at the anterior aspect of the capitellum, due to radiocapitellar impaction of the flexed elbow, often caused by throwing or gymnastics. Longitudinal sonography over the radiocapitellar joint of the extended elbow may demonstrate irregularity of the subchondral plate, fragmentation of the subchondral plate and overlying cartilage, or an osteochondral defect[99,100] (Fig. 4.57).

CONCLUSION

Sonography is excellent for the focused assessment of abnormalities of ligaments, tendons, nerves, and bursae around the elbow, and for assessing the joint itself. Additional advantages are its ability to perform dynamic scanning and guide percutaneous treatments.

REFERENCES

1. Conn JM, Annest JL, Gilchrist J. Sports and recreation related injury episodes in the US population, 1997-99. Inj Prev. 2003;9(2):117-123.

2. Yang NP, Chen HC, Phan DV, et al. Epidemiological survey of orthopedic joint dislocations based on nationwide insurance data in Taiwan, 2000-2005. BMC Musculoskelet Disord. 2011;12:253.
3. Reijneirse M, Miller TT. Sonography of the elbow: scanning technique and normal anatomy. AJR :200, June 2013, In Press.
4. Tsai P, Steinberg DR. Median and radial nerve compression about the elbow. Instr Course Lect. 2008;57:177-185.
5. Ferdinand BD, Rosenberg ZS, Schweitzer ME, et al. MR imaging features of radial tunnel syndrome: initial experience. Radiology. 2006;240(1):161-168.
6. Lee MJ, LaStayo PC. Pronator syndrome and other nerve compressions that mimic carpal tunnel syndrome. J Orthop Sports Phys Ther. 2004;34(10):601-609.
7. Andreisek G, Crook DW, Burg D, et al. Peripheral neuropathies of the median, radial, and ulnar nerves: MR imaging features. Radiographics. 2006;26(5):1267-1287.
8. Dunn AJ, Salonen DC, Anastakis DJ. MR imaging findings of anterior interosseous nerve lesions. Skeletal Radiol. 2007;36(12):1155-1162.
9. Miller TT, Adler RS. Sonography of tears of the distal biceps tendon. AJR Am J Roentgenol. 2000;175(4):1081-1086.
10. Kalume Brigido M, De Maeseneer M, Jacobson JA, et al. Improved visualization of the radial insertion of the biceps tendon at ultrasound with a lateral approach. Eur Radiol. 2009;19(7):1817-1821.
11. Smith J, Finnoff JT, O'Driscoll SW, et al. Sonographic evaluation of the distal biceps tendon using a medial approach: the pronator window. J Ultrasound Med. 2010;29(5):861-865.
12. Giuffre BM, Lisle DA. Tear of the distal biceps branchii tendon: a new method of ultrasound evaluation. Australas Radiol. 2005;49(5):404-406.
13. Tagliafico A, Michaud J, Capaccio E, et al. Ultrasound demonstration of distal biceps tendon bifurcation: normal and abnormal findings. Eur Radiol. 2010;20(1):202-208.
14. Skaf AY, Boutin RD, Dantas RW, et al. Bicipitoradial bursitis: MR imaging findings in eight patients and anatomic data from contrast material opacification of bursae followed by routine radiography and MR imaging in cadavers. Radiology. 1999;212(1):111-116.
15. Teixeira PA, Omoumi P, Trudell DJ, et al. Ultrasound assessment of the lateral collateral ligamentous complex of the elbow: imaging aspects in cadavers and normal volunteers. Eur Radiol. 2011;21(7):1492-1498.
16. Stewart B, Harish S, Oomen G, et al. Sonography of the lateral ulnar collateral ligament of the elbow: study of cadavers and healthy volunteers. AJR Am J Roentgenol. 2009;193(6):1615-1619.
17. Reichel LM, Milam GS, Sitton SE, et al. Elbow lateral collateral ligament injuries. J Hand Surg Am. 2013;38(1):184-201.
18. Yeh PC, Dodds SD, Smart LR, et al. Distal triceps rupture. J Am Acad Orthop Surg. 2010;18(1):31-40.
19. Calfee RP, Patel A, DaSilva MF, et al. Management of lateral epicondylitis: current concepts. J Am Acad Orthop Surg. 2008;16(1):19-29.
20. Abrams GD, Renstrom PA, Safran MR. Epidemiology of musculoskeletal injury in the tennis player. Br J Sports Med. 2012;46(7):492-498.
21. Bayes MC, Wadsworth LT. Upper extremity injuries in golf. Phys Sportsmed. 2009;37(1):92-96.
P. 71

22. Miller TT, Reinus WR. Nerve entrapment syndromes of the elbow, forearm, and wrist. AJR Am J Roentgenol. 2010;195(3):585-594.
23. Plancher KD, Halbrecht J, Lourie GM. Medial and lateral epicondylitis in the athlete. Clin Sports Med. 1996;15(2):283-305.
24. Walz DM, Newman JS, Konin GP, et al. Epicondylitis: pathogenesis, imaging, and treatment. Radiographics. 2010;30(1):167-184.
25. Nirschl RP. Elbow tendinosis/tennis elbow. Clin Sports Med. 1992;11(4):851-870.
26. Potter HG, Hannafin JA, Morwessel RM, et al. Lateral epicondylitis: correlation of MR imaging, surgical, and histopathologic findings. Radiology. 1995;196(1):43-46.
27. Regan W, Wold LE, Coonrad R, et al. Microscopic histopathology of chronic refractory lateral epicondylitis. Am J Sports Med. 1992;20(6):746-749.
28. Connell D, Burke F, Coombes P, et al. Sonographic examination of lateral epicondylitis. AJR Am J Roentgenol. 2001;176(3):777-782.
29. Miller TT, Shapiro MA, Schultz E, et al. Comparison of sonography and MRI for diagnosing epicondylitis. J Clin Ultrasound. 2002;30(4):193-202.
30. De Zordo T, Lill SR, Fink C, et al. Real-time sonoelastography of lateral epicondylitis: comparison of findings between patients and healthy volunteers. AJR Am J Roentgenol. 2009;193(1):180-185.
31. Levin D, Nazarian LN, Miller TT, et al. Lateral epicondylitis of the elbow: US findings. Radiology. 2005;237(1):230-234.
32. Struijs PA, Spruyt M, Assendelft WJ, et al. The predictive value of diagnostic sonography for the effectiveness of conservative treatment of tennis elbow. AJR Am J Roentgenol. 2005;185(5):1113-1118.
33. Lee MH, Cha JG, Jin W, et al. Utility of sonographic measurement of the common tensor tendon in patients with lateral epicondylitis. AJR Am J Roentgenol. 2011;196(6):1363-1367.
34. Park GY, Lee SM, Lee MY. Diagnostic value of ultrasonography for clinical medial epicondylitis. Arch Phys Med Rehabil. 2008;89(4):738-742.
35. McShane JM, Shah VN, Nazarian LN. Sonographically guided percutaneous needle tenotomy for treatment of common extensor tendinosis in the elbow: is a corticosteroid necessary? J Ultrasound Med. 2008;27(8):1137-1144.

36. McShane JM, Nazarian LN, Harwood MI. Sonographically guided percutaneous needle tenotomy for treatment of common extensor tendinosis in the elbow. J Ultrasound Med. 2006;25(10):1281-1289.
37. Suresh SP, Ali KE, Jones H, et al. Medial epicondylitis: is ultrasound guided autologous blood injection an effective treatment? Br J Sports Med. 2006;40(11):935-939.
38. Rantanen J, Orava S. Rupture of the distal biceps tendon. A report of 19 patients treated with anatomic reinsertion, and a meta-analysis of 147 cases found in the literature. Am J Sports Med. 1999;27(2):128-132.
39. Belli P, Costantini M, Mirk P, et al. Sonographic diagnosis of distal biceps tendon rupture: a prospective study of 25 cases. J Ultrasound Med. 2001;20(6):587-595.
40. Lobo Lda G, Fessell DP, Miller BS, et al. The role of sonography in differentiating full versus partial distal biceps tendon tears: correlation with surgical findings. AJR Am J Roentgenol. 2013;200(1):158-162.
41. Tagliafico A, Gandolfo N, Michaud J, et al. Ultrasound demonstration of distal triceps tendon tears. Eur J Radiol. 2012;81(6):1207-1210.
42. Downey R, Jacobson JA, Fessell DP, et al. Sonography of partial-thickness tears of the distal triceps brachii tendon. J Ultrasound Med. 2011;30(10):1351-1356.
43. Jacobson JA, Jebson PJ, Jeffers AW, et al. Ulnar nerve dislocation and snapping triceps syndrome: diagnosis with dynamic sonography—report of three cases. Radiology. 2001;220(3): 601-605.
44. Callaway GH, Field LD, Deng XH, et al. Biomechanical evaluation of the medial collateral ligament of the elbow. J Bone Joint Surg Am. 1997;79(8):1223-1231.
45. Floris S, Olsen BS, Dalstra M, et al. The medial collateral ligament of the elbow joint: anatomy and kinematics. J Shoulder Elbow Surg. 1998;7(4):345-351.
46. Magra M, Caine D, Maffulli N. A review of epidemiology of paediatric elbow injuries in sports. Sports Med. 2007;37(8):717-735.
47. Paletta GA Jr, Klepps SJ, Difelice GS, et al. Biomechanical evaluation of 2 techniques for ulnar collateral ligament reconstruction of the elbow. Am J Sports Med. 2006;34(10):1599-1603.
48. Dodson CC, Thomas A, Dines JS, et al. Medial ulnar collateral ligament reconstruction of the elbow in throwing athletes. Am J Sports Med. 2006;34(12):1926-1932.
49. Pollock JW, Brownhill J, Ferreira LM, et al. Effect of the posterior bundle of the medial collateral ligament on elbow stability. J Hand Surg Am. 2009;34(1):116-123.
50. Nazarian LN, McShane JM, Ciccotti MG, et al. Dynamic US of the anterior band of the ulnar collateral ligament of the elbow in asymptomatic major league baseball pitchers. Radiology. 2003;227(1):149-154.
51. Sasaki J, Takahara M, Ogino T, et al. Ultrasonographic assessment of the ulnar collateral ligament and medial elbow laxity in college baseball players. J Bone Joint Surg Am. 2002;84-A(4):525-531.
52. Popovic N, Ferrara MA, Daenen B, et al. Imaging overuse injury of the elbow in professional team handball players: a bilateral comparison using plain films, stress radiography, ultrasound, and magnetic resonance imaging. Int J Sports Med. 2001;22(1):60-67.
53. Cain EL Jr, Dugas JR, Wolf RS, et al. Elbow injuries in throwing athletes: a current concepts review. Am J Sports Med. 2003;31(4):621-635.
54. O'Holleran JD, Altchek DW. The thrower's elbow: arthroscopic treatment of valgus extension overload syndrome. HSS J. 2006;2(1):83-93.
55. Ahmad CS, ElAttrache NS. Valgus extension overload syndrome and stress injury of the olecranon. Clin Sports Med. 2004;23(4):665-676.
56. Miller TT, Adler RS, Friedman L. Sonography of injury of the ulnar collateral ligament of the elbow-initial experience. Skeletal Radiol. 2004;33(7):386-391.
57. Timmerman LA, Schwartz ML, Andrews JR. Preoperative evaluation of the ulnar collateral ligament by magnetic resonance imaging and computed tomography arthrography. Evaluation in 25 baseball players with surgical confirmation. Am J Sports Med. 1994;22(1):26-31.
58. Brogdon BG, Crow NE. Little leaguer's elbow. Am J Roentgenol Radium Ther Nucl Med. 1960;83:671-675.
59. Klingele KE, Kocher MS. Little league elbow: valgus overload injury in thepaediatric athlete. Sports Med. 2002;32(15): 1005-1015.
60. O'Driscoll SW. Classification and evaluation of recurrent instability of the elbow. Clin Orthop Relat Res. 2000;(370):34-43.
61. McKee MD, Schemitsch EH, Sala MJ, et al. The pathoanatomy of lateral ligamentous disruption in complex elbow instability. J Shoulder Elbow Surg. 2003;12(4):391-396.
62. Bredella MA, Tirman PF, Fritz RC, et al. MR imaging findings of lateral ulnar collateral ligament abnormalities in patients with lateral epicondylitis. AJR Am J Roentgenol. 1999; 173(5):1379-1382.
63. Kosuwon W, Mahaisavariya B, Saengnipanthkul S, et al. Ultrasonography of pulled elbow. J Bone Joint Surg Br. 1993; 75(3):421-422.
64. Kim MC, Eckhardt BP, Craig C, et al. Ultrasonography of the annular ligament partial tear and recurrent "pulled elbow". Pediatr Radiol. 2004;34(12):999-1004.

65. Bartels RH, Verbeek AL. Risk factors for ulnar nerve compression at the elbow: a case control study. Acta Neurochir (Wien). 2007;149(7):669-674.

66. van Rijn RM, Huisstede BM, Koes BW, et al. Associations between work-related factors and specific disorders at the elbow: a systematic literature review. Rheumatology (Oxford). 2009;48(5):528-536.
67. Gellman H. Compression of the ulnar nerve at the elbow: cubital tunnel syndrome. Instr Course Lect. 2008;57:187-197.
68. Darowish M, Lawton JN, Evans PJ. Q: What is cell phone elbow, and what should we tell our patients? Cleve Clin J Med. 2009;76(5):306-308.
69. Jensen A, Kaerlev L, Tüchsen F, et al. Locomotor diseases among male long-haul truck drivers and other professional drivers. Int Arch Occup Environ Health. 2008;81(7):821-827.
70. Cummins CA, Schneider DS. Peripheral nerve injuries in baseball players. Neurol Clin. 2008;26(1):195-215.
71. Husarik DB, Saupe N, Pfirrmann CW, et al. Elbow nerves: MR findings in 60 asymptomatic subjects—normal anatomy, variants, and pitfalls. Radiology. 2009;252(1):148-156.
72. Martinoli C, Bianchi S, Gandolfo N, et al. US of nerve entrapments in osteofibrous tunnels of the upper and lower limbs. Radiographics. 2000;20 Spec No:S199-S213.
73. Thoirs K, Williams MA, Phillips M. Ultrasonographic measurements of the ulnar nerve at the elbow: role of confounders. J Ultrasound Med. 2008;27(5):737-743.
74. Yoon JS, Walker FO, Cartwright MS. Ultrasonographic swelling ratio in the diagnosis of ulnar neuropathy at the elbow. Muscle Nerve. 2008;38(4):1231-1235.
75. Jacob D, Creteur V, Courthaliac C, et al. Sonoanatomy of the ulnar nerve in the cubital tunnel: a multicentre study by the GEL. Eur Radiol. 2004;14(10):1770-1773.
76. Childress HM. Recurrent ulnar-nerve dislocation at the elbow. Clin Orthop Relat Res. 1975;(108):168-173.
77. Okamoto M, Abe M, Shirai H, et al. Morphology and dynamics of the ulnar nerve in the cubital tunnel. Observation by ultrasonography. J Hand Surg Br. 2000;25(1):85-89.
78. Spinner RJ, Goldner RD. Snapping of the medial head of the triceps and recurrent dislocation of the ulnar nerve. Anatomical and dynamic factors. J Bone Joint Surg Am. 1998;80(2):239-247.
79. Spinner RJ, Goldner RD, Lee RA. Diagnosis of snapping triceps with US. Radiology. 2002;224(3):933-934.
80. Clavert P, Lutz JC, Adam P, et al. Frohse's arcade is not the exclusive compression site of the radial nerve in its tunnel. Orthop Traumatol Surg Res. 2009;95(2):114-118.
81. Xarchas KC, Psillakis I, Koukou O, et al. Ulnar nerve dislocation at the elbow: review of the literature and report of three cases. Open Orthop J. 2007;24:1-3.
82. Dang AC, Rodner CM. Unusual compression neuropathies of the forearm, Part I: radial nerve. J Hand Surg Am. 2009;34(10):1906-1914.
83. Bodner G, Harpf C, Meirer R, et al. Ultrasonographic appearance of supinator syndrome. J Ultrasound Med. 2002; 21(11):1289-1293.
84. Martinoli C, Bianchi S, Pugliese F, et al. Sonography of entrapment neuropathies in the upper limb (wrist excluded). J Clin Ultrasound. 2004;32(9):438-450.
85. Suranyi L. Median nerve compression by Struthers ligament. J Neurol Neurosurg Psychiatry. 1983;46(11):1047-1049.
86. Lordan J, Rauh P, Spinner RJ. The clinical anatomy of the supracondylar spur and the ligament of Struthers. Clin Anat. 2005;18(7):548-551.
87. Bilecenoglu B, Uz A, Karalezli N. Possible anatomic structures causing entrapment neuropathies of the median nerve: an anatomic study. Acta Orthop Belg. 2005;71(2):169-176.
88. Dang AC, Rodner CM. Unusual compression neuropathies of the forearm, part II: median nerve. J Hand Surg Am. 2009;34(10):1915-1920.
89. Kiloh LG, Nevin S. Isolated neuritis of the anterior interosseous nerve. Br Med J. 1952;1(4763):850-851.
90. Wong L, Dellon AL. Brachial neuritis presenting as anterior interosseous nerve compression—implications for diagnosis and treatment: a case report. J Hand Surg Am. 1997;22(3): 536-539.
91. Grainger AJ, Campbell RS, Stothard J. Anterior interosseous nerve syndrome: appearance at MR imaging in three cases. Radiology. 1998;208(2):381-384.
92. Hide IG, Grainger AJ, Naisby GP, et al. Sonographic findings in the anterior interosseous nerve syndrome. J Clin Ultrasound. 1999;27(8):459-464.
93. Blankstein A, Ganel A, Givon U, et al. Ultrasonographic findings in patients with olecranon bursitis. Ultraschall Med. 2006;27(6):568-571.
94. Liessi G, Cesari S, Spaliviero B, et al. The US, CT, and MR findings of cubital bursitis: a report of five cases. Skeletal Radiol. 1996;25(5):471-475.
95. Sofka CM, Adler RS. Sonography of cubital bursitis. AJR Am J Roentgenol. 2004;183(1):51-53.
96. Bianchi S, Martinoli C. Detection of loose bodies in joints. Radiol Clin North Am. 1999;37(4):679-690.
97. Frankel DA, Bargiela A, Bouffard JA, et al. Synovial joints: evaluation of intraarticular bodies with US. Radiology. 1998;206(1):41-44.
98. Miller JH, Beggs I. Detection of intraarticular bodies of the elbow with saline arthrosonography. Clin Radiol. 2001;56(3):231-234.
99. Harada M, Takahara M, Sasaki J, et al. Using sonography for the early detection of elbow injuries among young baseball players. AJR Am J Roentgenol. 2006;187(6):1436-1441.
100. Takahara M, Ogino T, Tsuchida H, et al. Sonographic assessment of osteochondritis dissecans of the humeral capitellum. AJR Am J Roentgenol. 2000;174(2):411-415.